

MECHANISM-BASED INHIBITORS OF LYSOSOMAL GLYCOSIDASES

by

ALEXANDER WILLIAM WONG

B.Sc., The University of Waterloo, 1994

A THESIS SUBMITTED IN PARTIAL FULFILMENT OF
THE REQUIREMENTS FOR THE DEGREE OF

DOCTOR OF PHILOSOPHY

in

THE FACULTY OF GRADUATE STUDIES

(Department of Chemistry)

We accept this thesis as conforming
to the required standard

THE UNIVERSITY OF BRITISH COLUMBIA

June 2001

© Alexander William Wong, 2001

In presenting this thesis in partial fulfilment of the requirements for an advanced degree at the University of British Columbia, I agree that the Library shall make it freely available for reference and study. I further agree that permission for extensive copying of this thesis for scholarly purposes may be granted by the head of my department or by his or her representatives. It is understood that copying or publication of this thesis for financial gain shall not be allowed without my written permission.

Department of Chemistry

The University of British Columbia
Vancouver, Canada

Date June 27, 2001

Abstract

The lysosomal storage disorders are genetic diseases arising from a deficiency of a lysosomal protein that is part of a catabolic pathway. Some of these enzymes are exoglycosidases that act in sequence on glycolipids and glycosaminoglycans, i.e. substrates are degraded by a stepwise removal of terminal sugar units. Thus, the deficiency of a single lysosomal enzyme causes the blockage of the entire pathway, leading to the accumulation of that substrate. Because of their clinical significance, interest in the lysosomal glycosidases is widespread.

The uronidases are a specific subset of lysosomal glycosidases. According to their sequence-based glycosidase family assignments, they are predicted to hydrolyze their substrates via a double displacement mechanism. In order to perform mechanistic studies upon these glycosidases, two classes of fluoro-sugar inactivators were developed – the 2-deoxy-2-fluoro- and the 5-fluoro-glycopyranosyluronic acids. These compounds function via the trapping of a covalent glycosyl-enzyme intermediate. Five new compounds - 2-deoxy-2-fluoro- β -D-glucopyranosyluronic acid fluoride (2FGlcAF), 2-deoxy-2-fluoro- β -D-mannopyranosyluronic acid fluoride (2FManAF), 2-deoxy-2-fluoro- α -L-idopyranosyluronic acid fluoride (2FIdoAF), 5-fluoro- β -D-glucopyranosyluronic acid fluoride (5FGlcAF) and 5-fluoro- α -L-idopyranosyluronic acid fluoride (5FIdoAF) were synthesized and evaluated with the appropriate enzymes.

The syntheses of both 2FGlcAF and 2FManAF were accomplished using a TEMPO-mediated oxidation of the primary C-6 alcohol group of the parent glycopyranosides while 2FIdoAF, 5FGlcAF and 5FIdoAF were synthesized from the parent glycopyranosyluronic acid fluorides via radical bromination of the C-5 carbon and displacement of the installed bromine with either tributyltin hydride (2FIdoAF) or silver tetrafluoroborate (5FGlcAF and 5FIdoAF). All five inactivators were evaluated using *E. coli* β -glucuronidase (EBG) as a model system. Further, labelling and identification of the catalytic nucleophile of EBG as Glu504 within the sequence ₅₀₂ITEYGVD₅₀₇ was accomplished by LC/MS analysis of proteolytic digests using 5FGlcAF. Both 2FGlcAF and 2FManAF were tested as inactivators of human β -glucuronidase, with its catalytic nucleophile being identified as Glu540 within the sequence ₅₃₉SEYGAET₅₄₅ through the use of 2FGlcAF. Finally, both 5FIdoAF and 2FIdoAF were tested on human α -L-iduronidase, with its catalytic nucleophile being identified through the use of 5FIdoAF and 2FIdoAF.

Gaucher disease is a lysosomal storage disorder caused by a deficiency in glucocerebrosidase (GCase). Current treatment of the Type I version for this disease involves enzyme replacement therapy, whereby the patient is administered recombinant enzyme intravenously. A non-invasive technique of assessing *in vivo* localization of the enzyme would be beneficial in patient care. To this end, ¹⁸F-labelled 2,6-dideoxy-2,6-difluoro- β -D-glucopyranosyl fluoride was developed as a potential positron emission tomographic imaging agent. Starting with 3,4-di-O-acetyl-6-O-trifluoromethanesulfonyl-2-deoxy-2-fluoro- β -D-glucopyranosyl fluoride, the triflate group was displaced with ¹⁸F-

fluoride, and the acetyl groups were removed under Zemplén conditions to give the radiolabelled inactivator in 8% radiochemical yield (corrected for decay). Attempts at radiolabelling GCase *in vitro* have so far failed. Explanations for this result are offered, with suggestions as to what may be done.

Table of Contents

Abstract.....	ii
Table of Contents	v
List of Figures.....	ix
List of Tables	xii
List of Abbreviations	xiii
Acknowledgments	xv

Chapter 1 General Introduction 1

1.1 Classification of glycosidases	2
1.2 The catalytic mechanism of retaining glycosidases.....	5
1.3 Evidence for a double displacement mechanism in retaining glycosidases	7
1.3.1 Presence of active site carboxylates	7
1.3.2 Nature of the glycosyl-enzyme intermediate	7
1.3.2.1 Kinetic studies.....	7
1.3.2.2 Oxocarbenium ion-like transition states	9
1.4 Glycosidase inhibitors and covalent labeling of active site residues	12
1.4.1 Affinity labels.....	12
1.4.2 Conduritol epoxides	14
1.4.3 2-Fluoro glycosides	16
1.4.4 5-Fluoro glycosyl fluorides	18
1.5 Lysosomal storage disorders	20
1.6 Aims of this thesis	21

Chapter 2 Fluoro-Sugar Inhibitors of Glycuronidases 22

2.1	Introduction	23
2.1.1	Fluoro-glycosides – Good inhibitors of glycosidases	23
2.1.2	Glycuronidases - Background	24
2.1.2.1	Human β -glucuronidase	25
2.1.2.2	<i>E. coli</i> β -glucuronidase	27
2.1.2.3	Human α -L-iduronidase	28
2.2	Specific aims	30
2.3	Syntheses of 2-deoxy-2-fluoro- and 5-fluoro glycopyranosyluronic acid fluoride inactivators	31
2.3.1	Syntheses of 2-deoxy-2-fluoro-glycopyranosyluronic acid fluorides	31
2.3.1.1	2-Deoxy-2-fluoro- β -D-glucopyranosyluronic acid fluoride, 2FGlcAF (5)	31
2.3.1.2	2-Deoxy-2-fluoro- β -D-mannopyranosyluronic acid fluoride, 2FManAF (8)	33
2.3.1.3	2-Deoxy-2-fluoro- α -L-idopyranosyluronic acid fluoride, 2FIdoAF (14)	34
2.3.2	Synthesis of 5-fluoro- β -D-glucopyranosyluronic acid fluoride, 5FGlcAF (25) and 5-fluoro- α -L-idopyranosyluronic acid fluoride, 5FIdoAF (26) ...	38
2.4	Spontaneous hydrolysis studies of fluoro-sugar inactivators	41
2.5	Studies employing EBG	42
2.5.1	Inactivation Kinetics	42
2.5.1.1	2FGlcAF and 2FManAF	43
2.5.1.2	5FGlcAF	48
2.5.1.3	5FIdoAF	53
2.5.1.4	2FIdoAF	59
2.5.1.5	Interpretation of the kinetic results obtained using the various fluoroglycopyranosyluronic acid fluoride inactivators	62
2.5.2	Identification of the catalytic nucleophile by electrospray MS	65
2.5.3	Conclusion	70
2.6	Studies employing HBG	71
2.6.1	Stereochemistry of HBG hydrolysis	71
2.6.2	Inactivation Kinetics using 2FGlcAF and 2FManAF	74
2.6.3	Identification of the catalytic nucleophile by electrospray MS	78
2.6.4	Conclusion	83
2.7	Studies employing IDUA	84

2.7.1	Previous studies using 5FIdoAF	84
2.7.2	Inactivation kinetics using 2FIdoAF	85
2.7.3	Identification of the catalytic nucleophile by electrospray MS	87
2.7.4	Conclusion.....	92

Chapter 3 Attempted Radiolabelling of Glucocerebrosidase 98

3.1	Introduction	99
3.1.1	Positron emission tomography (PET)	101
3.1.2	Earlier Studies using ¹⁸ F-labelled glycosidase inactivators	103
3.2	Specific Aims	104
3.3	Results and Discussion	105
3.3.1	Synthesis	105
3.3.2	Radiosynthesis.....	106
3.3.3	Kinetic analysis of the reaction of 2,6diFGF with Abg and GCase.....	109
3.3.4	Attempted radiolabelling of GCase.....	113
3.3.5	Conclusions	115

Chapter 4 Materials and Methods 117

4.1	Synthetic Procedures	118
4.1.1	Analytical methods.....	118
4.1.2	Solvents and reagents	119
4.1.3	General work-up procedure.....	119
4.1.4	Synthesis of 2-deoxy-2-fluoro-β-D-glucopyranosyluronic acid fluoride (2FGlcAF) 5	120
4.1.5	Synthesis of 2-deoxy-2-fluoro-β-D-mannopyranosyluronic acid fluoride (2FManAF) 8	122
4.1.6	Synthesis of 2-deoxy-2-fluoro-α-L-idopyranosyluronic acid fluoride (2FIdoAF) 14	124
4.1.7	Syntheses of 5-fluoro-glycopyranosyluronic fluorides (5FGlcAF and 5FIdoAF) 25 and 26	128
4.1.8	Synthesis of 2,6-dideoxy-2,6-trifluoro-β-D-glucopyranosyl fluoride (2,6diFGF) 30.....	135
4.1.9	Radiosynthesis of 2,6-dideoxy-6- ¹⁸ F-2-fluoro-β-D-glucopyranosyl fluoride 32 139	

4.2	Spontaneous Hydrolysis of Glycosyl Fluorides	140
4.3	Enzyme Kinetics	141
4.3.1	General Materials and Methods	141
4.3.2	Time-dependent inactivation.....	143
4.3.3	Protection against inactivation	144
4.3.4	Reactivation of inactivated enzyme	144
4.3.5	Determination of apparent K_i ' values	145
4.4	Determination of the Stereochemical Course of Hydrolysis of HBG	145
4.5	Labelling and proteolysis of glycosidases for electrospray MS analysis.....	146
4.6	Electrospray MS conditions for peptide analysis	147
4.6.1	MS scan mode parameters - HBG.....	148
4.6.2	MS scan mode parameters - EBG	148
4.6.3	MS scan mode parameters - IDUA	149
4.7	Radiolabelling of glucocerebrosidase.....	149
Appendix I: Enzyme Kinetics		151
	Fundamental Equations of Enzyme Kinetics	152
	Enzyme Kinetics in the Presence of a Reversible Competitive Inhibitor	158
	Enzyme Kinetics in the Presence of a Mechanism-Based Inactivator .	161
Appendix II: Graphical Representation of Spontaneous Hydrolysis Data.....		166
References.....		171

List of Figures

Figure 1.1: Reaction normally catalyzed by a glycosidase	2
Figure 1.2: Possible stereochemical outcome of glycosidase-catalyzed hydrolyses of glycosides	4
Figure 1.3: Presumed mechanism of a retaining glycosidase.	6
Figure 1.4: Comparison of a ground state glucoside and a transition state glucosyl oxocarbenium ion	10
Figure 1.5: Resonance structures of aldonolactones (top) and aldonolactams (bottom). ..	11
Figure 1.6: Nojirimycin in both hydrated and dehydrated forms (top), and nojiritetrazole (bottom)	12
Figure 1.7: Affinity labels of glycosidases: glycosyl epoxide, N-bromoacetyl glycosylamine, and glycosyl isothiocyanate.	13
Figure 1.8: Affinity labels of glycosidases: C-glycosyl epoxide and C-glycosyl bromoketone	14
Figure 1.9: Reaction of conduritol B epoxide with a β -glucosidase	15
 Figure 2.1: Synthesis of 2-deoxy-2-fluoro- β -D-glucopyranosyluronic acid fluoride 5	32
Figure 2.2: Synthesis of 2-deoxy-2-fluoro- β -D-mannopyranosyluronic acid fluoride 8 ..	34
Figure 2.3: Synthesis of 2-deoxy-2-fluoro- α -L-idopyranosyluronic acid fluoride 14	35
Figure 2.4: Crystal structure of phenacyl (3,4-di-O-acetyl-2-deoxy-2-fluoro- α -L-idopyranosyl fluoride)uronate	36
Figure 2.5: Synthesis of 5-fluoro- β -D-glucopyranosyluronic acid fluoride 25 and 5-fluoro- α -L-idopyranosiduronic acid fluoride 26	40
Figure 2.6: Inactivation of EBG by 2FGlcAF	43
Figure 2.7: Inactivation of EBG by 2FManAF	44
Figure 2.8: Protection against inactivation of EBG with 2FGlcAF and 2FManF.....	45
Figure 2.9: Reactivation of 2F-glycuronyl EBG species in buffer	46
Figure 2.10: Reactivation of (●) 2FGlcA-EBG species and (○) 2FManA-EBG species in the presence of 20 mM BnOH	47
Figure 2.11: Reactivation of 2F-glycuronyl-EBG species in the presence of 50 mM pNPG	48
Figure 2.12: Inactivation of <i>E. coli</i> β -glucuronidase by 5FGlcAF. Lines shown in each case are those for the best fit to the data.....	49
Figure 2.13: Protection against inactivation of EBG with 100 μ M 5FGlcAF in: A) the absence and B) the presence of 50 μ M D-saccharic acid 1,4-lactone	50
Figure 2.14: Reactivation of 5FGlcA-EBG in buffer.....	51
Figure 2.15: Turnover of 5FGlcA-EBG in the presence of reactivation ligands	52
Figure 2.16: Reversible K_i for 5FGlcAF with EBG determined under steady-state conditions.....	53

Figure 2.17: Inactivation of <i>E. coli</i> β -glucuronidase by 5FIIdoAF. Lines shown in each case are those for the best fit to the data.....	54
Figure 2.18: Protection against inactivation of EBG with 16 mM 5FIIdoAF in: A) the absence and B) the presence of 50 μ M D-saccharic acid 1,4-lactone	55
Figure 2.19: Reactivation of 5F-iduronyl-EBG in buffer	57
Figure 2.20: Reactivation of 5F-iduronyl-EBG in 20 mM benzyl alcohol	58
Figure 2.21: Reversible K_i for 5FIIdoAF with EBG determined under steady-state conditions.....	59
Figure 2.22: Inactivation of <i>E. coli</i> β -glucuronidase by 2FIIdoAF.....	60
Figure 2.23: Protection against inactivation of EBG with 10 mM 2FIIdoAF in (●) the absence and (○) the presence of 50 μ M D-saccharic acid 1,4-lactone.....	60
Figure 2.24: Reactivation of 2F-idopyranosyluronic acid-EBG in buffer (●) and in 20 mM benzyl alcohol (○).....	61
Figure 2.25: Reversible K_i for 2FIIdoAF with EBG determined under steady-state conditions.....	62
Figure 2.26: Electrospray mass spectrometry experiments on EBG proteolytic digests	67
Figure 2.27: Electrospray tandem MS daughter ion spectrum of labeled peptides.....	69
Figure 2.28: Proton NMR spectra showing the stereochemical course of hydrolysis of pNPGlcA by HBG.....	73
Figure 2.29: Inactivation of HBG by 2FGlcAF.	74
Figure 2.30: Inactivation of HBG by 2FManAF.....	75
Figure 2.31: Inactivation with 150 μ M 2FGlcAF in the absence (○) and presence (●) of 0.68 μ M D-saccharic acid 1,4-lactone.....	76
Figure 2.32: Reactivation of 2F-glucopyranosyluronic acid glucuronidase	78
Figure 2.33: ESMS experiments on a peptic digest of human β -glucuronidase	80
Figure 2.34: ESMS/MS daughter ion spectrum of the 2F-glucopyranosyluronic acid peptide (m/z 934, in the singly charged state)	82
Figure 2.35: Sequence of the 2FGlcA-HBG peptide.	82
Figure 2.36: Testing of 2FIIdoAF as a time-dependent inactivator of IDUA.....	86
Figure 2.37: Reversible K_i for 2FIIdoAF with IDUA determined under steady-state conditions.....	87
Figure 2.38: Electrospray mass spectrometry experiment on labelled IDUA proteolytic digest.....	88
Figure 2.39: ESMS/MS daughter ion spectrum of the 2F-iduronyl peptide (m/z 885). .	90
Figure 2.40: Sequence of the 2FIIdoA-IDUA peptide	91
Figure 2.41: Proposed reactions of different fluoro-sugar inactivators with an enzyme active site nucleophilic carboxylate residue	94
Figure 2.42: 2,5 B conformations of different pyranose sugars	96
Figure 2.43: Proposed reactions of 2FIIdoAF and 5FIIdoAF with IDUA	97
Figure 3.1: Structure of glucosyl ceramide	99
Figure 3.2: Structures of 2,6-dideoxy-2,6-difluoro- β -D-glucopyranosyl fluoride and 2,6-dideoxy-2-fluoro-6-[18 F]-fluoro- β -D-glucopyranosyl fluoride	104
Figure 3.3: Synthetic scheme of 2,6-dideoxy-2,6-difluoro- β -D-glucopyranosyl fluoride	
30.	105

Figure 3.4: Synthetic scheme of 3,4-di-O-acetyl-6-O-trifluoromethanesulfonyl-2-deoxy-2-fluoro- β -D-glucopyranosyl fluoride 31	107
Figure 3.5: Synthetic scheme of 2,6-dideoxy-2,6-difluoro- β -D-glucopyranosyl fluoride 3.1 and 2,6-dideoxy-2-fluoro-6-[^{18}F]-fluoro- β -D-glucopyranosyl fluoride 3.2 using fluoride anion.....	107
Figure 3.6: Inactivation of <i>Agrobacterium</i> sp. β -glucosidase by 2,6diFGF.	109
Figure 3.7: Inactivation of Abg with 4 mM 2,6diFGF in the absence (●) and the presence (○) of 3.8 μM castanospermine.....	110
Figure 3.8: Inactivation of human glucocerebrosidase by 2,6diFGF.....	111
Figure 3.9: Inactivation of GCase with 200 mM 2,6diFGF in the absence (○) and the presence (●) of 8.0 μM castanospermine.....	111
Figure 3.10: A) Reactivation of inactivated <i>Agrobacterium</i> sp. β -glucosidase. B) Reactivation of inactivated human glucocerebrosidase.....	113
Figure AII-1: Spontaneous hydrolysis of 2FGF (2.5 mM) at 50°C, pH 6.8.....	167
Figure AII-2: Spontaneous hydrolysis of 2FMF (7.5 mM) at 50°C, pH 6.8.....	167
Figure AII-3: Spontaneous hydrolysis of 2,6diFGF (5 mM) at 50°C, pH 6.8	168
Figure AII-4: Spontaneous hydrolysis of 2FGlcAF (5 mM) at 50°C, pH 6.8.....	168
Figure AII-5: Spontaneous hydrolysis of 2FManAF (2.5 mM) at 50°C, pH 6.8	169
Figure AII-6: Spontaneous hydrolysis of 5FGlcAF (5 mM) at 50°C, pH 6.8.....	169
Figure AII-7: Spontaneous hydrolysis of 5FIIdoAF (5 mM) at 50°C, pH 6.8	170
Figure AII-8: Spontaneous hydrolysis of 2FIIdoAF (10 mM) at 50°C, pH 6.8	170

List of Tables

Table 2.1: The repeating disaccharide units of the glycosaminoglycan substrates of human β -glucuronidase and human α -L-iduronidase	25
Table 2.2: Torsion angles obtained from the X-ray crystal structure of 2FIdoAF.....	37
Table 2.3: Spontaneous hydrolysis data for various 2-deoxy-2-fluoro- β -D- and 5-fluoro- β -D-glycopyranosyl fluorides and -glycopyranosyluronic acid fluorides.....	41
Table 2.4: Kinetic parameters for reaction of pNPGlcA, 2FGlcAF, 2FManAF, 5FGlcAF, 5FIdoAF, and 2FIdoAF with <i>E. coli</i> β -glucuronidase.....	63
Table 2.5: Conserved active site residues of Family 2 glycosidases. The enzymes are grouped according to substrate specificity.	70
Table 2.6: Observed peptide fragments resulting from fragmentation of the labelled parent peptide ($m/z = 885$). Bolded sequences contain the 2FIdoA label.....	91
Table 2.7: Values of k_{re} and K_i' obtained for 2F α GF and 5F α GF (yeast α -glucosidase), and 2FIdoAF and 5FIdoAF (EBG and IDUA).....	95
Table 3.1: The clinical manifestations of the three types of Gaucher disease.	100
Table 3.2: Kinetic parameters determined for the inactivation of Abg and GCase by 2,6-dideoxy-2,6-difluoro- β -D-glucopyranosyl fluoride (2,6diFGF). For comparison, values previously reported using 2-deoxy-2-fluoro- β -D-glucopyranosyl fluoride (2FGF) and 2-deoxy-2-fluoro- β -D-mannopyranosyl fluoride (2F β MF) are also shown. ^{43,76}	112
Table 3.3: Presence (+) or absence (-) of both enzymatic activity and radioactivity of eluted fractions obtained from purification of GCase radiolabelling experiment using a Hi-Trap desalting column.	114

List of Abbreviations

2,6diFGF:	2,6-dideoxy-2,6-difluoro- β -D-glucopyranosyl fluoride
2F α G-Abg:	2-deoxy-2-fluoro- α -D-glucosyl-Abg
2F α GF:	2-deoxy-2-fluoro- α -D-glucosyl fluoride
2F α M-Abg:	2-deoxy-2-fluoro- α -D-mannosyl-Abg
2F β GF:	2-deoxy-2-fluoro- β -D-glucosyl fluoride
2F β MF:	2-deoxy-2-fluoro- β -D-mannosyl fluoride
2FGlcA-EBG:	2-deoxy-2-fluoro- α -D-glucopyranosyluronic acid-EBG
2FGlcA-HBG:	2-deoxy-2-fluoro- α -D-glucopyranosyluronic acid-HBG
2FGlcAF:	2-deoxy-2-fluoro- β -D-glucopyranosyluronic acid fluoride
2FI α A-EBG:	2-deoxy-2-fluoro- β -L-idopyranosyluronic acid-IDUA
2FI α AF:	2-deoxy-2-fluoro- α -L-idopyranosyluronic acid fluoride
2FManAF:	2-deoxy-2-fluoro- β -D-mannopyranosyluronic acid fluoride
2FManA-EBG:	2-deoxy-2-fluoro- α -D-mannopyranosyluronic acid-EBG
5F α G-Abg:	5-fluoro- α -D-glucosyl-Abg
5F α GF:	5-fluoro- α -D-glucosyl fluoride
5F α IF:	5-fluoro- α -L-idosyl fluoride
5F β GF:	5-fluoro- β -D-glucopyranosyl fluoride
5FGlcA-EBG:	5-fluoro- α -D-glucopyranosyluronic acid-EBG
5FGlcAF:	5-fluoro- β -D-glucopyranosyluronic acid fluoride
5FI α A-EBG:	5-fluoro- β -L-idopyranosyluronic acid-IDUA
5FI α AF:	5-fluoro- α -L-idopyranosyluronic acid fluoride
Abg:	<i>Agrobacterium</i> sp. β -glucosidase
AcCl:	acetyl chloride
DAST:	diethylaminosulfur trifluoride
DMF:	<i>N,N</i> -dimethyl formamide
DNP:	2,4-dinitrophenyl
EBG:	<i>E. coli</i> β -D-glucuronidase
EBGal:	<i>E. coli</i> β -D-galactosidase
ESMS:	electrospray ionization mass spectrometry
ESMS/MS:	electrospray ionization tandem mass spectrometry
GAG:	glycosaminoglycan
GCase:	human glucocerebrosidase
GlcNAc:	<i>N</i> -acetylglucosamine
HBG:	human β -D-glucuronidase
HPLC:	high performance liquid chromatography
IDUA:	human α -L-iduronidase
ISV:	ion source voltage
LC/MS:	liquid chromatography-mass spectrometry
MeOH:	methanol

MPS:	mucopolysaccharidosis
MS:	mass spectrometry
MS/MS:	tandem mass spectrometry
MUI:	4- methylumbelliferyl- α -L-iduronide
NBS:	<i>N</i> -bromosuccinimide
NMR:	nuclear magnetic resonance spectroscopy
OR:	orifice plate energy
PET:	positron emission tomography
pNPG:	<i>p</i> -nitrophenyl β -D-glucoside
pNPGlcA:	<i>p</i> -nitrophenyl β -D-glucuronide
pNPIdoA:	<i>p</i> -nitrophenyl α -L-iduronide
TEMPO:	2,2,6,6-tetramethyl-1-piperidinyloxy
TIC:	total ion chromatogram
TLC:	thin layer chromatography

Amino acid abbreviations

Ala	(A)	Alanine
Arg	(R)	Arginine
Asn	(N)	Asparagine
Asp	(D)	Aspartic acid
Cys	(C)	Cysteine
Glu	(E)	Glutamic acid
Gln	(Q)	Glutamine
Gly	(G)	Glycine
His	(H)	Histidine
Ile	(I)	Isoleucine
Leu	(L)	Leucine
Lys	(K)	Lysine
Met	(M)	Methionine
Phe	(F)	Phenylalanine
Pro	(P)	Proline
Ser	(S)	Serine
Thr	(T)	Threonine
Trp	(W)	Tryptophan
Tyr	(Y)	Tyrosine
Val	(V)	Valine

Acknowledgments

I would like to thank a number of people whose help was invaluable during the course of my research at UBC. First of all, I would like to thank my supervisors Dr. Steve Withers and Dr. Michael Adam, for their advice, encouragement, and, most of all, patience. Secondly, the technical assistance of Ms. Karen Rupitz and Mr. Shouming He was greatly appreciated. My thanks to Mr. Jeffrey Grubb and Dr. William Sly of the E.A. Doisy Department of Biochemistry and Molecular Biology, St. Louis University School of Medicine, St. Louis, Missouri, USA for providing human β -glucuronidase, and to Dr. Lorne Clarke of the British Columbia Research Institute for Children's and Women's Health, Vancouver, Canada for providing human α -L-iduronidase and glucocerebrosidase. A special thanks to all members of the Withers group, past and present, for their friendships and help during my stay at UBC. My thanks to the Medical Research Council of Canada for providing me with a studentship and to the Department of Chemistry, University of British Columbia for providing me with a Gladys Estella Laird Research Fellowship.

On a more personal note, I would like to thank my parents for all the love and support they've given and continue to provide over the years. I only hope that I've come close to meeting your expectations. To my brother John – what can I say to the biggest Leck Doy around? This Oogleemba salutes you! To all my friends – thanks for being there for me all these years, especially during my stay here at UBC. Last, and certainly not least, to

my dearest Naoko I reserve my most heartfelt gratitude. Your love and laughter has brought renewed joy to my life.

For Naoko

And for my family

Chapter 1 General Introduction

1.1 Classification of glycosidases

Glycosidases, or glycoside hydrolases, constitute a large family of enzymes that catalyze the hydrolysis of glycosidic linkages by the cleavage of the C-O bond between a sugar and an aglycone (which may be a second sugar, or another group). These glycoside substrates are composed of two structural units: the sugar glycone, which is bound in the catalytic site of the enzyme; and the aglycone, which is bound in an adjacent subsite. Although the glycone in many natural substrates is another sugar residue, many glycosidases exhibit liberal aglycone specificity, catalyzing the cleavage of a variety of anomeric substituents, including C-O-aryl, C-S, C-N, and C-F bonds. Interest in these enzymes is fuelled by their applications in industry, e.g. invertase for the production of 'invert' sugar, cellulases for the degradation of cellulosic biomass, xylanases in pulp-and-paper production; and by their relevance to cancer metastasis, influenza, AIDS and other viral diseases, diabetes, and lysosomal storage disorders.

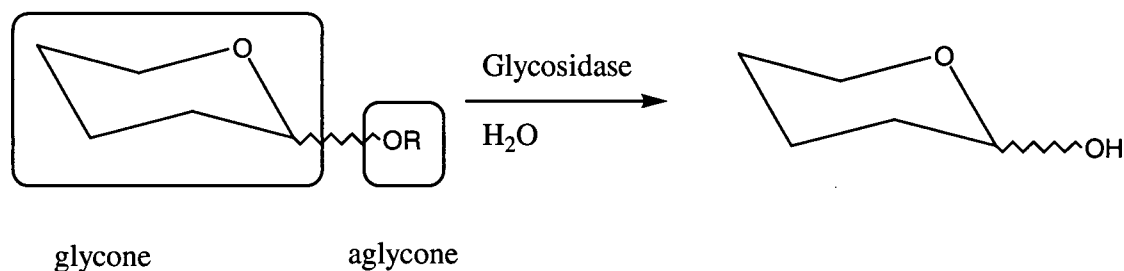


Figure 1.1: Reaction normally catalyzed by a glycosidase.

Glycosidases may be divided into smaller subgroups according to:

1) Anomeric configuration (α or β) of the substrate. In general, a β -glucosidase will catalyze the hydrolysis of β -glucosides but not of α -glucosides, while an α -glucosidase is specific for α -glucosides.

2) Glycone specificity. A particular glycosidase usually exhibits maximal activity with a specific glycone, and is generally classified according to the glycone against which it is most active. An α -glucosidase, for example, is most active against α -glucosides, but other α -glycosides may be substrates as well.

3) Stereochemical outcome of the reaction. A glycosidase is termed “inverting” or “retaining” depending on the relative anomeric configurations of the substrate and of the product initially released from the enzyme. Hydrolysis catalyzed by a retaining glycosidase leads to the formation of a product with the same initial anomeric configuration as the substrate, while hydrolysis via an inverting enzyme gives a product of the opposite anomeric configuration to that of the substrate.

These different stereochemical outcomes reflect the existence of two distinct mechanistic classes of glycosidases – inverting and retaining. Inverting glycosidases operate via a direct displacement of the leaving group with water, while retaining glycosidases utilize a double-displacement mechanism involving a glycosyl-enzyme intermediate. Despite

these differences, it is noteworthy that both classes employ a pair of carboxylic acids in the active site. With inverting enzymes, one residue acts as a general acid and the other acts as a general base, whereas with retaining glycosidases one functions as a general acid and a general base while the other acts as a nucleophile and a leaving group.

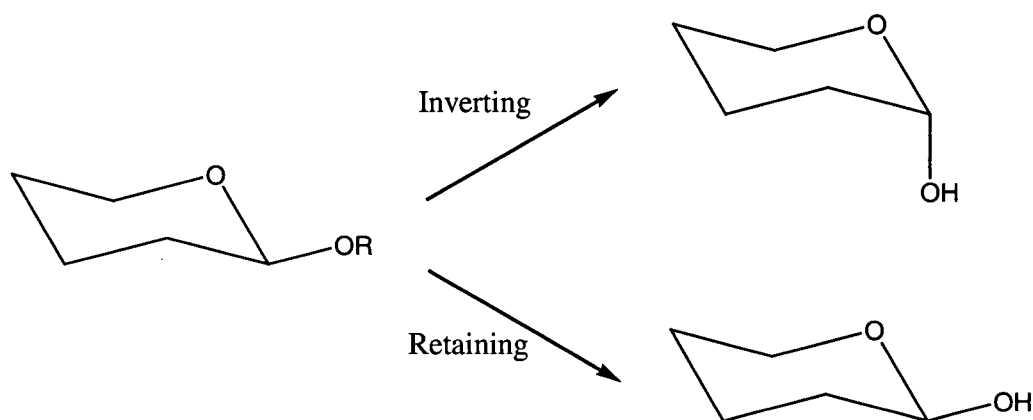


Figure 1.2: Possible stereochemical outcome of glycosidase-catalyzed hydrolyses of glycosides.

In addition to the general criteria listed above, it is possible to group enzymes together into families based on sequence similarities.¹⁻⁵ To date, over 3000 glycosidases have been categorized into 85 families (see the web-site <http://afmb.cnrs-mrs.fr/~pedro/CAZY/db.html>). Members within the same family have the same three-dimensional fold. Additionally, since the overall fold is more conserved than their primary sequence it turns out that several families have similar folds even though this is not evident from the sequence and these families have been assigned to clans on this basis. This similarity has proven useful in helping to identify the residues responsible for

specificity and catalysis since once a structural motif is established for one member of the family, comparisons can be made to other enzymes within the group whose structures have not yet been solved.

1.2 The catalytic mechanism of retaining glycosidases

A general mechanism for retaining glycosidases, which are the focus of this study, was first proposed by Koshland in 1953.⁶ The first step involves displacement of the aglycone by an appropriately positioned carboxylate nucleophile in the active site to form a glycosyl-enzyme intermediate (the 'glycosylation' step). In a second step, the intermediate is hydrolyzed to yield a product with the same anomeric configuration as the starting substrate (the deglycosylation step). Both the formation and the hydrolysis of the glycosyl-enzyme intermediate occur via oxocarbenium ion-like transition states. Cleavage of the C-O bond in this model is assisted by general acid catalysis from an appropriately positioned carboxylic acid residue while hydrolysis of the intermediate likely occurs with general base catalysis by the same residue.

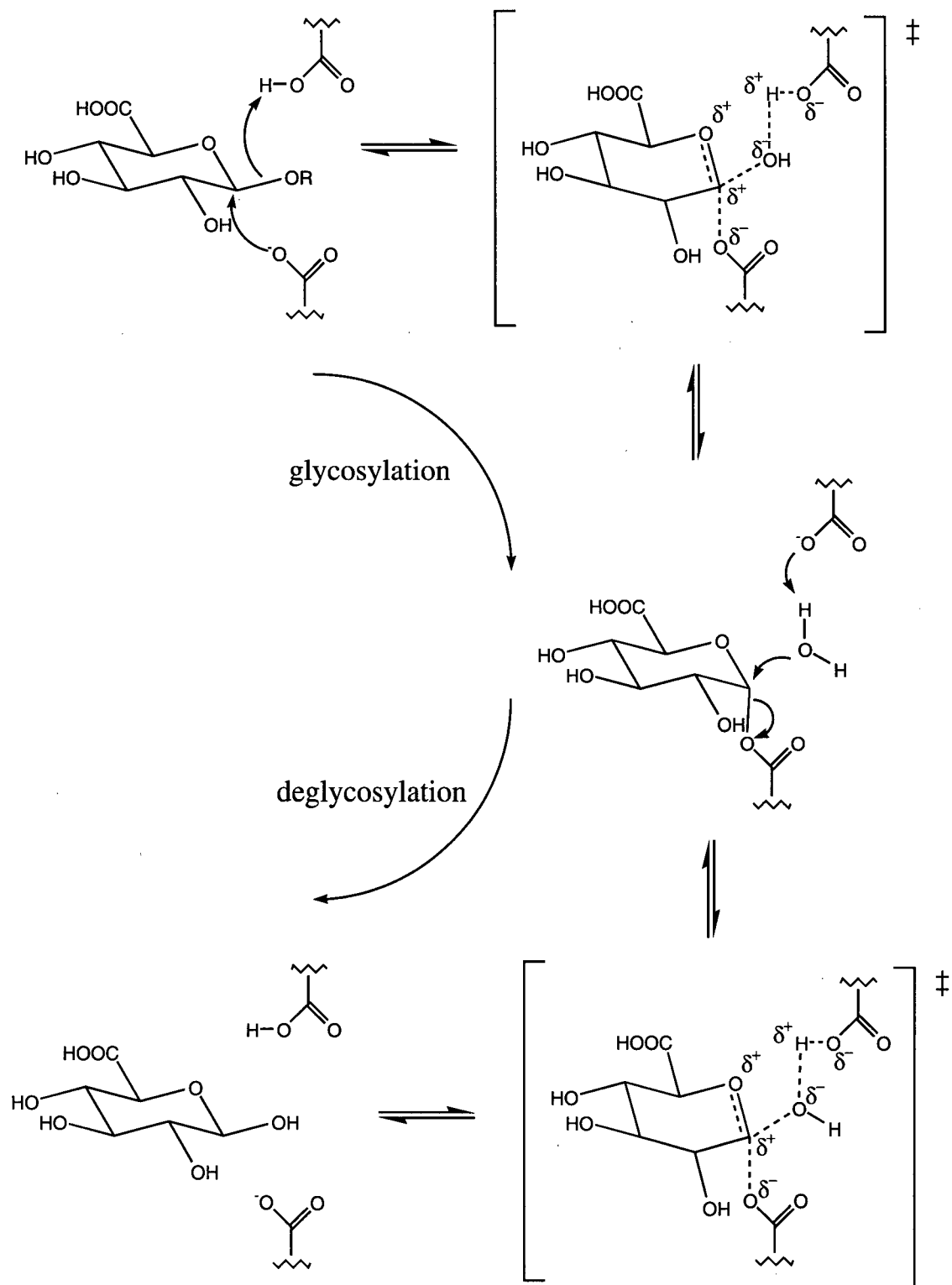


Figure 1.3: Presumed mechanism of a retaining glycosidase.

1.3 Evidence for a double displacement mechanism in retaining glycosidases

1.3.1 Presence of active site carboxylates

X-ray crystallographic studies have invariably revealed the presence of glutamic or aspartic acid residues in the active sites of glycosidases. Active site carboxylic acids have been identified, for example, in the retaining β -glycosidases *Cellulomonas fimi* exoglycanase, *E. coli* β -galactosidase, and human β -glucuronidase.⁷⁻⁹ More compelling evidence derives from X-ray crystal structures of glycosidases co-crystallized with either inhibitors or substrates in the active site.¹⁰⁻¹² While the residues important to catalysis are often apparent in such structures and the identities of the residues in close spatial proximity to the substrate or inhibitor are known, their specific roles in catalysis frequently cannot be predicted with certainty from X-ray structural data alone. Other evidence for active site carboxylates is derived from labeling and mutagenesis studies, and will be discussed later.

1.3.2 Nature of the glycosyl-enzyme intermediate

1.3.2.1 Kinetic studies

The double displacement mechanism for retaining glycosidases initially proposed by Koshland described the formation of a *covalent* glycosyl-enzyme intermediate. Indeed,

low temperature and rapid-quench studies with radiolabelled versions of natural substrates have resulted in the trapping of covalent glycosyl-enzyme intermediates in porcine pancreatic α -amylase and in *Streptococcus sobrinus* α -glucosyltransferase.^{13,14} However, it has been suggested, based on X-ray structural studies with hen egg white lysozyme, that a negatively charged active site carboxylate (Asp52) could stabilize a positively charged oxocarbenium ion intermediate sufficiently to allow diffusion of the leaving group out of the active site and attack of this ion-pair by a glycosyl acceptor (water or another sugar). While ion-pair intermediates are still regularly evoked, particularly for lysozyme, there is considerable evidence that favours the existence of a covalent glycosyl-enzyme intermediate for many retaining glycosidases.

Strong evidence for the covalent nature of a glycosyl-enzyme intermediate is derived from α -secondary deuterium kinetic isotope effect measurements with substrates (deuterated at C-1) for which deglycosylation is rate-limiting. Isotope effects for the deglycosylation step of $k_H/k_D = 1.20$ - 1.25 have been determined for *E. coli* (lac Z) β -galactosidase, and $k_H/k_D = 1.10$ - 1.12 for *Agrobacterium* sp. β -glucosidase.^{15,16} These large, positive kinetic isotope effects reflect sp^3 to sp^2 rehybridization at the anomeric centre as the reaction proceeds from a ground state glycosyl-enzyme intermediate to the transition state of the deglycosylation step. This strongly implies that the intermediate has considerably more sp^3 character than the subsequent transition state, consistent with a covalent glycosyl-enzyme that is hydrolyzed *via* a transition state with significant oxocarbenium ion character. If the intermediate were truly an ion pair, an inverse kinetic isotope effect would be expected.

As well, spontaneous (non-enzymatic) hydrolysis studies of various glycosides indicate that glycosyl cations are very unstable species with extremely brief lifetimes (estimated to be 10^{-10} to 10^{-12} s in aqueous solution) while the lifetimes of covalent glycosyl-enzymes at ambient temperatures are 1 to 100 ms.¹⁷⁻¹⁹ Thus, an unstable ion-pair would seem unlikely to exist long enough, even within an extremely favourable enzyme active site microenvironment, to allow diffusion of the leaving group out of the active site and attack by water prior to collapse to a covalent species.²⁰

1.3.2.2 Oxocarbenium ion-like transition states

Kinetic isotope effect studies provide evidence for oxocarbenium ion-like transition states associated with both the glycosylation and deglycosylation steps of glycosidase-catalyzed hydrolysis. By selection of appropriate aglycones, it is possible to obtain substrates for which either step is rate-limiting, and the isotope effect on each step may then be determined. The *E. coli* (lac Z) β -galactosidase-catalyzed hydrolysis of β -galactosyl pyridinium salts exhibited α -secondary deuterium kinetic isotope effects of $k_H/k_D = 1.15$ - 1.20 , indicating substantial sp^2 character in the transition state for formation of the galactosyl-enzyme since glycosylation is rate-limiting for these substrates.²¹ Even larger isotope effects are reported for this enzyme when deglycosylation is rate-limiting, with $k_H/k_D = 1.20$ - 1.25 for 2,4-dinitrophenyl β -galactosides.²⁰ Similar results were obtained

with *Agrobacterium* sp. β -glucosidase, with k_H/k_D values for the glycosylation and deglycosylation steps of $k_H/k_D = 1.06$ and $k_H/k_D = 1.11$, respectively.¹⁶

Glycosidases are strongly inhibited by compounds that appear to mimic a glycosyl oxocarbenium ion in conformation or charge, presumably functioning as transition state analogues. In a glycosyl oxocarbenium ion, in contrast to a ground state glucoside, C-1 and O-5 share a full positive charge, while C-1, C-2, C-5, and O-5 are required to be planar.²² To fulfill these requirements, the glycosyl oxocarbenium ion may theoretically adopt either a half-chair (4H_3 or 3H_4), or a boat ($^{2,5}B$ or $B_{2,5}$) conformation.

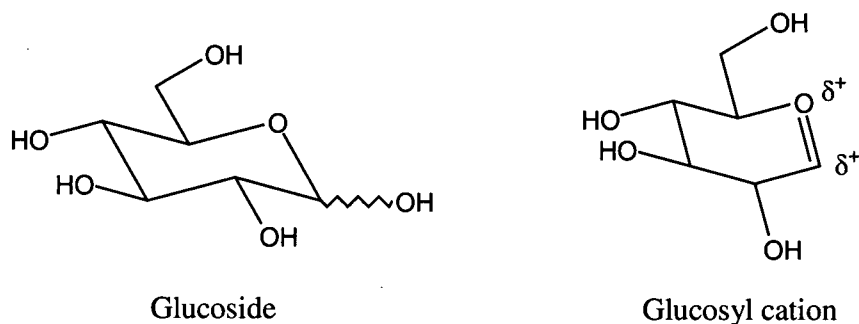


Figure 1.4: Comparison of a ground state glucoside and a transition state glucosyl oxocarbenium ion.

Putative transition state analogues include aldonolactones and aldonolactams that resemble the glycosyl oxocarbenium ion both in geometry, and to some extent, in charge. Their half-chair like geometry and resonance charge distribution closely resemble that of

the oxocarbenium ion. K_i values for these compounds are often 10^2 to 10^4 -fold lower than K_i values for the corresponding glycosides.²³

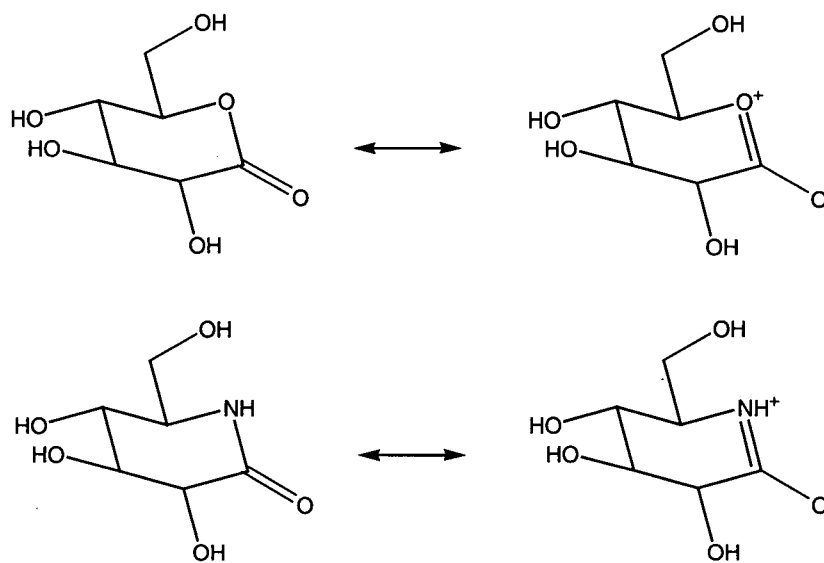


Figure 1.5: Resonance structures of aldonolactones (top) and aldonolactams (bottom).

Other potent glycosidase inhibitors include the amino sugar nojirimycin and its various analogues. Such compounds may bind up to 10^4 -fold tighter than the corresponding ground state analogues.²³ K_i values of these inhibitors with the corresponding glycosidases are typically in the micro- or submicromolar range. The K_i values of nojirimycin, galactonojirimycin, and mannonojirimycin with *Aspergillus wentii* β -glucosidase, *E. coli* β -galactosidase, and Jack bean α -mannosidase are 0.36, 0.045, and 1.2 μ M, respectively. Nojirimycins are presumed to resemble a glycosyl oxocarbenium ion in geometry and charge. Upon protonation, nojirimycin is isoelectronic with a glucosyl oxocarbenium ion; the dehydrated form would appear to be nearly isosteric as

well. However, for such inhibitors to be true transition state analogues, their inhibitory efficiencies should correlate with the glycone specificities of the corresponding substrates.^{24,25} This is not always the case, and tight binding may result from fortuitous interactions between the inhibitors and residues in the enzyme active site. However, a correlation has indeed been shown between a class of transition state analogues, the nojiritetrazoles, and a series of glycosidases.²⁶

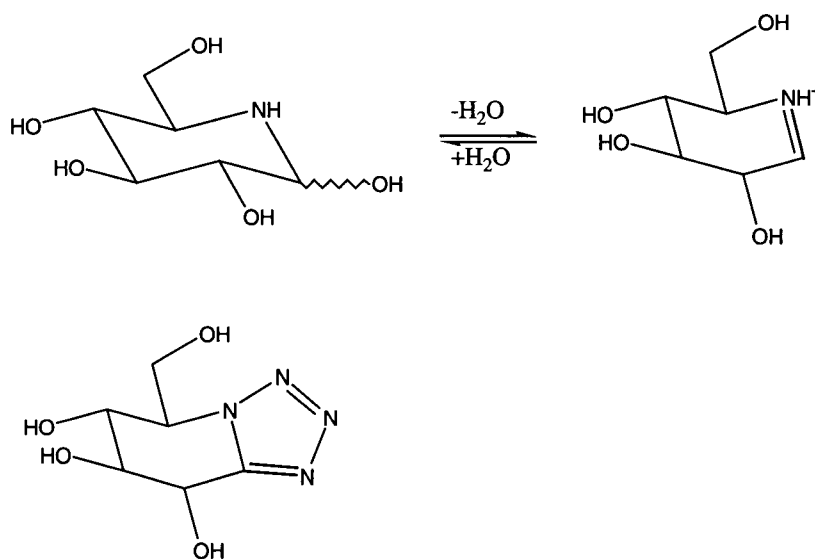


Figure 1.6: Nojirimycin in both hydrated and dehydrated forms (top), and nojiritetrazole (bottom).

1.4 Glycosidase inhibitors and covalent labeling of active site residues

1.4.1 Affinity labels

Affinity labels consist of a reactive functional group that can react with certain residues on the enzyme and a sugar moiety that provides affinity for the active site. Since the functional group of the molecule can react with a number of amino acids on the enzyme, the results of affinity labeling must be interpreted with caution as a specific means of identifying catalytic residues. However, in selected cases, these compounds have proven useful in the labeling of the acid/base catalyst.

Common affinity labels for β -glycosidases include glycosyl epoxides, *N*-bromoacetyl-glycosylamines and glycosyl isothiocyanates.

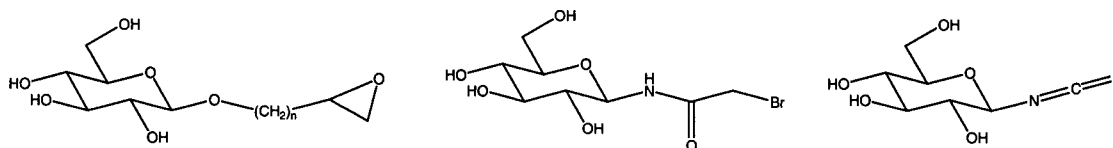


Figure 1.7: Affinity labels of glycosidases: glycosyl epoxide, *N*-bromoacetyl glycosylamine, and glycosyl isothiocyanate.

The main drawback of the O-linked affinity labels is their susceptibility to enzyme-catalyzed hydrolysis while the N-linked labels have the advantage of being inert in this respect. Examples where affinity labels have proven successful in determining the identity of the acid/base catalyst include the labeling of Glu127 from *Cellulomonas fimi* β -(1,4)-glucanase with *N*-bromoacetyl- β -D-cellobiosylamine, and the labeling of Glu198 from Cassava β -glucosidase with *N*-bromoacetyl- β -D-glucosylamine.^{27,28} The variety of affinity labels available for α -glycosidases is more limited. One example of a

successful α -configured affinity label is 1,2-epoxy-3-(α -D-glucopyranosyl)propane which was shown to be an effective inactivator of two α -glucosyltransferases from *Streptococcus mutans*.²⁹ Another example is the bromo-ketone α -C-mannoside that was used to target the acid/base catalyst of α -glucosidase from *Saccharomyces cerevisiae*.³⁰ In this case, it was possible to use the manno configuration of the label as the enzyme has a similar binding affinity for mannosides and glucosides.

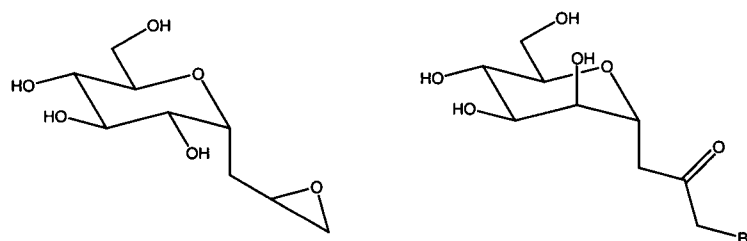


Figure 1.8: Affinity labels of glycosidases: C-glycosyl epoxide and C-glycosyl bromoketone.

1.4.2 Conduritol epoxides

The conduritol epoxides are a related class of inhibitors that incorporates an endocyclic epoxide within a cyclitol ring, this structure resembling the sugar ring of the natural substrate. A number of these epoxides, with structures corresponding to those of the substrates of a range of glycosidases, have been synthesized, e.g. conduritol B epoxide is the *gluco* analogue. The mechanism of inactivation is similar to that of the epoxyalkyl glycosides, with protonation of the epoxide and attack by an enzymic nucleophile leading to formation of a covalent adduct. These inactivators are likely to be more specific since

nucleophilic attack of the endocyclic epoxide occurs at a centre analogous to the anomeric centre of the substrate. A wide range of glycosidases has been successfully inactivated by these compounds.²³ These have also been used *in vivo* to inactivate glucocerebrosidase in mice, providing a possible animal model for Gaucher disease.³¹

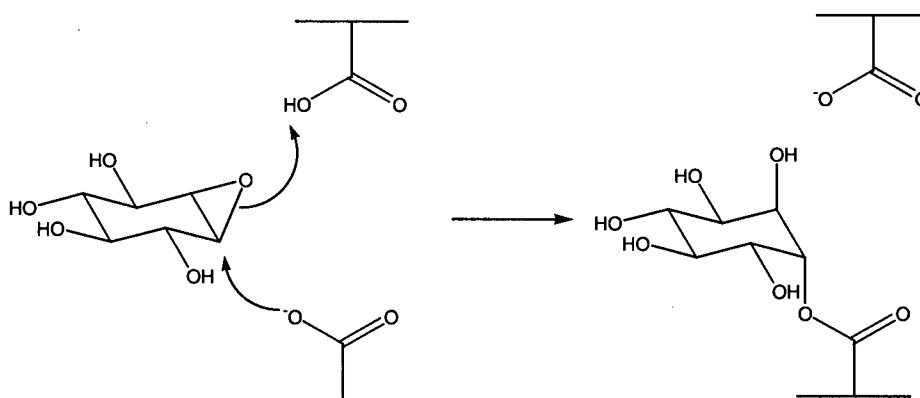


Figure 1.9: Reaction of conduritol B epoxide with a β -glucosidase. The residues involved in protonation and nucleophilic attack may not necessarily be the catalytic residues in the normal mechanism.

Since rotation of the molecule by 180° about an axis bisecting the epoxide ring places the epoxide and all the hydroxyls in the correct orientations to mimic an α -glucoside, conduritol B epoxide is an effective inactivator of both β - and α -glucosidases. With β -glucosidases, attack of the catalytic nucleophile from the α -face of the cyclitol ring would give products with the favoured *trans*-diaxial stereochemistry, while with α -glucosidases, attack of this catalytic residue from the β -face would produce the less favoured *trans*-diequatorial products. Indeed, β -glycosidases are more effectively

inactivated by these compounds than are α -glycosidases.²³ However, conduritol epoxides have shown an unfortunate propensity to specifically, but 'incorrectly', label active site residues *other* than the normal catalytic nucleophiles, on occasion leading to incorrect assignment of the catalytic nucleophile. For example, inactivation of *E. coli* β -galactosidase with the appropriate conduritol epoxide resulted in labelling of Glu461.³² Subsequent mutagenesis studies revealed that the glycine mutant modified at this position displayed a significant level of activity inconsistent with removal of the catalytic nucleophile, suggesting that this epoxide had originally labeled another residue in the active site. Re-investigation of this enzyme using another class of inactivators, the 2-deoxy-2-fluoro glycosides, resulted in the identification of the actual nucleophile, Glu537.^{33,34} Mutations of this residue exhibited the expected kinetic behaviour. The absence of the C-6 hydroxymethylene substituent in conduritol epoxides present in the sugar substrates likely accounts for the 'incorrect' labeling observed, by permitting alternative binding modes in the enzyme active site, and subsequent reactions with other residues.

1.4.3 2-Fluoro glycosides

The 2-deoxy-2-fluoro- β -D-glycosides have proven to be extremely useful in the labelling of the catalytic nucleophiles of β -retaining glycosidases, thus providing evidence for the existence of a covalent glycosyl-enzyme intermediate. The presence of the electronegative fluorine at C-2 destabilizes the oxocarbenium ion-like transition states of

both glycosylation and deglycosylation steps, thereby slowing both the formation and the hydrolysis of the intermediate. The replacement of the C-2 hydroxyl also results in the disruption of important hydrogen bonding interactions that stabilize the transition state. Together, this results in a decrease of 10^5 to 10^8 fold in the rates of both glycosylation and deglycosylation. However, the presence of a good leaving group (typically fluoride or 2,4-dinitrophenolate) helps to accelerate the glycosylation step, leading to the accumulation of the intermediate and inactivation of the enzyme. This trapped intermediate is catalytically competent and can be turned over in the presence of a suitable acceptor to give fully active enzyme. This strategy has been used successfully to identify the catalytic nucleophiles for many glycosidases.³⁵

The first nucleophile to be identified in this manner was Glu358 of *Agrobacterium* sp. β -glucosidase (Abg).³⁶ The reaction of Abg with 2,4-dinitrophenyl-2-deoxy-2-fluoro- β -D-glucopyranoside resulted in a glycosyl-enzyme intermediate whose half-life was over 500 hours. This extended lifetime allowed for the intermediate's covalent nature to be proven by ^{19}F NMR.³⁷

The long-lived nature of the 2-deoxy-2-fluoro glycosyl enzyme intermediates has proven useful for crystallographic studies of the inactivator bound at the enzyme active site. Examples include the retaining β -1,4 glycanase from *Cellulomonas fimi* (Cex) co-crystallized in the presence of DNP-2-deoxy-2-fluoro-cellobioside and the retaining xylanase from *B. circulans* co-crystallized in the presence of DNP-2-deoxy-2-fluoro-xylobioside.^{10,12}

Although the 2-fluoro sugars have worked very well for retaining β -glycosidases, they have been less successful for retaining α -glycosidases. For example, 2-deoxy-2-fluoro- α -maltosyl fluoride was found to act as a slow substrate for human pancreatic α -amylase.³⁸ Furthermore, substitution of a C-2 hydroxyl with fluorine is not possible for those enzymes whose substrates do not possess such a hydroxyl group, e.g. *N*-acetylhexosaminidase. A solution to these problems lay in the development of the 5-fluoro glycosyl fluorides.

1.4.4 5-Fluoro glycosyl fluorides

The 5-fluoro glycosyl fluorides have been shown to be a useful alternative to their 2-deoxy-2-fluoro counterparts. Having a fluorine atom at C-5 in a pyranose ring is analogous to its being at C-2, as they are both adjacent to centres of developing positive charge. In the case of the 5-fluoro compound, the electron withdrawing fluorine is adjacent to the developing positive charge of the ring oxygen while in the corresponding 2-deoxy-2-fluoro case, the fluorine is closest to the developing charge at C-1. It has been suggested through modelling studies that the greatest difference in partial charge between the ground state and the developing transition state actually occurs at O-5 rather than at C-1. Therefore, substitution of fluorine at C-5 rather than at C-2 would serve to inductively destabilize the transition state to a greater extent. This is further magnified since the fluorine atom at C-5 replaces a hydrogen atom while that at C-2 replaces a significantly electronegative oxygen atom. Thus, on electronic grounds, 5-fluoro

glycosides might prove more advantageous than 2-deoxy-2-fluoro glycosides in trapping a glycosyl-enzyme intermediate. In addition, some of the reduction in the rates of glycosylation and deglycosylation with 2-deoxy-2-fluoro glycosides presumably results from the disruption in binding interactions as a consequence of the replacement of the C-2 hydroxyl group. Substitution of the hydrogen at C-5 with a relatively small fluorine atom might be expected to result in less severe disruptions in binding affinity as the C-2 hydroxyl group is unaltered. Hence, for a given enzyme, the degree to which the glycosyl-enzyme intermediate will accumulate depends on the relative importance of how a particular substitution affects the transition state binding affinity versus the charge development at the transition state.

The utility of the 5-fluoro strategy toward retaining β -glycosidases was first demonstrated using the two 5-fluoro epimers, 5-fluoro- β -D-glucosyl fluoride and 5-fluoro- α -L-idosyl fluoride, as inhibitors for *Agrobacterium* sp. β -glucosidase.³⁹ Incubation of either epimer with Abg resulted in a time-dependent inactivation of the enzyme. This inactivation was shown to be active site-directed as protection from inactivation was provided by appropriate inhibitors known to bind at the active site. As with the 2-fluoro-glycosyl-enzyme intermediates, the 5-fluoro glycosyl-enzyme intermediates are catalytically competent. Mass spectral analysis of the protein incubated with either inactivator (both intact and proteolytically digested) demonstrated the attachment of a 5-fluoro glycosyl moiety on Glu358, the catalytic nucleophile.

The 5-fluoro approach proved useful in the identification of the catalytic nucleophiles of several retaining α -glycosidases which had not previously been labelled with 2-deoxy-2-fluoro glycosides. Examples include yeast α -glucosidase and jack bean α -mannosidase.^{40,41}

1.5 Lysosomal storage disorders

The lysosomal storage disorders comprise a group of more than 30 different diseases.⁴² The common feature of these diseases is the deficiency of a lysosomal protein that is part of a catabolic pathway. These proteins are mainly exoglycosidases whose dysfunctions result in the cessation of the stepwise breakdown of glycosaminoglycans, glycolipids and sphingolipids. The accumulation of these undegraded molecules leads to an increase in size and number of lysosomes, severely disrupting normal cellular turnover functions. Examples of lysosomal disorders include Gaucher disease, Sly syndrome and Hurler Scheie syndrome.

Because of their clinical significance, interest in the lysosomal glycosidases is widespread. One such enzyme, glucocerebrosidase, the deficiency of which causes Gaucher disease, is currently used to treat patients with Type 1 Gaucher disease by enzyme replacement therapy. The efficacy and mode of administration of this treatment is still in question and a technique to monitor *in vivo* localization of the protein would be of great benefit.

Two of the storage disorders, Sly syndrome and Hurler Scheie syndrome, are caused by a deficiency in a particular class of glycosidase, the glucuronidases. The substrates for these enzymes are glycopyranosides whose C-6 hydroxymethylene group is oxidized to the carboxylic acid.

1.6 Aims of this thesis

The aims of this thesis are two-fold:

1. The synthesis of new fluoro-sugar inactivators for the study of glucuronidases.
This would expand the repertoire of inactivators currently available for the mechanistic study of glycosidases.
2. The development of a radiolabel for use as a positron emission tomography imaging agent. This would allow for real-time observation of the *in vivo* localization of administered enzyme in patients undergoing enzyme replacement therapy.

Chapter 2 Fluoro-Sugar Inhibitors of Glycuronidases

2.1 Introduction

2.1.1 Fluoro-glycosides – Good inhibitors of glycosidases

As previously mentioned, the 2-deoxy-2-fluoro-glycosides and 5-fluoro-glycosides were developed as specific mechanism-based inactivators of retaining glycosidases. Both classes function by the same mechanism, the fluorine substituent serving to inductively destabilize the oxocarbenium ion-like transition states for both the formation and the hydrolysis of the glycosyl-enzyme intermediate, thereby slowing *both* steps. The presence of a good leaving group (typically fluoride) at the anomeric centre accelerates the first step, thereby ensuring that the intermediate is kinetically accessible, thus that it accumulates.

The first fluoro-sugar inhibitors to be developed were the 2-deoxy-2-fluoro-glycosides.⁴³ Since their development, the β -D-glycosides of this type have proven to be extremely useful in the labelling and identification of the catalytic nucleophiles of various β -retaining glycosidases.³⁵ However, the 2-deoxy-2-fluoro- α -D-glycosides have not proven useful as inactivators of α -retaining glycosidases, acting instead as slow substrates for which glycosylation is rate-limiting. This problem was circumvented by the introduction of the 5-fluoro-glycosides.³⁹ Instead of replacing the C-2 hydroxyl group with a fluorine atom, these inactivators are obtained by the conservative replacement of the C-5 hydrogen atom with a fluorine atom. Interestingly, the epimers of C-5 have turned out to be effective inactivators also. Their usefulness was demonstrated

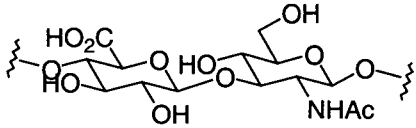
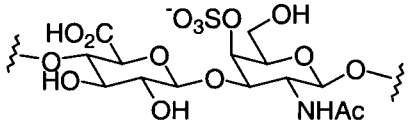
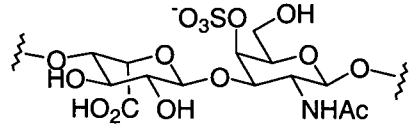
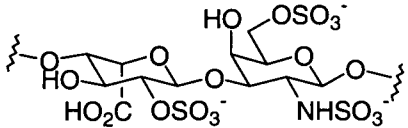
in the case of jack bean α -mannosidase, where the 5-fluoro- β -L-gulosyl fluoride was used to inactivate the enzyme but the 2-deoxy-2-fluoro- α -D-mannosyl fluoride failed to do so.^{41,43}

While a number of 2-deoxy-2-fluoro- and 5-fluoro-glycopyranosyl fluorides have been made, no uronic acid versions of these inactivators have been synthesized to date. Such molecules would be useful tools in the mechanistic studies of glycuronidases such as human β -D-glucuronidase and human α -L-iduronidase, enzymes whose deficiencies lead to the lysosomal storage disorders Sly syndrome and Hurler-Scheie syndrome, respectively.

2.1.2 Glycuronidases - Background

Glycuronic acids are those sugars in which the C-6 OH has been oxidized to a carboxylic acid. They are usually found as one of the two alternating monosaccharides of glycosaminoglycans (GAGs), the other saccharide being a N-acetylhexosamine. The enzymes that cleave these uronic acids thus play an important role in the biological turnover process. The two classes of glycosidases responsible are the glucuronidases and the iduronidases. In this study the action of the various fluorosugar-inhibitors synthesized on the human lysosomal enzymes β -glucuronidase and α -L-iduronidase along with *E. coli* β -glucuronidase were studied.

Table 2.1: The repeating disaccharide units of the glycosaminoglycan substrates of human β -glucuronidase and human α -L-iduronidase⁴⁴

 <p>hyaluronic acid</p>	 <p>chondroitin-4-sulphate</p>
 <p>dermatan sulphate</p>	 <p>heparin</p>

2.1.2.1 Human β -glucuronidase

Human β -glucuronidase (HBG, EC# 3.2.1.31) is a lysosomal exoglycosidase that cleaves β -D-glucuronic acid residues from the non-reducing termini of glycosaminoglycans such as chondroitin sulphate and hyaluronic acid, and is an essential enzyme for the normal restructuring and turnover of these extracellular matrix components (see Table 2.1).⁴⁵ As mentioned earlier, these GAGs are composed of alternating glucuronic acid and *N*-acetyl-glycosamine residues. The latter residues may be either *N*-acetyl-glucosamine or *N*-acetyl-galactosamine, and may be sulfated.

Mutations in the β -glucuronidase gene result in the human lysosomal storage disease mucopolysaccharidosis type VII (MPS VII) or Sly Syndrome.⁴⁶⁻⁴⁹ Patients suffering from this disease exhibit a wide variety of symptoms, including skeletal dysplasias,

hepatosplenomegaly, and moderate mental retardation.⁴² Currently, there is no treatment available although studies using enzyme replacement therapy with animals is currently underway. Such therapies entail the administration of the appropriate recombinant protein to the patient in order to replace the enzyme they are lacking.

HBG exists in its native state as a homotetramer of MW 332,000 Da, the monomer consisting of 651 amino acids. It is a member of the sequence-related glycosyl hydrolase family 2 that includes β -glucuronidases, β -galactosidases and β -mannosidases.¹ Enzymes in this family hydrolyze their substrates with net retention of anomeric configuration, presumably via the double displacement mechanism previously mentioned.⁵⁰

The three-dimensional structure of HBG is one of two that have been solved for Family 2 β -glycosidases, the other being that of *Escherichia coli* lacZ β -galactosidase (EBGal).^{8,9} The two enzymes have a similar multidomain structure each possessing a jelly roll barrel, an immunoglobulin constant domain, and a TIM barrel. The active sites, however, are significantly different since EBGal is a metalloenzyme, binding Mg^{2+} at the active site, while HBG does not. Removal of this metal ion severely reduces activity on most substrates. The role of this metal ion is unclear, one suggestion being that it acts as an electrophilic catalyst, interacting directly with the departing phenolate.⁵⁰ Alternatively, it may function to correctly position the acid/base catalyst. Importantly, HBG shows no metal ion dependence and no metal ion is found in the X-ray crystal structure. In this case it appears that Glu451 functions as the acid/base catalyst. The equivalent residue in

EBGal (Glu461) was previously suggested to play the role of the acid/base catalyst on the basis of affinity labelling studies and kinetic analyses of mutants.^{33,51-53} Both residues are on the C-terminal side of a conserved asparagine which has been shown in other enzymes of clan GH-A to hydrogen bond to the 2-hydroxyl group of the sugar substrate.⁵⁴ The catalytic nucleophile of EBGal was identified as Glu537 by trapping of a glycosyl-enzyme intermediate and sequencing of the labelled peptide. Based on the above information and amino acid sequence similarity, Glu540 has been suggested to be the catalytic nucleophile of HBG. However, another residue (Asp207) has been proposed as an alternative candidate based upon its position in the active site.⁹ Thus, confirmation of the identity of this important residue is necessary.

2.1.2.2 *E. coli* β -glucuronidase

E. coli β -glucuronidase (EBG, EC# 3.2.1.31) is also a member of the Family 2 of β -glycosidases. Similar to HBG, the enzyme is tetrameric, with a monomeric molecular weight of 68200 Da and a length of 603 amino acids.⁵⁵ The natural habitat of *E. coli* is the mammalian gut, where numerous glucuronic acid conjugates of endogenous and xenobiotic compounds can be found. In mammals, glucuronidation is a principal means of detoxifying or inactivating compounds. *E. coli*'s β -glucuronidase cleaves glucuronic acid from these conjugates, enabling the organism to use the sugar as its sole carbon source. In general, the aglycone is not used and passes back across the bacterial membrane into the gut and is reabsorbed into the bloodstream. This back-and-forth cycling of compounds via glucuronidation in the liver and deglucuronidation in the gut is termed enterohepatic circulation. Because of this important phenomenon, many

compounds are not eliminated from the body all at once; rather, their levels in the bloodstream oscillate. *E. coli* is one of the only bacterial species known to have glucuronidase activity. Indeed, the presence of EBG activity is a widely accepted diagnostic test for *E. coli* in natural populations of bacteria isolated from sources such as urine, feces, and contaminated water or food.^{56,57}

The enzyme is quite robust, having a pH range of 5.0-7.8. EBG has no cofactors or ionic requirements and is known to be inhibited by some divalent metal ions: 70% inhibition by Mn^{2+} and Ca^{2+} at 10 mM, and complete inhibition by Cu^{2+} and Zn^{2+} at comparable concentrations. EBG catalyzes the hydrolysis of a wide range of β -D-glucuronides, and some β -D-galacturonides as well, but will not cleave other glycosides, such as α - or β -glycoside substrate types. On the basis of amino acid sequence similarities, Glu504 has been suggested to be the catalytic nucleophile of EBG.

EBG holds an important place in research by virtue of its use as a reporter enzyme for plant genetic research. This is due to the fact that glucuronidase activity is largely if not completely absent from higher plants, mosses, algae and ferns. In our hands, it proved to be a useful enzyme in the study of the various fluoroglycoside inhibitors synthesized.

2.1.2.3 Human α -L-iduronidase

Human α -L-iduronidase (IDUA, EC# 3.2.1.76) is a lysosomal exoglycosidase that cleaves α -L-iduronic acid residues from the non-reducing termini of glycosaminoglycans (GAGs) such as dermatan sulphate and heparin, and is an essential enzyme for the normal

restructuring and turnover of these extracellular matrix components (see Table 2.1). The mature enzyme consists of 627 amino acids with a molecular weight of 74 kDa and has been assigned to the family 39 of glycosidases.⁵⁸

Mutations in the α -L-iduronidase gene result in the human lysosomal storage disease mucopolysaccharidosis type I (MPS I).⁴² There is a wide variation in clinical phenotypes observed in this disease. Patients with the mildest form, Scheie syndrome, exhibit very little or no neurologic involvement, have mild hepatosplenomegaly, joint stiffness and deformities, and may have a normal lifespan. At the other end of the spectrum, patients with the severest form – known as Hurler syndrome – exhibit hepatosplenomegaly, skeletal dysplasias, corneal clouding, short stature and mental retardation. Intermediate phenotypes have been termed Hurler/Scheie Syndrome.

Currently, the only medical treatment for the disease is bone marrow transplantation. However, research into using recombinant IDUA for enzyme replacement therapy, initially with dogs and more recently in humans, has shown that this form of therapy can improve patient health.⁵⁹⁻⁶¹

Although much is known about the genetic and clinical aspects of iduronidase, little is known about the mechanism of this enzyme. All known iduronidases are grouped according to amino acid similarities into the family 39 of glycosyl hydrolases, which also contains some β -D-xylosidases. This family, by extension from stereochemical outcome studies of *Thermoanaerobacterium saccharolyticum* β -D-xylosidase, operates via a

retaining mechanism.⁶² On the basis of hydrophobic cluster analysis, IDUA's catalytic nucleophile was predicted to be Glu299.^{63,64} Recently, IDUA was shown to hydrolyze its substrates with net retention of anomeric configuration via ¹H-NMR spectroscopy.⁶⁵ The author then proceeded to show that Glu299 is indeed the catalytic nucleophile through the use of 5FIIdoAF (see below). However, the results were not unequivocal and further confirmation is necessary.

2.2 Specific aims

The syntheses of five novel compounds - 2-deoxy-2-fluoro- β -D-glucopyranosyluronic acid fluoride (2FGlcAF), 2-deoxy-2-fluoro- β -D-mannopyranosyluronic acid fluoride (2FManAF), 2-deoxy-2-fluoro- α -L-idopyranosyluronic acid fluoride (2FIIdoAF), 5-fluoro- β -D-glucopyranosyluronic acid fluoride (5FGlcAF) and 5-fluoro- α -L-idopyranosyluronic acid fluoride (5FIIdoAF) – will be performed.

These compounds will then be evaluated as inactivators using three different enzymes: *E. coli* β -D-glucuronidase, human β -D-glucuronidase and human α -L-iduronidase. As well, the labelling and identification of the catalytic nucleophiles of these glycosidases will be performed using the appropriate inactivators through a combination of proteolysis and liquid chromatography-electrospray mass spectrometric analysis.

2.3 Syntheses of 2-deoxy-2-fluoro- and 5-fluoro glycopyranosyluronic acid fluoride inactivators

2.3.1 Syntheses of 2-deoxy-2-fluoro-glycopyranosyluronic acid fluorides

It is only natural that we begin the synthesis of the fluoroglycopyranosyluronic acid inactivators with the 2-deoxy-2-fluoro- β -D-glycopyranosyluronic acid fluorides. Since the original fluorosugar inactivator, 2-deoxy-2-fluoro- β -D-glucopyranosyl fluoride, was first synthesized, a wide variety of 2-deoxy-2-fluoro- β -D-glycopyranosides have been made and proven to be extremely useful over the years in the mechanistic studies of glycosidases. These include 2-deoxy-2-fluoro- β -D-cellobiosides, -galactosides, -glucosides, -mannosides, -xylosides, and -xylobiosides. However, the 2-deoxy-2-fluoro- β -D-glycopyranosyluronic acids are conspicuous by their absence from this list. We thus undertook the task of synthesizing both 2-deoxy-2-fluoro- β -D-glucopyranosyluronic acid fluoride **5** and 2-deoxy-2-fluoro- β -D-mannopyranosyluronic acid fluoride **8** for use as inactivators of glucuronidases. Also, the synthesis of 2-deoxy-2-fluoro- α -L-idopyranosyluronic acid fluoride **14** was accomplished for use with human α -L-iduronidase.

2.3.1.1 2-Deoxy-2-fluoro- β -D-glucopyranosyluronic acid fluoride, 2FGlcAF (5**)**

The synthesis of 2-deoxy-2-fluoro- β -D-glucopyranosyluronic acid fluoride **5** is outlined in Figure 2.1.

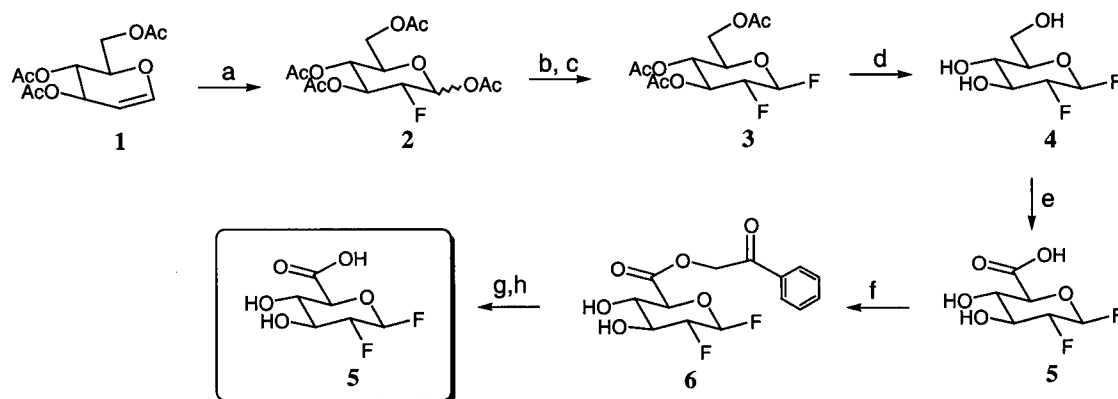


Figure 2.1: Synthesis of 2-deoxy-2-fluoro- β -D-glucopyranosyluronic acid fluoride **5**. a) SelectfluorTM, acetic anhydride, acetic acid; b) 45% HBr/acetic acid; c) AgF, acetonitrile; d) NaOMe/MeOH; e) TEMPO, NaOCl, NaBr; f) phenacyl bromide, triethylamine, DMF; g) 10% Pd-C, H₂; h) H⁺-cation exchange resin.

The key steps involved the use of SelectfluorTM to introduce fluorine at the C-2 position and the use of TEMPO in the selective oxidation of the C-6 alcohol to the carboxylic acid.

SelectfluorTM (1-chloromethyl-4-fluoro-1,4-diazoniabicyclo[2.2.2]octane bis(tetrafluoroborate)) is an electrophilic fluorinating agent that is both stable and easy to use.⁶⁶ It reacts with olefins in the presence of a weak nucleophile such as water or acetic acid to yield the addition product and it has previously been shown to react with glycals to yield a variety of 2-deoxy-2-fluoro-glycosides.^{67,68} In particular, tri-*O*-acetyl-D-glucal was shown to react with Selectfluor in dimethylformamide/water to give predominantly the *manno* epimer. We found that by changing the solvent/nucleophile system to acetic anhydride/acetic acid the *gluco* epimer was obtained in satisfactory quantities, albeit at lower yield relative to the *manno* epimer (2:3 *gluco:manno*, 23% and 32%, respectively). Fortunately, separation of the *gluco* and *manno* products is readily achieved by silica gel chromatography, and the *gluco* epimer was converted to the 2-

deoxy-2-fluoro- β -D-glucopyranosyl fluoride by a series of steps involving bromination, displacement of the bromine by fluoride, and deprotection.

The 2-deoxy-2-fluoro- β -D-glucopyranosyluronic acid was obtained via TEMPO (2,2,6,6-tetramethyl-1-piperidinyloxy) mediated oxidation of the C-6 alcohol of 2-deoxy-2-fluoro- β -D-glucopyranosyl fluoride in water (maintained at pH 10 with sodium hydroxide) with hypobromite (formed by the reaction of hypochlorite and bromide) as the regenerating oxidant.⁶⁹⁻⁷¹ This reaction is both mild and selective for the primary C-6 alcohol. In order to facilitate purification of the product away from the inorganic salts present in the reaction mixture after the oxidation, the uronic acid was first converted to its phenacyl ester and then purified by flash chromatography. The choice of the phenacyl ester was based upon the need for a protecting group that can be easily removed under mild conditions, i.e. non-acidic and non-basic conditions. This particular ester is easily cleaved via catalytic hydrogenolysis.⁷² While the oxidation step proceeded to completion (as evidenced by TLC), the overall yield for the oxidation and purification steps was modest (33%). This is probably due to the inefficiency of the esterification step. Hydrogenolysis of **6**, followed by flash chromatography, afforded the final product **5** in 87% yield.

2.3.1.2 2-Deoxy-2-fluoro- β -D-mannopyranosyluronic acid fluoride, 2FManAF (8**)**

The synthesis of 2-deoxy-2-fluoro- β -D-mannopyranosyluronic acid fluoride **8** is outlined in Figure 2.2.

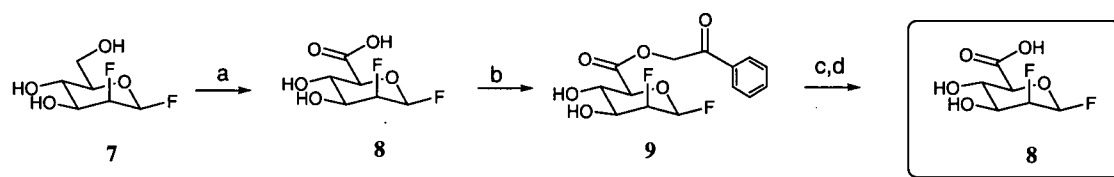


Figure 2.2: Synthesis of 2-deoxy-2-fluoro- β -D-mannopyranosyluronic acid fluoride **8**. a) TEMPO, NaOCl, NaBr; b) phenacyl bromide, triethylamine, DMF; c) 10% Pd-C, H₂; d) H⁺-cation exchange resin.

The starting sugar 2-deoxy-2-fluoro- β -D-mannosyl fluoride was oxidized and purified in an analogous manner to that described above. Again, the oxidation/purification steps were not efficient, resulting in a 29% yield of the phenacyl ester **9**. Hydrogenolysis of **9** gave the desired product **8** in 84% yield.

2.3.1.3 2-Deoxy-2-fluoro- α -L-idopyranosyluronic acid fluoride, 2FIdoAF (**14**)

The synthesis of 2-deoxy-2-fluoro- α -L-idopyranosyluronic acid fluoride **14** is outlined in Figure 2.3.

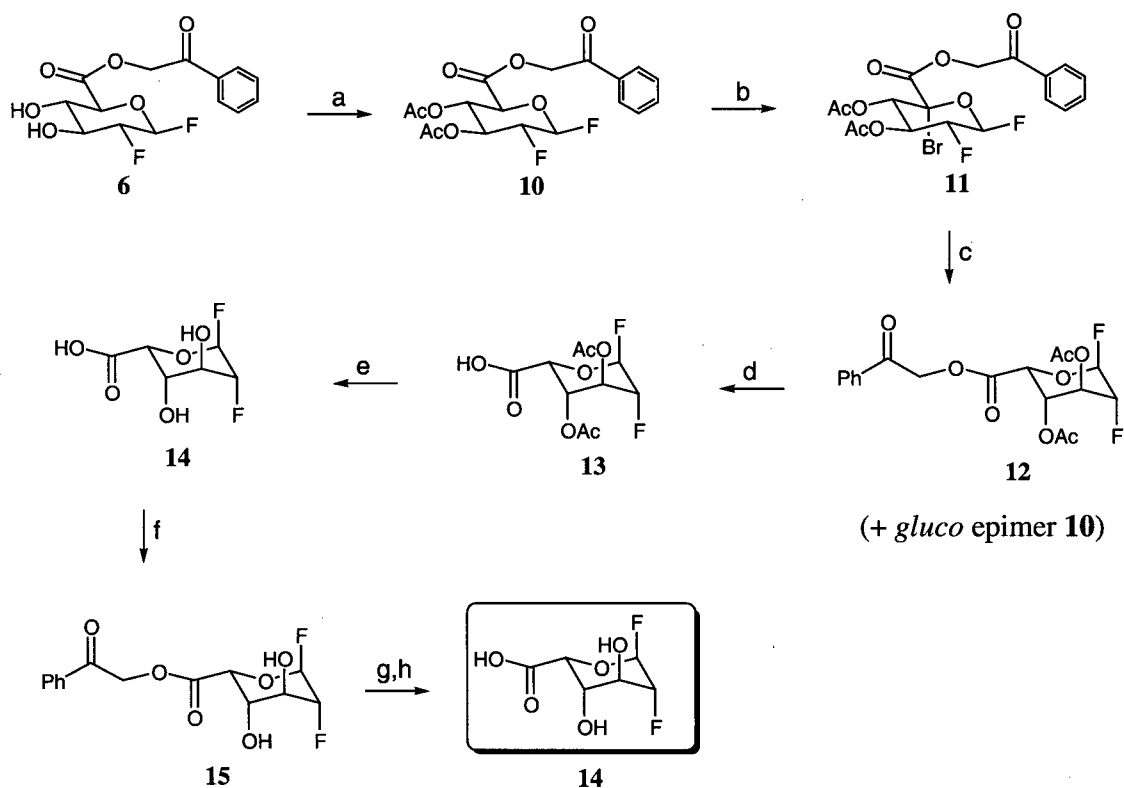
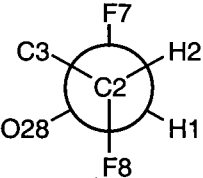
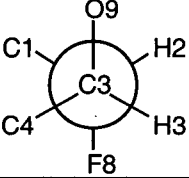
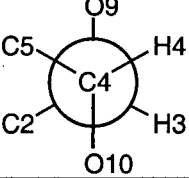
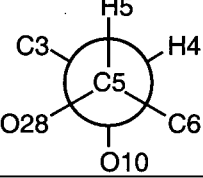


Figure 2.3: Synthesis of 2-deoxy-2-fluoro- α -L-idopyranosyluronic acid fluoride **14**. a) AcCl ; b) NBS , CCl_4 , $h\nu$; c) Bu_3SnH , toluene, Δ ; d) 10 % Pd-C , H_2 ; e) NaOMe , MeOH ; f) phenacyl bromide, triethylamine, DMF ; g) 10% Pd-C , H_2 ; h) H^+ -cation exchange resin.

The synthesis of **14** hinged upon the radical bromination of C-5 of the protected phenacyl (3,4-di-O-acetyl-2-deoxy-2-fluoro- β -D-glucopyranosyl fluoride)uronate **10** (obtained by acetylation of **6** with acetyl chloride in 80% yield) to give **11** in 51% yield.⁷³ This was followed by displacement of the bromide under radical conditions with tributyltin hydride to give **12** in 30% yield.⁷⁴ A nearly identical yield (29%) of the *gluco* epimer **10** was also obtained.

between H1-H2 approaches 90° since there is no apparent coupling of H1 to H2, the resonances corresponding to hydrogen atoms H2, H3, and H4 appear as complex multiplets and are of no help. However, the observed coupling constant between H4 and H5 – 1.7 Hz – indicates that they are in a gauche orientation.

Table 2.2: Torsion angles obtained from the X-ray crystal structure of 2FidoAF. Angles listed are between substituents attached to C1, C2, C3, C4, C5 and the endocyclic oxygen.

Newman projection	Atoms	Torsion Angles
	O28-C1-C2-C3 F7-C1-C2-C3 F8-C2-C1-O28 F7-C1-C2-F8	-39.0(3) 82.1(2) 78.8(2) -160.2(2)
	C1-C2-C3-C4 O9-C3-C2-C1 F8-C2-C3-C4 F8-C2-C3-O9	37.2(3) -78.3(2) -80.4(2) 164.1(2)
	C2-C3-C4-C5 O9-C3-C4-C5 O10-C4-C3-C2 O9-C3-C4-O10	-46.4(2) 71.3(2) 70.8(2) -171.5(2)
	O28-C5-C4-C3 O10-C4-C5-O28 O10-C4-C5-C6 C3-C4-C5-C6	57.7(2) -61.5(2) 58.0(2) -182.7(8)

The deprotection of **12** was somewhat problematic: while the removal of the phenacyl ester proceeded smoothly, the acetate groups were recalcitrant toward removal with ammonia dissolved in methanol; addition of sodium methoxide was required. However, after deprotection, the material was impure as observed by NMR spectroscopy. In order

to purify this material, re-esterification with phenacyl bromide followed by removal of the protecting group was required. This gave the desired 2-deoxy-2-fluoro- α -L-idopyranosyluronic acid fluoride **14**.

2.3.2 Synthesis of 5-fluoro- β -D-glucopyranosyluronic acid fluoride, 5FGlcAF (25) and 5-fluoro- α -L-idopyranosyluronic acid fluoride, 5FIdoAF (26)

The synthetic strategy employed for the 5-fluorosugar inhibitors hinges upon a radical bromination reaction at C-5 of the appropriate protected glycosyl fluoride, displacement of the bromide by fluoride, and then deprotection using ammonia in methanol.^{73,75} It is important that the anomeric substituent be installed prior to bromination since these C-5 halo derivatives contain two reactive anomeric centres, and thus are quite labile. In addition, once the C-5 fluorine substituent has been installed it is not possible to generate intermediates with free hemiacetals at C-1 since they would rapidly decompose via ring opening and elimination of HF. This synthetic approach has been applied to the generation of 5-fluoro glucosides, galactosides, mannosides and even N-acetylhexosaminides, but has never been used to generate 5-fluoroglucopyranosyluronic acid derivatives. Indeed, glucuronides are particularly attractive candidates for such chemistry since generation of a radical at C-5 should be considerably facilitated by the adjacent acid/ester functionality.

A major stumbling block in the syntheses of the 5-fluoro-glycopyranosyluronic acid fluorides was the choice of protecting group for the acid functionality. Simple alkyl esters

such as a methyl ester are unsuitable since the conditions required for their removal result in the decomposition of the difluoride product. Benzyl esters, which could be removed hydrogenolytically, are also of no use, being incompatible with the photobromination conditions. Silicon-based protecting groups are also out of the question since they are incompatible with the use of fluoride salts. The protecting group ultimately employed was the phenacyl ester, which is compatible with all the reaction conditions used, and is readily removed by hydrogenolysis.

The synthesis of the 5-fluoro- β -D-glucopyranosyluronic acid fluoride **25** and 5-fluoro- α -L-idopyranosyluronic acid fluoride **26** is illustrated in Figure 2.5. Acetylation of D-glucuronic acid was carried out with acetic anhydride under acidic conditions to give the 1,2,3,4-tetra-O-acetate **17** in 62% yield. Selective anomeric deprotection was achieved by the use of hydrazine acetate in DMF, the hemiacetal product partially purified by liquid extraction, and then directly converted to the phenacyl ester via reaction with 2-bromoacetophenone in the presence of triethylamine to give **18**; the overall yield for these two steps was 47%. Conversion of this protected hemiacetal **18** to the β -glycosyl fluoride **19** was achieved by reaction with diethylaminosulfur trifluoride (DAST), yielding a mixture of the β - and α -anomers, of which the β -anomer was the predominant species. Fortunately, the β -anomer selectively crystallized from dichloromethane and petroleum ether to yield **19** (56%). Compound **20** was obtained in 43% yield by brominating C-5 under radical conditions using *N*-bromosuccinimide and light. While this reaction proceeds slowly for the per-O-acetylated β -glucosyl fluoride (over four hours), the phenacyl (2,3,4-tri-O-acetyl- β -D-glucopyranosyl fluoride)uronate starting

material was consumed within two hours, presumably reflecting captodative stabilization of the radical generated at C5 by the adjacent carbonyl group (electron-withdrawing) and the adjacent oxygen atom (electron-donating).⁷³

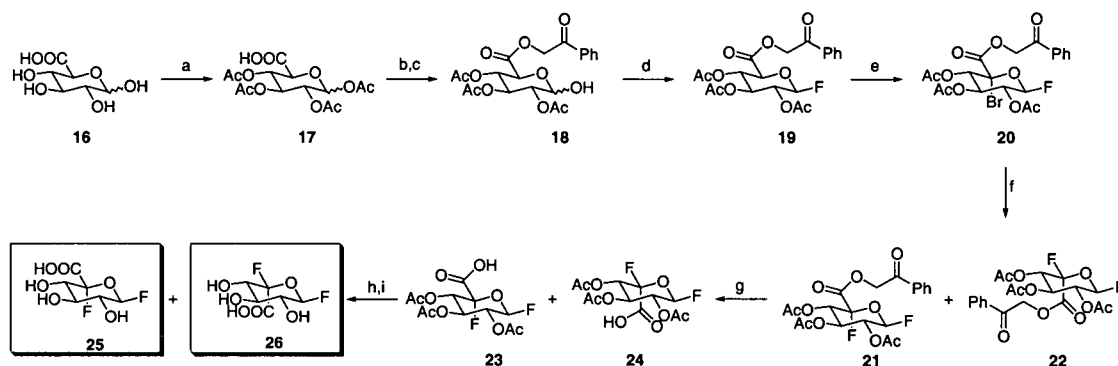


Figure 2.5: Synthesis of 5-fluoro-β-D-glucopyranosyluronic acid fluoride **25** and 5-fluoro-α-L-idopyranosiduronic acid fluoride **26**. a) acetic anhydride, acetonitrile, H₂SO₄ (cat.); b) hydrazine acetate, DMF; c) phenacyl bromide, triethylamine, ethyl acetate; d) DAST, CH₂Cl₂; e) NBS, CCl₄; f) AgBF₄, Et₂O, 0 °C; g) 10% Pd-C, H₂; h) NH₃, MeOH; i) AG 1X-8 (H⁺) resin.

Reaction of the 5-bromo sugar with silver tetrafluoroborate in diethyl ether afforded a mixture of the 5-fluoro D-*gluco* and L-*ido* uronic acid fluorides (**21** and **22**), but unfortunately only in low yields (12 and 31%, respectively). Use of silver fluoride in acetonitrile afforded only the *ido* epimer in 32% yield. However, the bromide displacement step using silver tetrafluoroborate provided sufficient amounts of both **21** and **22** for deprotection, characterization, and testing as an inactivator. Deprotection of **21** and **22** was achieved via a two-step process: the phenacyl protecting group was removed via hydrogenolysis in methanol:water to give **23** and **24** in 90% yield each, while the acetate groups were cleaved using ammonia in methanol to yield the desired final products **25** and **26**, both in 85% yield.

2.4 Spontaneous hydrolysis studies of fluoro-sugar inactivators

The rate constants and half-lives for the spontaneous hydrolysis of 2-deoxy-2-fluoro- β -D- and 5-fluoro- β -D-glycopyranosyl fluorides and -glycopyranosyluronic acid fluorides in 50 mM sodium phosphate buffer, pH 6.8, containing 1 M NaClO₄, at 50°C, are outlined in the following table.

Table 2.3: Spontaneous hydrolysis data for various 2-deoxy-2-fluoro- β -D- and 5-fluoro- β -D-glycopyranosyl fluorides and -glycopyranosyluronic acid fluorides.

Compound	k at 50°C (h ⁻¹)	t _{1/2} (h)
2F β GF ^a	0.057±0.008	12
2F β MF ^b	0.023±0.001	30
2,6diFGF ^c	0.028±0.001	25
5F β GF ^{d,e}	0.0014	510
5F α IF ^{d,f}	0.063	11
2FGlcAF	0.0075±0.0002	92
2FManAF	0.019±0.002	36
5FGlcAF	0.0011±0.0001	630
5FIdoAF	0.010±0.001	69
2FIdoAF	0.020±0.002	35

^a 2-deoxy-2-fluoro- β -D-glucopyranosyl fluoride

^b 2-deoxy-2-fluoro- β -D-mannopyranosyl fluoride

^c 2,6-dideoxy-2,6-trifluoro- β -D-glucopyranosyl fluoride (synthesis and kinetic studies outlined in Chapter 3)

^d Taken from ref. 76

^e 5-fluoro- β -D-glucopyranosyl fluoride

^f 5-fluoro- α -L-idopyranosyl fluoride

The first thing one notes is that the rate of hydrolysis of 2F β MF is actually lower than that of 2F β GF by a factor of 2.5. It is difficult to rationalize why this is observed, especially when one considers that the rate of hydrolysis of 2FManAF is greater than that of 2FGlcAF by the same factor. Also worth noting is that replacement of the 6-OH with fluorine caused a 2-fold decrease in rate from 2F β GF to 2,6diFGF, presumably due to a field effect from the fluorine at the 6-position.

A general trend can be seen that changing the oxidation state of the C-5 substituent from a hydroxymethyl group to a carboxylic acid has the effect of lowering the rate of spontaneous hydrolysis. This is what would be expected since the carboxylic acid is electron-withdrawing and would destabilize the formation of an oxocarbenium ion transition state. For example, 2FGlcAF undergoes hydrolysis 7.5-fold slower as compared to the parent glucopyranoside and 5FIdoAF hydrolyzes 6-fold more slowly than the parent idoside. Interestingly, however, 5FGlcAF hydrolyzed only 1.2-fold more slowly than the parent glucoside, but in this case it is likely that the fluorine at C-5 departs before the anomeric fluoride.

2.5 Studies employing EBG

2.5.1 Inactivation Kinetics

2.5.1.1 2FGlcAF and 2FManAF

Incubation of EBG with 2FGlcAF resulted in inactivation of the enzyme in a time dependent manner according to pseudo first order kinetics (Figure 2.6A). However, no saturation was observed, even at the highest inactivator concentrations studied (Figure 2.6B). Yet higher concentrations could not be investigated due to the rapidity of inactivation, which precluded accurate sampling. However, good estimates for the values of the inactivation rate constant (k_i) and the reversible dissociation constant (K_i) could be made ($3.7 \pm 0.2 \text{ min}^{-1}$ and $11.7 \pm 0.9 \text{ mM}$, respectively). From these data a second order rate constant of $k_i/K_i = 0.32 \pm 0.04 \text{ min}^{-1} \text{ mM}^{-1}$ was calculated.

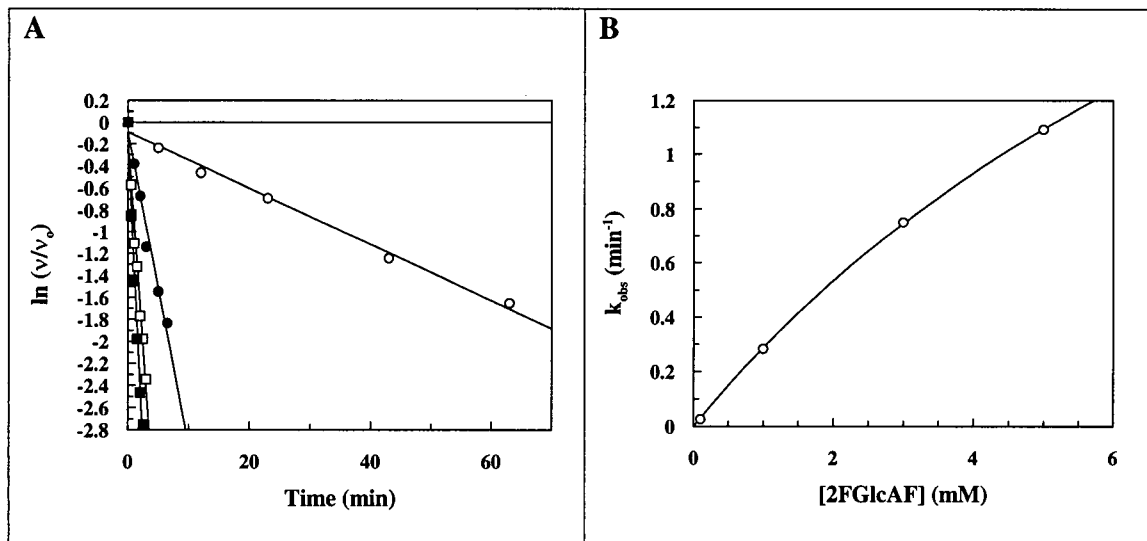


Figure 2.6: Inactivation of EBG by 2FGlcAF. A) semilogarithmic plot of residual activity versus time at the indicated inactivator concentrations: 0.1 mM (○), 1 mM (●), 3 mM (□), and 5 mM (■). B) replot of the first-order rate constants from A.

Similar inactivation kinetics were obtained with 2FManAF, however separate values for k_i and K_i could not be determined (Figure 2.7). Instead, a value of $k_i/K_i = 0.35 \pm 0.01 \text{ min}^{-1} \text{ mM}^{-1}$ was calculated from the slope of the plot of k_{obs} vs [2FManAF].

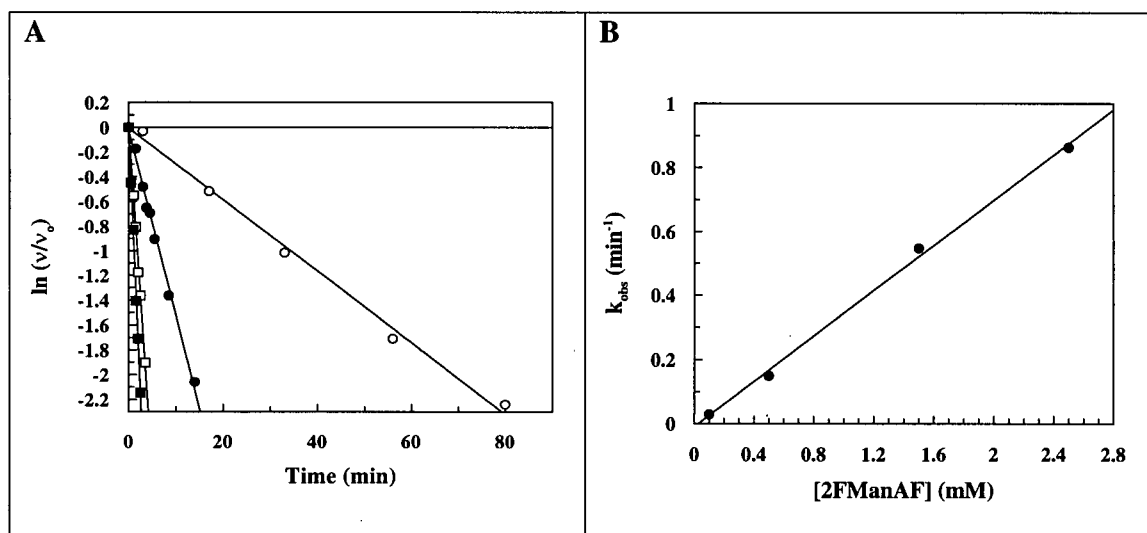


Figure 2.7: Inactivation of EBG by 2FManAF. A) semilogarithmic plot of residual activity versus time at the indicated inactivator concentrations: 0.1 mM (○), 0.5 mM (●), 1.5 mM (□), and 2.5 mM (■). B) replot of the first-order rate constants from A.

Both 2FGlcAF and 2FManAF were shown to be active-site directed by incubating EBG with the inactivators in the presence and absence of the known competitive inhibitor D-saccharic acid 1,4-lactone (100 μM , $K_i = 22 \mu\text{M}$) (Figure 2.8). In both cases, the apparent rate constants were reduced by the amount expected if these compounds were competing for the same site on the enzyme: from $0.210 \pm 0.011 \text{ min}^{-1}$ to $0.034 \pm 0.001 \text{ min}^{-1}$ for 1 mM 2FGlcAF and from $0.122 \pm 0.003 \text{ min}^{-1}$ to $0.019 \pm 0.001 \text{ min}^{-1}$ for 1 mM 2FManAF.

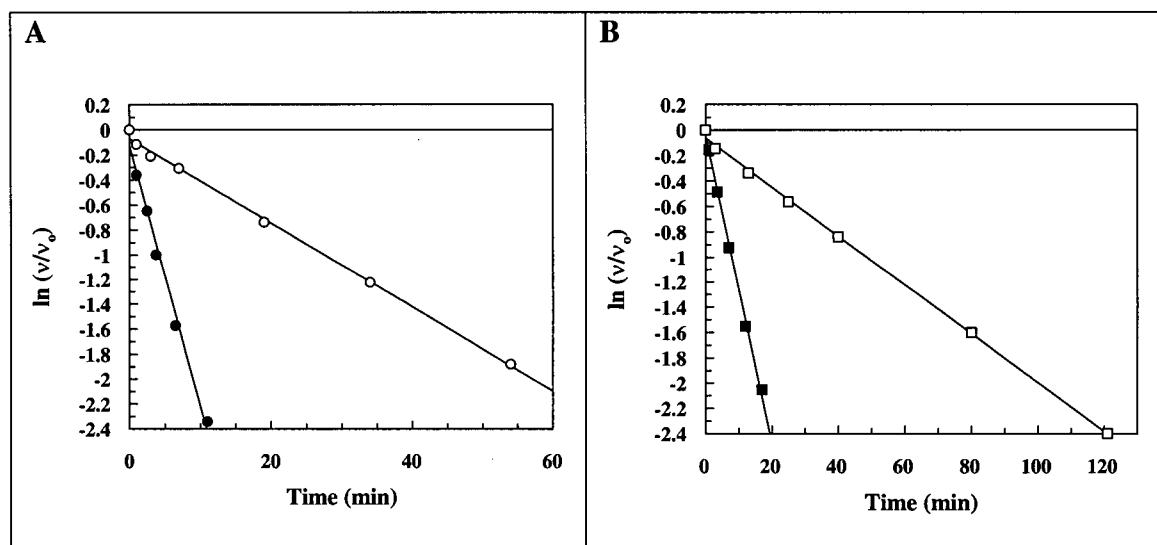


Figure 2.8: Protection against inactivation of EBG with 2FGlcAF and 2FManF. **A)** inactivation with 1 mM 2FGlcAF in the absence (●) and presence (○) of 100 μ M D-saccharic acid 1,4-lactone. **B)** inactivation with 1 mM 2FManAF in the absence (■) and presence (□) of 100 μ M D-saccharic acid 1,4-lactone.

Catalytic Competence

Further evidence supporting the trapping of relevant covalent 2F-glucopyranosyluronic acid- and 2F-mannopyranosyluronic acid-enzyme species arises from demonstration of the catalytic competence of the trapped intermediates as follows: excess inactivator was removed from the labeled enzyme samples, they were then incubated at 37°C in the presence of buffer and the recovery of activity associated with the regeneration of the free enzyme was monitored. Reactivation of the 2F-glucopyranosyluronic acid-enzyme in buffer followed a first order process with an apparent rate constant of $k_{re} = 0.0020 \pm 0.0001 \text{ min}^{-1}$ ($t_{1/2} = 350 \pm 20 \text{ min}$) (Fig. 2.9A) while reactivation of the 2F-mannopyranosyluronic acid-enzyme proceeded much more slowly ($k_{re} = 0.00046 \pm 0.00029 \text{ min}^{-1}$, $t_{1/2} = 1500 \pm 950 \text{ min}$) (Fig. 2.9B).

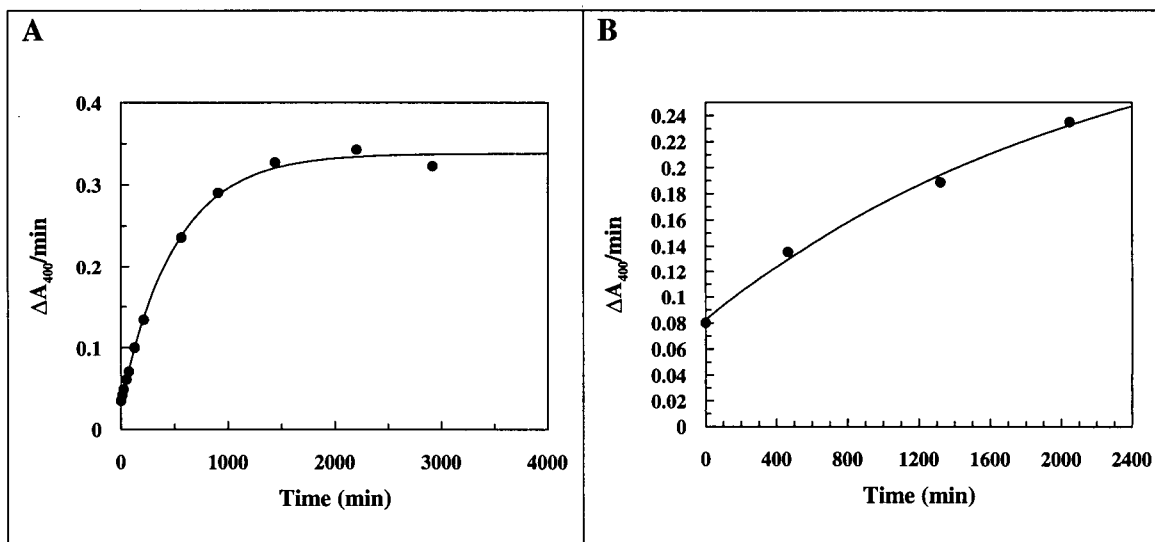


Figure 2.9: Reactivation of 2F-glycuronyl EBG species in buffer. A) 2FGlcA-EBG; B) 2FManA-EBG.

Reactivation of the glycosyl-enzyme species was also observed in the presence of 20 mM benzyl alcohol (Figure 2.10). The presence of the aromatic alcohol had the effect of accelerating the rates of reactivation as evidenced by the increased rate constants (lowered half-life values): $k_{re} = 0.022 \pm 0.002 \text{ min}^{-1}$ ($t_{1/2} = 32 \pm 3 \text{ min}$) for the 2FGlcA-EBG species; $k_{re} = 0.0017 \pm 0.0003 \text{ min}^{-1}$ ($t_{1/2} = 400 \pm 70 \text{ min}$) for the 2FManA-EBG species. These increased rates of reactivation are not surprising since EBG's natural substrates comprise a wide variety of aromatic glucuronides and the enzyme therefore likely has an aglycone binding pocket that preferentially binds aromatic compounds.

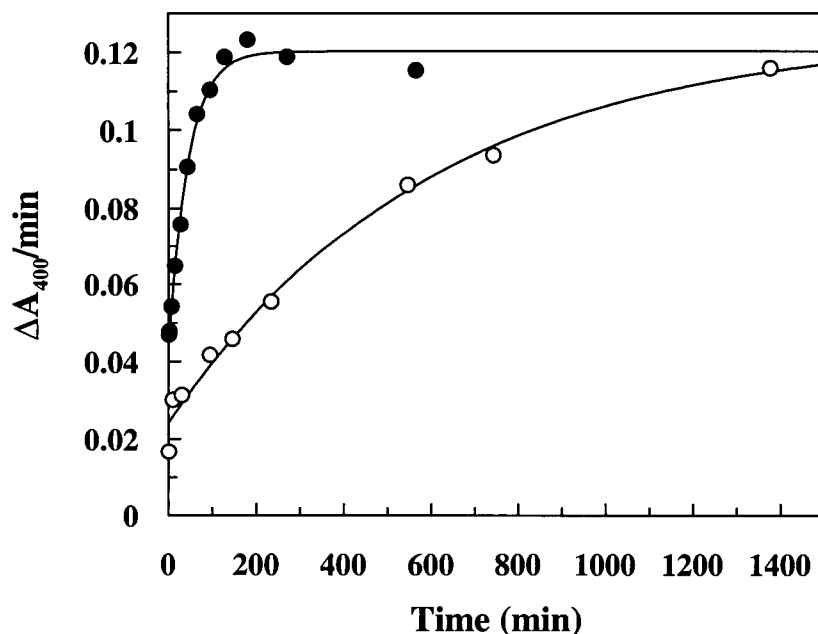


Figure 2.10: Reactivation of (●) 2FGlcA-EBG species and (○) 2FManA-EBG species in the presence of 20 mM BnOH.

We also attempted to increase the rate of reactivation using an acceptor sugar (50 mM pNP-glucose). Again, an increase in the reactivation rate was observed for the 2FManA-EBG species: $k_{re} = 0.0062 \pm 0.0018 \text{ min}^{-1}$ ($t_{1/2} = 110 \pm 32 \text{ min}$) (Figure 2.11B). However, in the case of the 2FGlcA-EBG species, the expected maximum return of enzymatic activity was not obtained. Instead, at longer incubation times, the enzymatic rate was observed to drop dramatically, even below the initial rate (Figure 2.11A). Thus, no reliable reactivation rate constant could be calculated from the data. Why this occurred is still a mystery; however, qualitatively, one can say that there was an increase in the rate of reactivation for the 2FGlcA-EBG species.

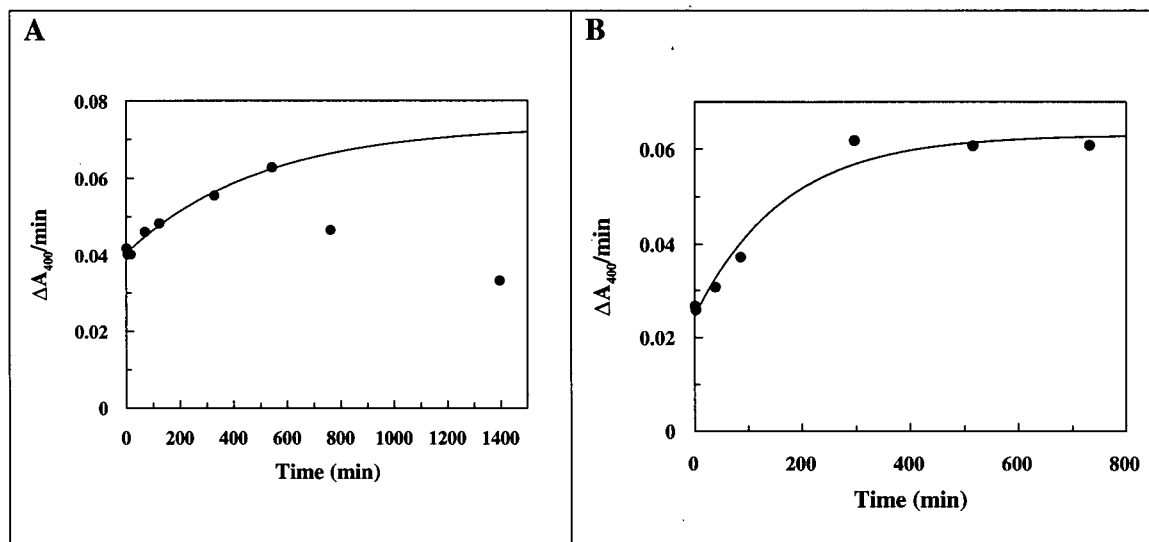


Figure 2.11: Reactivation of 2F-glycuronyl-EBG species in the presence of 50 mM pNPG. A) 2FGlcA-EBG species; B) 2FManA-EBG species.

2.5.1.2 5FGlcAF

Incubation of EBG with 5FGlcAF resulted in inactivation of the enzyme in a time dependent manner according to essentially pseudo-first order kinetics, though inactivation, particularly at low inactivator concentrations, did not proceed to completion (Fig. 2.12A). This is consistent with a kinetic model in which, at high concentrations of inactivator, the rate of formation of the glycosyl-enzyme intermediate is significantly greater than that of its breakdown, but not at low concentrations.⁷⁷ A plot of these observed rate constants versus inactivator concentration revealed that full saturation of the enzyme was not achieved, even at the highest inactivator concentrations studied (Fig. 2.12B). Unfortunately, yet higher concentrations could not be investigated due to the rapidity of inactivation, which precluded accurate sampling. Nevertheless, approximate values for the inactivation rate constant of $k_i = 4.8 \pm 0.6 \text{ min}^{-1}$ and of the reversible dissociation constant $K_i = 455 \pm 95 \text{ } \mu\text{M}$ were determined, and a value of the second order

rate constant $k_i/K_i = 10.4 \pm 1.9 \text{ min}^{-1}\text{mM}^{-1}$ was extracted from the initial slope of this plot (obtained by performing a linear regression on the first three points of the data). This latter value can also be calculated from the observed values of $k_i = 4.8 \pm 0.6 \text{ min}^{-1}$ and $K_i = 455 \pm 95 \text{ }\mu\text{M}$ to give $k_i/K_i = 10.5 \pm 3.5 \text{ min}^{-1}\text{mM}^{-1}$, in good agreement with the value obtained from low inactivator concentrations.

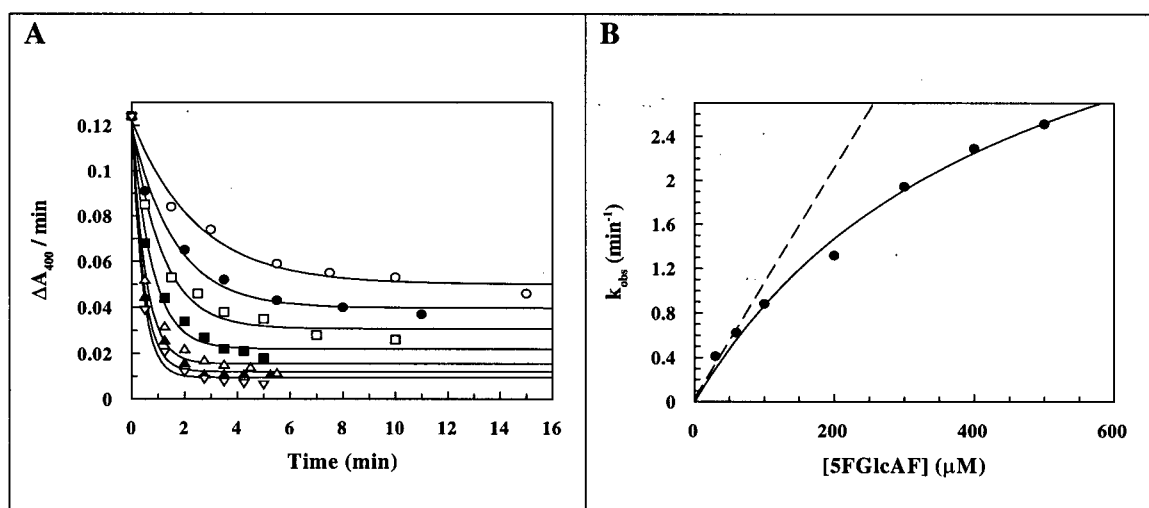


Figure 2.12: Inactivation of *E. coli* β -glucuronidase by 5FGlcAF. Lines shown in each case are those for the best fit to the data. A) Plot of residual activity vs. time at the indicated inactivator concentrations: (\circ) 30 μM , (\bullet) 60 μM , (\square) 100 μM , (\blacksquare) 200 μM , (\triangle) 300 μM , (\blacktriangle) 400 μM , (∇) 500 μM . B) Replot of the first order rate constants from panel A. The dashed line represents the initial slope of the plot.

5FGlcAF was then shown to be active site-directed by incubating EBG with the inactivator (100 μM) in the presence and absence of the known competitive inhibitor D-saccharic acid 1,4-lactone (50 μM , $K_i = 22 \text{ }\mu\text{M}$) (Figure 2.13). In the presence of the inhibitor and 5FGlcAF, the plot of enzyme activity versus time cannot be fit to a simple first order exponential decay function with an offset. However, as an estimate, we fitted the initial portion of the data ($t < 25 \text{ min}$) to this model in order to calculate a reactivation

rate constant for comparison. The apparent reactivation rate constant was reduced from $0.54 \pm 0.05 \text{ min}^{-1}$ to $0.18 \pm 0.02 \text{ min}^{-1}$; this is the expected amount of rate reduction.

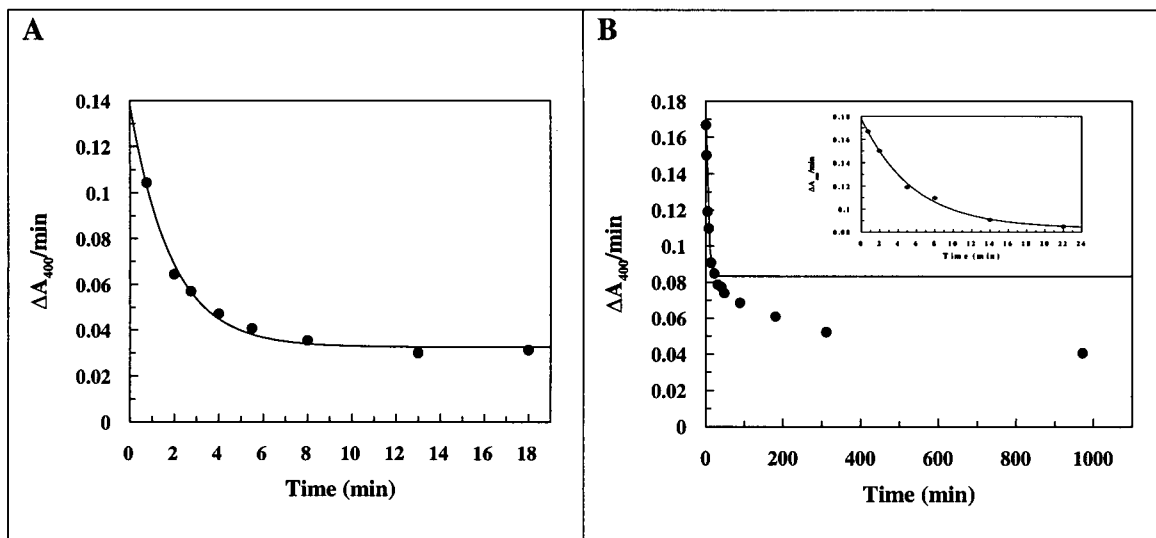


Figure 2.13: Protection against inactivation of EBG with 100 μM 5FGlcAF in: **A)** the absence and **B)** the presence of 50 μM D-saccharic acid 1,4-lactone; the inset shows an expansion of the initial portion of the curve.

Catalytic Competence

Further evidence supporting the trapping of a relevant covalent 5F-glucopyranosyluronic acid-enzyme arises from demonstration of the catalytic competence of the trapped intermediate. Following removal of excess inactivator from the labeled enzyme, the sample was incubated at 37°C in the presence of buffer and the recovery of activity associated with the regeneration of the free enzyme was monitored. Reactivation of the 5F-glucopyranosyluronic acid-enzyme in buffer followed a first order process with an apparent rate constant of $k_{re} = 0.073 \pm 0.006 \text{ min}^{-1}$ ($t_{1/2} = 9.5 \pm 0.8 \text{ min}$) (Fig. 2.14).

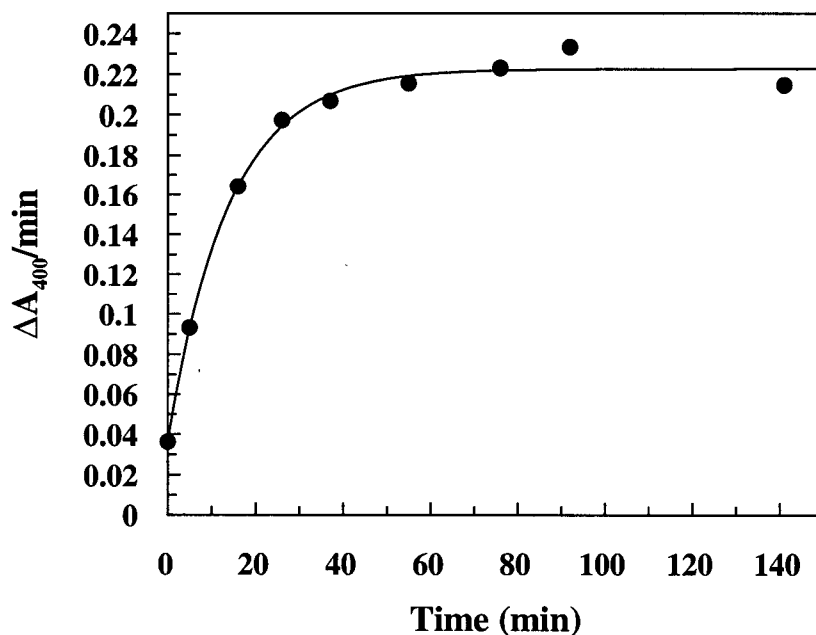


Figure 2.14: Reactivation of 5FGlcA-EBG in buffer.

Reactivation of the 5FGlcA-EBG species was also monitored in the presence of a variety of ligands - 10 mM glucuronic acid, 50 mM cellobiose, 20 mM pNPG and 20 mM benzyl alcohol (Figure 2.15). As with the 2FGlcA-EBG and the 2FManA-EBG glycosyl-enzyme species, both pNPG and benzyl alcohol were good reactivating ligands, increasing the apparent reactivation rate constants from $k_{re} = 0.073 \pm 0.006 \text{ min}^{-1}$ ($t_{1/2} = 9.5 \pm 0.8 \text{ min}$, buffer) to $k_{re} = 0.252 \pm 0.028 \text{ min}^{-1}$ ($t_{1/2} = 2.8 \pm 0.3 \text{ min}$, pNPG) and $k_{re} = 0.50 \pm 0.05 \text{ min}^{-1}$ ($t_{1/2} = 1.4 \pm 0.1 \text{ min}$, benzyl alcohol), respectively. However, neither D-glucuronic acid nor cellobiose changed the rate of reactivation significantly at the concentrations assayed (data not shown).

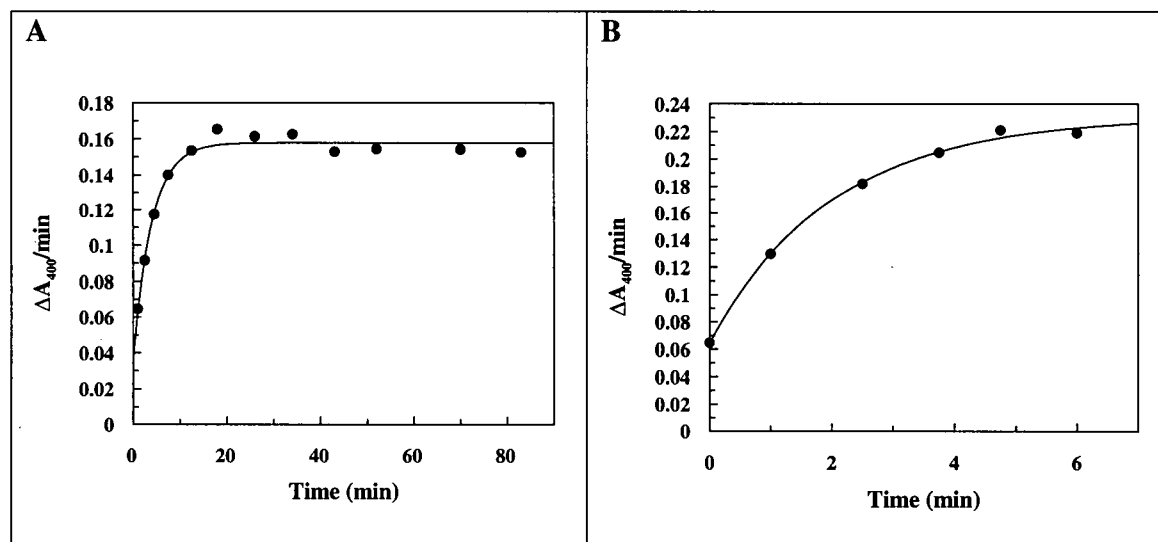


Figure 2.15: Turnover of 5FGlcA-EBG in the presence of reactivation ligands. A) 20 mM pNPG; B) 20 mM benzyl alcohol.

Competitive Inhibition

Since we observed that 5FGlcAF did not inactivate EBG completely at all concentrations assayed, we also tested it as a reversible competitive inhibitor. To do this, the kinetic parameters K_m and V_{\max} were first determined for the substrate pNPGlcA ($87 \mu\text{M}$, 0.15 min^{-1}). An assay of enzyme activity in the presence of $100 \mu\text{M}$ pNPGlcA and varying concentrations of 5FGlcAF yielded a linear plot of $1/V$ versus $[5\text{FGlcAF}]$ described by the equation of $y = 475x + 15$. Intersection of this line with $y = 1/V_{\max}$ yielded a value of $K_i' = 18 \mu\text{M}$ (Figure 2.16). It is noteworthy that this K_i' is considerably lower than the K_i value determined for 5FGlcAF as an inactivator. This is because the inactivation K_i value is a true dissociation constant while the competitive K_i' value also reflects the accumulated enzyme species.

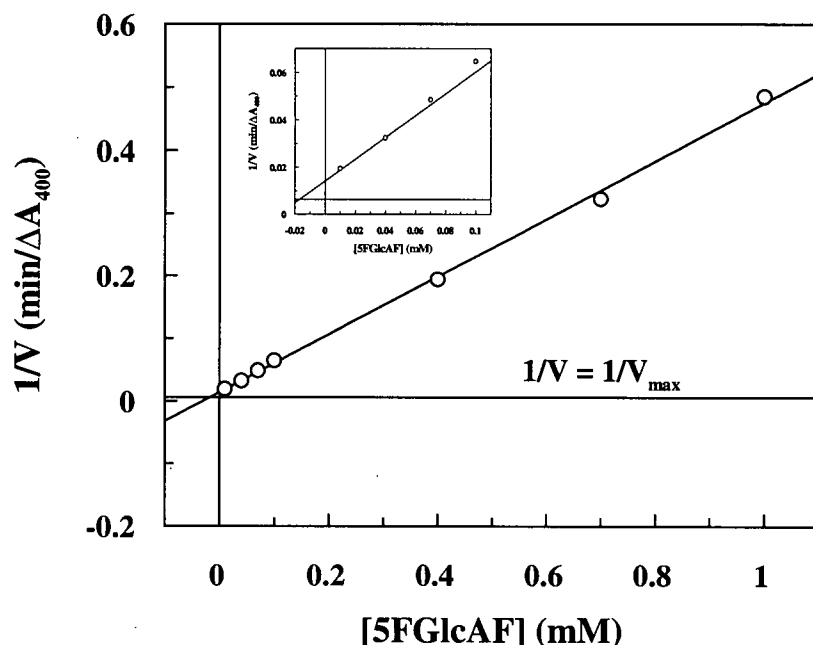


Figure 2.16: Reversible K_i for 5FGlcAF with EBG determined under steady-state conditions. Intersection of the plot $1/V$ versus $[5FGlcAF]$ intersects a line given by $1/V_m$ at $-K_i$. Inset shows expansion of the plot near the origin.

2.5.1.3 5FIdoAF

Incubation of EBG with 5FIdoAF resulted in inactivation of the enzyme in a time dependent manner. Surprisingly, the observed data could not be fit to a single exponential decay equation; rather, the data was best fit to a double exponential decay model (Figure 2.17A). This unexpected behaviour may be explained by the presence of a contaminant in the 5FIdoAF or the EBG preparation used may contain more than one glucuronidase with different activities. Nevertheless, plots of both the higher and lower observed rate constants (k_{obs1} and k_{obs2} , respectively) versus inactivator concentration revealed that full saturation of the enzyme was not achieved, even at the highest inactivator concentrations studied (Figures 2.17B and 2.17C, respectively). Values of k_i and K_i were calculated, though, from the plot of k_{obs1} versus $[5FIdoAF]$ ($0.81 \pm 0.13 \text{ min}^{-1}$

and 16.5 ± 3.9 mM, respectively), while a second order rate constant $k_i/K_i = 0.0013 \pm 0.0001 \text{ min}^{-1}\text{mM}^{-1}$ was calculated from the slope of the plot of $k_{\text{obs}2}$ vs [5FIduAF].

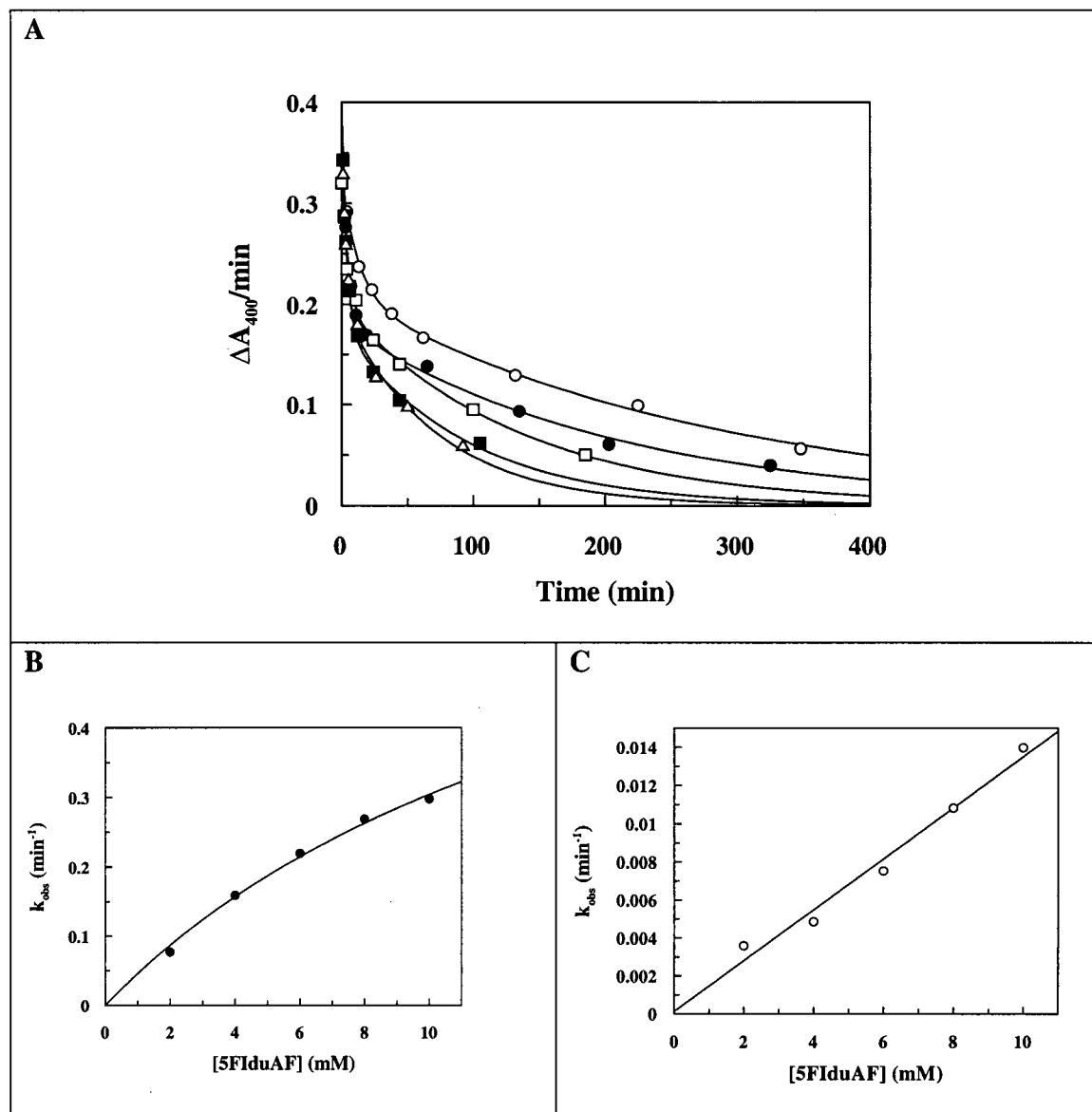


Figure 2.17: Inactivation of *E. coli* β -glucuronidase by 5FIduAF. Lines shown in each case are those for the best fit to the data. **A)** Plot of residual activity vs. time at the indicated inactivator concentrations: (○) 2 mM, (●) 4 mM, (□) 6 mM, (■) 8 mM, and (△) 10 mM. **B)** Replot of the initial first order rate constants from panel A. **C)** Replot of the final first order rate constants from panel A.

5FIIdoAF was then shown to be active site-directed by incubating EBG with the inactivator (16 mM) in the presence and absence of the competitive inhibitor D-saccharic acid 1,4-lactone (50 μ M, $K_i = 22 \mu$ M) (Figure 2.18).

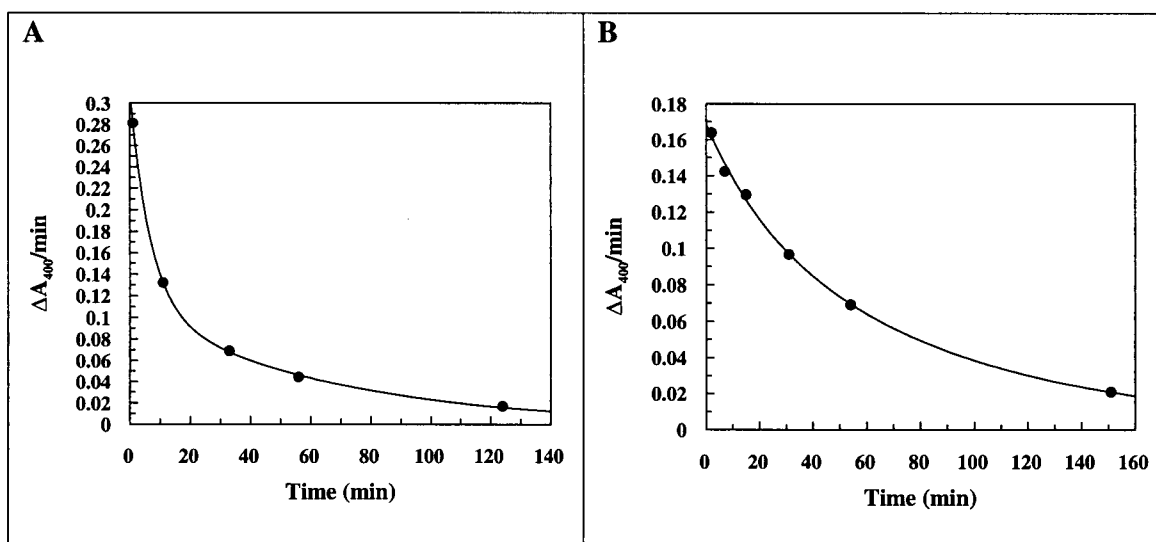


Figure 2.18: Protection against inactivation of EBG with 16 mM 5FIIdoAF in: **A)** the absence and **B)** the presence of 50 μ M D-saccharic acid 1,4-lactone. Both plots were fitted to a double exponential decay function.

One notices immediately that in the presence of D-saccharic acid 1,4-lactone, the decay curve appears dissimilar in shape to the curve generated with no inhibitor present. In fact, while the curve in Figure 2.18A can be best fit only to a double exponential decay function, the curve in Figure 2.18B can now be fit with either a single or a double exponential decay function. Values of $k_{\text{obs1}} = 0.15 \pm 0.01 \text{ min}^{-1}$ and $k_{\text{obs2}} = 0.016 \pm 0.002 \text{ min}^{-1}$ were determined in the absence of inhibitor, while values of $k_{\text{obs1}} = 0.046 \pm 0.051 \text{ min}^{-1}$ and $k_{\text{obs2}} = 0.012 \pm 0.004 \text{ min}^{-1}$ were determined in its presence. If we assume that there is a small amount of contaminating 5FGlcAF present in the 5FIIdoAF used, then a

value of $k_{\text{obs1}} = 0.15 \pm 0.01 \text{ min}^{-1}$ in the absence of inhibitor would correspond to a concentration of $14 \text{ }\mu\text{M}$ (calculated using the value of $k_i/K_i = 10.4 \pm 1.9 \text{ min}^{-1}\text{mM}^{-1}$ for 5FGlcAF). This value is consistent with the decrease in k_{obs1} in the presence of D-saccharic acid 1,4-lactone. That would mean that the amount of contamination would be only 0.09%, thus explaining why it could not be observed in the NMR data of the prepared 5FIdoAF sample. The absence of this anomalous behaviour of EBG with any other substrate or inactivator in this study further suggests that this behaviour arises from an impurity within the prepared 5FIdoAF sample and not the presence of an isozyme of EBG. Regardless, it can be safely concluded that 5FIdoAF did label the enzyme as the time-dependent inactivation process was dependent on the presence of both impurity and 5FIdoAF.

Catalytic Competence

The covalent 5F-idopyranosyluronic acid-enzyme intermediate was shown to be present in the usual manner: after removal of excess inactivator from the labeled enzyme, the sample was incubated at 37°C in the presence of buffer and the recovery of activity associated with the regeneration of the free enzyme was monitored. Reactivation of the 5F-idopyranosyluronic acid-enzyme in buffer followed a first order process with an apparent rate constant of $k_{\text{re}} = 0.0010 \pm 0.0001 \text{ min}^{-1}$ ($t_{1/2} = 690 \pm 70 \text{ min}$) (Fig. 2.19A). From the plot, one can see that the initial points (at time < 100 minutes) do not fall upon the fitted curve. In fact, when this region is expanded, one observes that this plot can be fitted to a first order rate equation as well (Figure 2.19B). In this case, an apparent rate

constant of $k_{re} = 0.022 \pm 0.003 \text{ min}^{-1}$ ($t_{1/2} = 32 \pm 4 \text{ min}$) was calculated. This value is similar to the value determined for the 5FGlcA-EBG species, thus supporting the hypothesis that the contaminant in the 5FIdoAF sample was indeed 5FGlcAF. Reactivation of the 5FIdoA-EBG was also followed in the presence of 20 mM benzyl alcohol, with an apparent rate constant of $k_{re} = 0.0038 \pm 0.0004 \text{ min}^{-1}$ ($t_{1/2} = 180 \pm 20 \text{ min}$) being obtained (Figure 2.20).

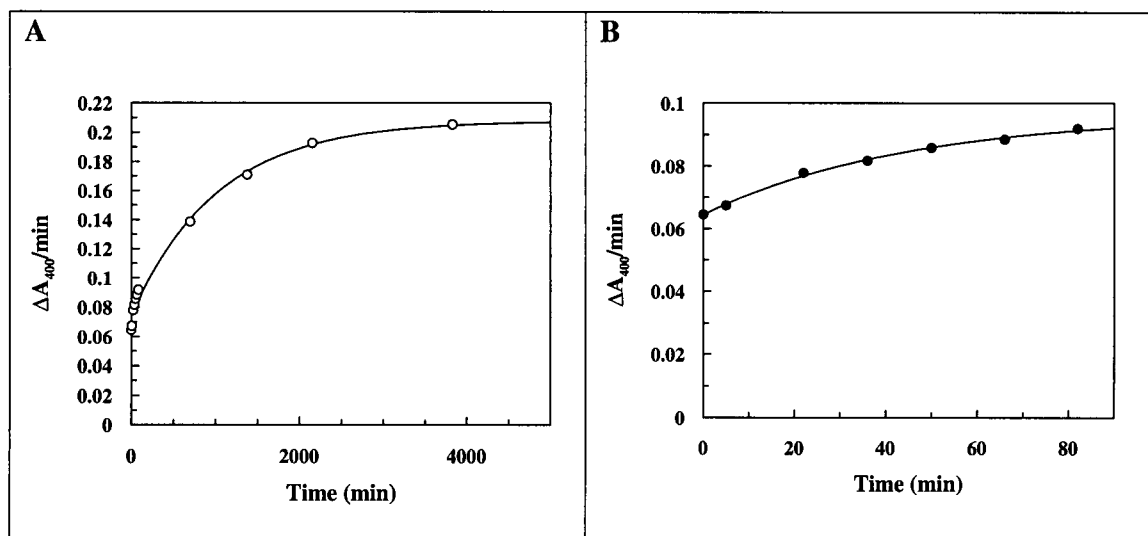


Figure 2.19: Reactivation of 5F-iduronyl-EBG in buffer. A) Plot of enzyme activity versus time. B) Expansion of A from t=0 min to t=100 min.

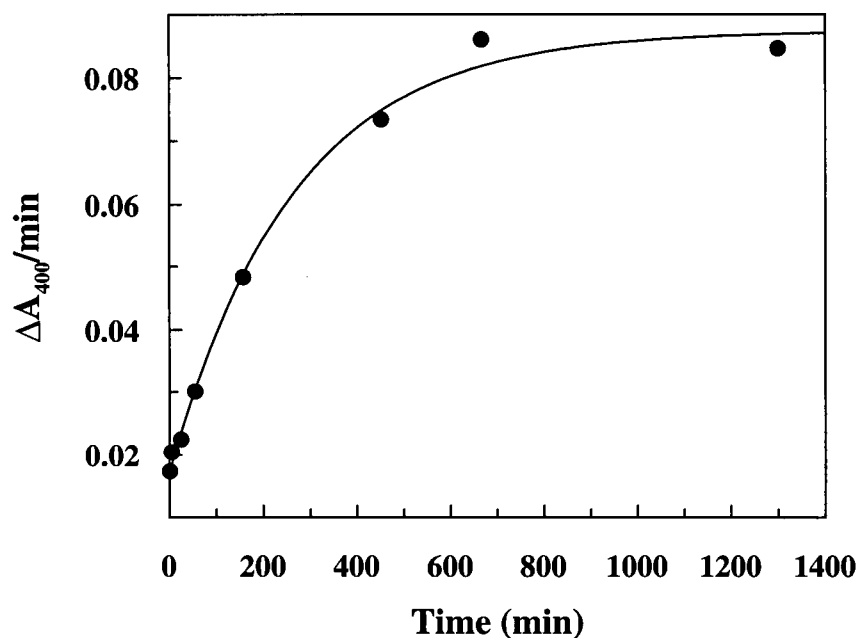


Figure 2.20: Reactivation of 5F-iduronyl-EBG in 20 mM benzyl alcohol.

Competitive Inhibition

For comparison to the other K_i' values obtained, 5FIIdoAF was also tested as a reversible competitive inhibitor of EBG. An assay of enzyme activity in the presence of 100 μM pNPGlcA ($K_m = 100 \mu\text{M}$, $V_{\max} = 0.19 \text{ min}^{-1}$) and varying concentrations of 5FIIdoAF yielded a linear plot of $1/V$ versus [5FIIdoAF] described by the equation of $y = 215x + 1009$. Intersection of this line with $y = 1/V_{\max}$ yielded a value of $K_i' = 4.6 \text{ mM}$ (Figure 2.21). This value is much larger than that observed for 5FGlcAF and reflects the fact that 5FIIdoAF is a poor inactivator of EBG.

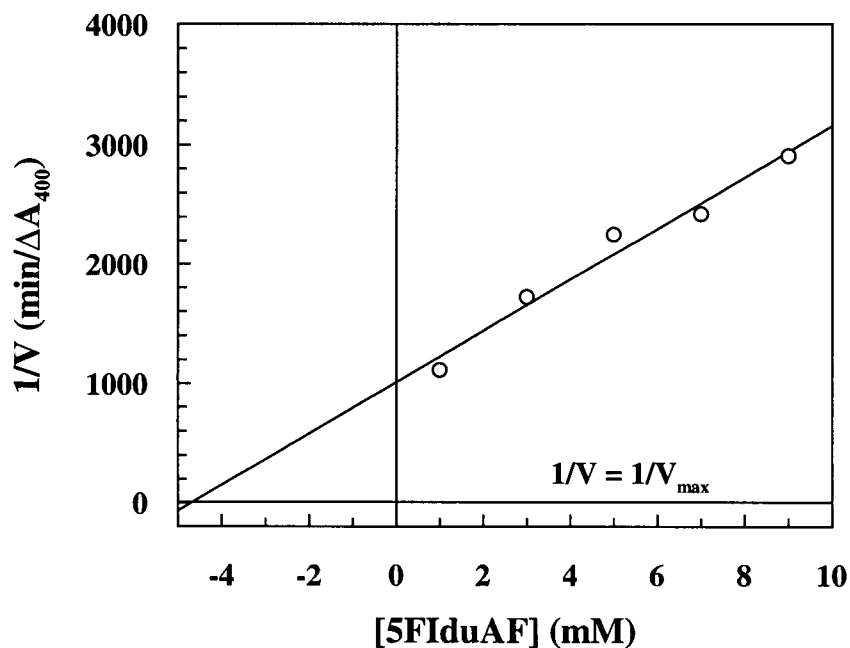


Figure 2.21: Reversible K_i for 5FIdoAF with EBG determined under steady-state conditions. The plot of $1/V$ versus $[5FGlcAF]$ intersects a line given by $1/V_m$ at $-K_i$.

2.5.1.4 2FIdoAF

Incubation of EBG with 2FIdoAF resulted in inactivation of the enzyme in a time dependent manner according to essentially pseudo-first order kinetics, though inactivation did not proceed to completion (Fig. 2.22A). A second order rate constant $k_i/K_i = 0.0009 \pm 0.0001 \text{ min}^{-1} \text{ mM}^{-1}$ was calculated from the slope of the plot of k_{obs} vs $[2FIdoAF]$ (Figure 2.22B).

2FIdoAF was then shown to be active site-directed by incubating EBG with the inactivator (10 mM) in the presence and absence of the competitive inhibitor D-saccharic acid 1,4-lactone (50 μM , $K_i = 22 \mu\text{M}$) (Figure 2.23). The apparent reactivation rate

constant was reduced from $0.011 \pm 0.001 \text{ min}^{-1}$ to $0.0023 \pm 0.0002 \text{ min}^{-1}$, consistent with the amount expected if both compounds are competing for the same site on the enzyme.

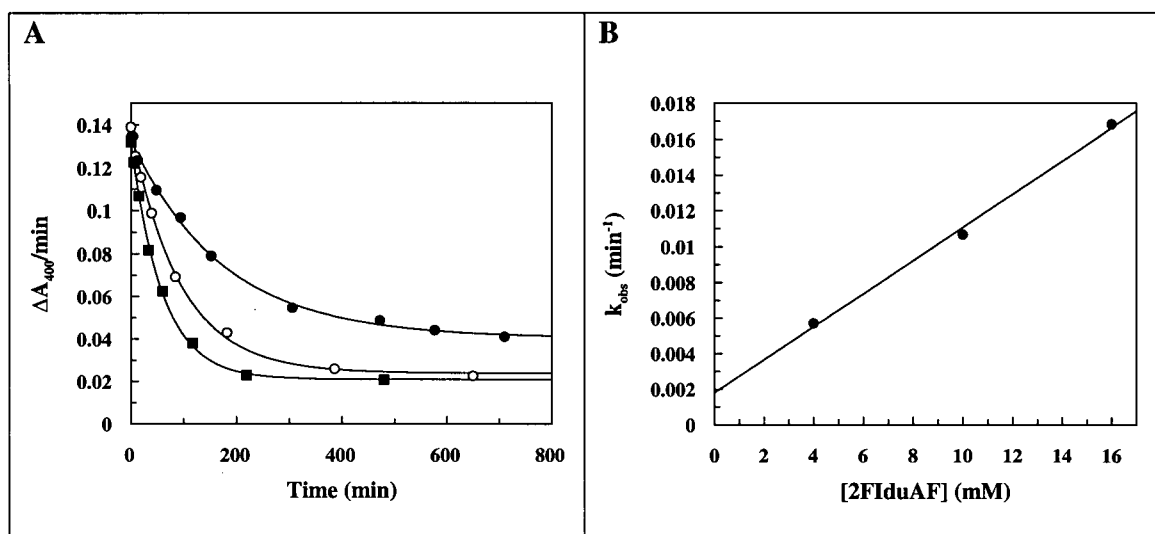


Figure 2.22: Inactivation of *E. coli* β -glucuronidase by 2FIdoAF. Lines shown in each case are those for the best fit to the data. A) Plot of residual activity vs. time at the indicated inactivator concentrations: (○) 4 mM, (●) 10 mM, (■) 16 mM. B) Replot of the first order rate constants from panel A.

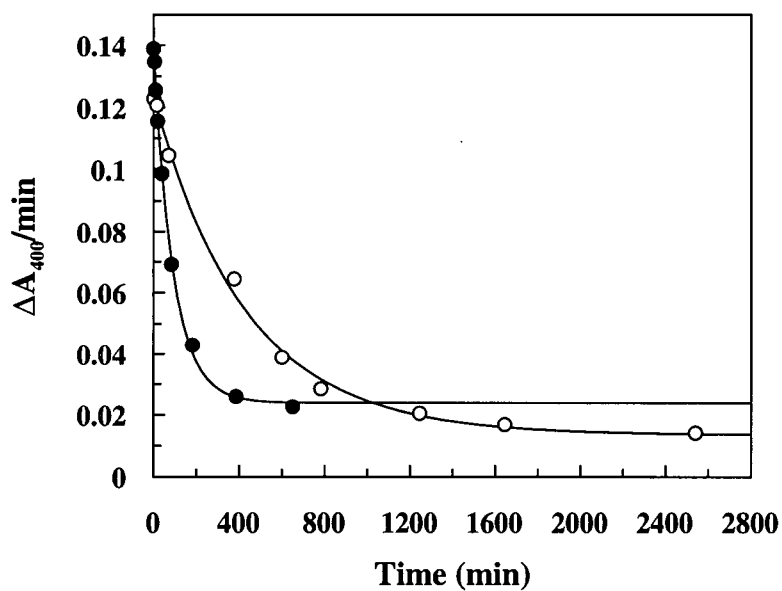


Figure 2.23: Protection against inactivation of EBG with 10 mM 2FIdoAF in (●) the absence and (○) the presence of 50 μM D-saccharic acid 1,4-lactone.

Catalytic Competence

The covalent 2F-idopyranosyluronic acid-enzyme intermediate was shown to be present in the usual manner: after removal of excess inactivator from the labeled enzyme by ultrafiltration, the sample was incubated at 37°C in the presence of buffer or 20 mM benzyl alcohol and the recovery of activity associated with the regeneration of the free enzyme was monitored. Reactivation of the 2F-idopyranosyluronic acid-enzyme in buffer followed a first order process with an apparent rate constant of $k_{re} = 0.0023 \pm 0.0003 \text{ min}^{-1}$ ($t_{1/2} = 300 \pm 39 \text{ min}$); this increased to $k_{re} = 0.019 \pm 0.002 \text{ min}^{-1}$ ($t_{1/2} = 36 \pm 4 \text{ min}$) in the presence of 20 mM benzyl alcohol (Figure 2.24).

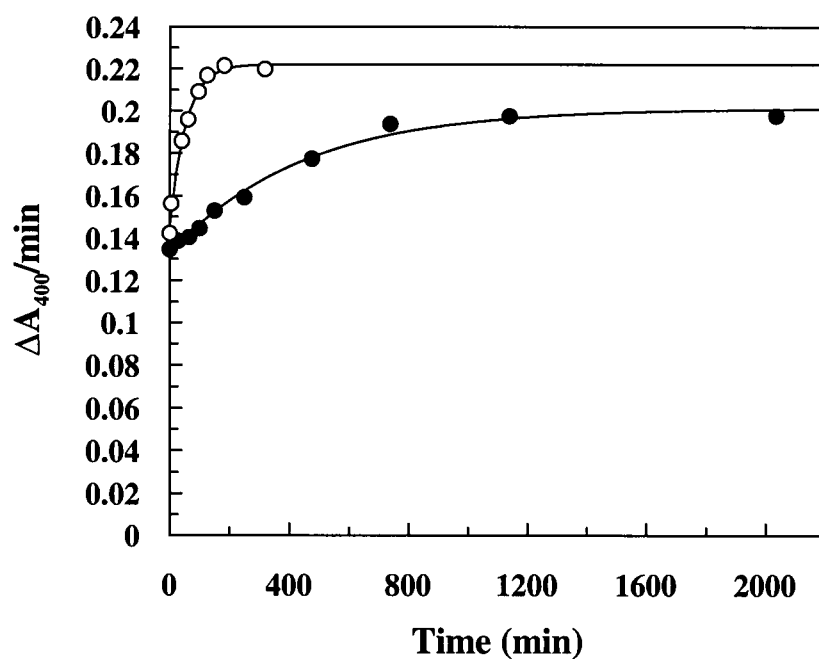


Figure 2.24: Reactivation of 2F-idopyranosyluronic acid-EBG in buffer (●) and in 20 mM benzyl alcohol (○).

Competitive Inhibition

2FIdoAF was also tested as a reversible competitive inhibitor of EBG. An assay of enzyme activity in the presence of 100 μM pNPGlcA ($K_m = 76 \mu\text{M}$, $V_{\max} = 0.001 \text{ min}^{-1}$) and varying concentrations of 2FIdoAF yielded a linear plot of $1/V$ versus $[2\text{FIdoAF}]$ described by the equation of $y = 330x + 1486$. Intersection of this line with $y = 1/V_{\max}$ yielded a value of $K_i' = 1.5 \text{ mM}$ (Figure 2.25).

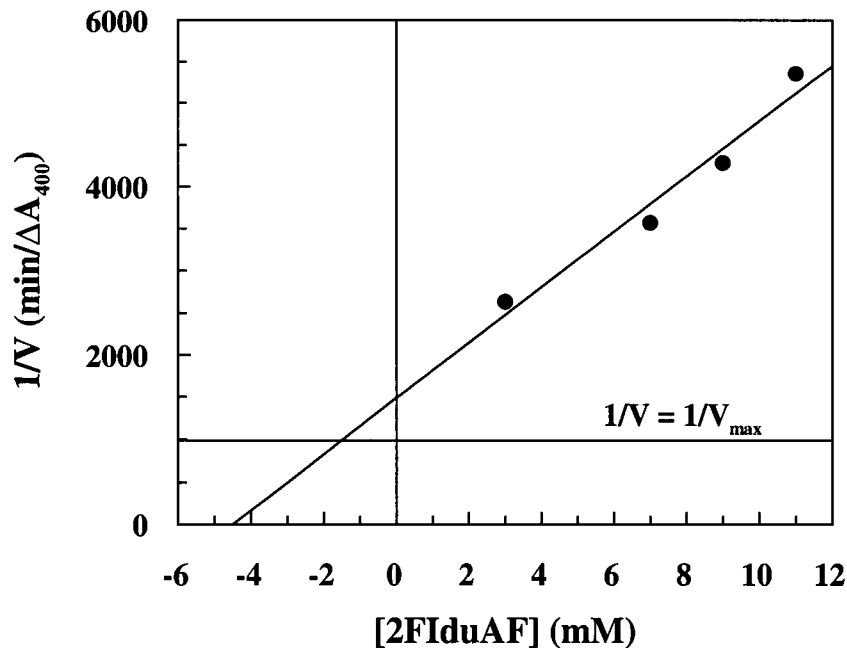


Figure 2.25: Reversible K_i' for 2FIdoAF with EBG determined under steady-state conditions. Intersection of the plot $1/V$ versus $[2\text{FIduAF}]$ intersects a line given by $1/V_m$ at $-K_i'$.

2.5.1.5 Interpretation of the kinetic results obtained using the various fluoroglycopyranosyluronic acid fluoride inactivators

The kinetic parameters for reaction of the various fluoroglycopyranosyluronic acid fluoride inactivators with EBG are summarized in Table 2.4.

As expected, both 2FGlcAF and 2FManAF were good inactivators of EBG. What was unexpected was that both had similar values of k_i/K_i and that the 2FManA-EBG species turned over more slowly compared to the 2FGlcA-EBG species. This is the opposite of what was observed with *Agrobacterium* sp. β -glucosidase (Abg), where the 2F α M-Abg species turned over 100 times faster compared to the 2F α G-Abg species (1.0×10^{-3} vs $1.2 \times 10^{-5} \text{ min}^{-1}$).

Table 2.4: Kinetic parameters for reaction of pNPGlcA, 2FGlcAF, 2FManAF, 5FGlcAF, 5FIdoAF, and 2FIdoAF with *E. coli* β -glucuronidase.

Compound	k_{re} or k_{cat} (min^{-1}) ^a	K_m or K_i' (mM)	k_i (min^{-1})	K_i (mM)	k_{cat}/K_m or k_i/K_i ($\text{min}^{-1}\text{mM}^{-1}$)
pNPGlcA ^b	12000	0.087	-	-	1.4×10^5
2FGlcAF	0.0020 ± 0.0001	0.0063^c	3.7 ± 0.2	11.7 ± 0.9	0.32 ± 0.04
2FManAF	0.00046 ± 0.00029	-	-	-	0.35 ± 0.01
5FGlcAF	0.073 ± 0.006	0.018	4.8 ± 0.6	0.455 ± 0.095	10.5 ± 3.5
5FIdoAF	0.0010 ± 0.0001	4.6	-	-	0.0013 ± 0.0001
2FIdoAF	0.0023 ± 0.0003	1.5	-	-	0.0009 ± 0.0001

^a For inactivators, reactivation rate constants listed

^b Kinetic data determined experimentally

^c K_i' calculated using the equation $K_i' = K_i/(1 + k_i/k_{cat})$

5FGlcAF caused rapid inactivation and exhibited a significant turnover rate relative to the 2-deoxy-2-fluoro analogues. This situation parallels what was observed with Abg. However, whereas the turnover rate for 2F α G-Abg was ~6800-fold lower than 5F α G-Abg, the turnover rate for 2FGlcA-EBG was only ~160-fold lower than for 5FGlcA-EBG.

In the case of both 5FIdoAF and 2FIdoAF, very similar kinetic parameters are observed, leading one to believe that both bind in a similar fashion and that the enzyme-bound sugar is in a conformation that minimizes the difference in electronic effects between a C-2 fluorine and a C-5 fluorine. What is surprising is the fact that turnover of 5FIdoA-EBG and 2FIdoA-EBG proceeded at rates similar to that of 2FGlcA-EBG. Because glucuronic acid and iduronic acid have very different conformations, one would expect that the stability of 2FGlcA-EBG should differ significantly from that of 5FIdoA-EBG and 2FIdoA-EBG, and hence their rates of spontaneous reactivation should also differ. However, perhaps this difference may be offset by the difference in energy between the bound conformation of the *ido* inactivators and the conformation required for its enzymatic hydrolysis.

In summary, we have synthesized five novel fluoroglycopyranosyluronic acid fluoride inactivators. All of them were shown to inactivate EBG in a time-dependent fashion, albeit at widely different rates. These compounds should prove useful in the mechanistic studies of other uronidases.

2.5.2 Identification of the catalytic nucleophile by electrospray MS

Previous studies identifying the catalytic nucleophiles of β -retaining glycosidases have successfully employed both the 2-deoxy-2-fluoro- and the 5-fluoro- β -D-glycosides.³⁵ Indeed, we will later show that this was true in the labelling and identification of the catalytic nucleophile of human β -glucuronidase using 2FGlcAF (see section 2.4.3). However, we wanted to demonstrate that the 5-fluoro-glycopyranosyluronic acid fluorides were also useful in this regard. We thus undertook the task of labelling and identifying the catalytic nucleophile of EBG using 5FGlcAF.

The initial strategy for identification of the active site nucleophile involved first labelling a sample of EBG with 5FGlcAF, then carrying out comparative LC/MS analyses of samples of labelled and unlabeled enzyme that had been subjected to proteolytic digestion. Searching of the total ion chromatograms for a pair of unique peptides differing in mass by exactly the mass of the 5-fluoroglucopyranosyluronic acid moiety (195 Da) should allow the identification of a candidate peptide containing the catalytic nucleophile and bearing the fluorosugar label, which could then be sequenced by tandem mass spectrometry to determine the precise site at which the label was attached.

Peptic hydrolysis of native EBG or 5F-glucopyranosyluronic acid-enzyme resulted in a mixture of peptides that were separated by reverse-phase HPLC using the ESMS as detector. When scanned in the normal LC/MS mode the total ion chromatograms (TIC)

showed a large number of peaks, each corresponding to one or more peptides in the digest mixture. The masses under each peak in the labelled sample were compared with the masses of the corresponding peptides in the native sample, searching for a peptide present only in the labelled sample that was 195 Da greater than a peptide present only in the unlabelled sample. However, no peptide was found matching this criterion.

The absence of such a match did not rule out the presence of a labelled peptide in the treated sample since it was possible that the presence of the sugar moiety could modify the cleavage pattern of pepsin, thereby masking the mass difference. Comparative mapping was therefore performed between EBG labelled with 5FGlcAF and EBG labelled with 2FGlcAF. The difference in mass between 5FGlcAF and 2FGlcAF is 16, allowing for comparative searching of the chromatograms from proteolytic digests of the two labeled samples. These samples would likely have very similar proteolytic digestion profiles, thereby sidestepping the problem of different digestion patterns. Only one pair of peaks with this difference in mass was found, these being a peak with m/z 990 in the 5FGlcAF-treated sample, which was not observed in the 2FGlcAF-treated sample and a peak with m/z 974 in the 2FGlcAF-treated sample that was not observed in that of the 5FGlcAF-treated sample (Figure 2.26). The labeled parent ions (m/z 974 and 990) thus appear as singly charged species. Subtracting 179 and 195 (the masses of the 2FGlcAF and 5FGlcAF labels) from these observed masses gives the molecular weight of the native peptide as 795.

Candidate peptides with a mass of 795 ± 1 Da were then identified by inspection of the amino acid sequence of the enzyme and searching for all possible peptides with this mass. Three such peptides were identified, but one of these was eliminated because its sequence did not contain either an aspartate or a glutamate residue. Precedent with retaining glycosidases to date would predict that the nucleophile should be one of these two amino acids⁷⁸. The candidate peptides are $_{115}\text{EADVTPY}_{121}$ and $_{502}\text{ITEYGVD}_{507}$. The sequence of the peptide was then unambiguously determined by tandem mass spectrometry.

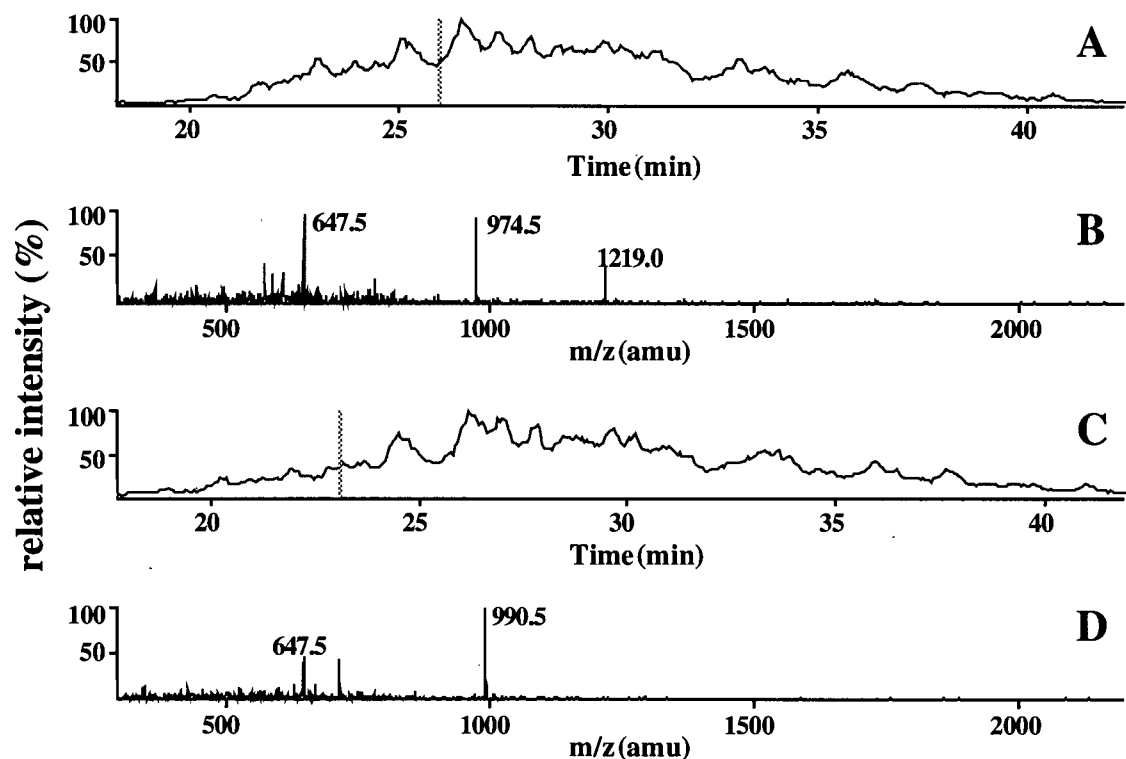


Figure 2.26: Electrospray mass spectrometry experiments on EBG proteolytic digests. A, total ion chromatogram (TIC) of EBG+2FGlcAF. B, mass spectrum of peptides at 26 min in A. C, TIC of EBG+5FGlcAF. D, mass spectrum of peptides at 23 min in C. Vertical grey lines in A and C indicate the regions of the chromatograms for which mass spectra are shown in B and D.

Peptide Sequencing

Information on the sequence was obtained by additional fragmentation of the peptides of interest (m/z 974 and 990) in the daughter ion scan mode (Fig. 2.27).

The parent ion of interest was selected in the first quadrupole and subjected to collision-induced fragmentation, and then the masses of the daughter ions were detected in the third quadrupole. In each sample, peaks with a mass difference of 16 arising from B ions bearing either a 2FGlcAF or a 5FGlcAF label include ITE (m/z 523 and 539), ITEY (m/z 686 and 702), ITEYG (m/z 743 and 759), and ITEYGV (m/z 842 and 858). Because the B ions bearing the label include only one amino acid with a carboxylic acid group (glutamic acid), we can infer that the label is linked to Glu504. This information, in conjunction with the mass of the labeled peptide and the primary sequence of the enzyme, permits identification of the peptide containing the active site nucleophile as $_{502}\text{ITEYGVD}_{507}$. Comparison of this sequence with those of the other Family 2 glycosidase sequences shows that the dipeptide EY is conserved throughout the known family members (Table 2.5). However, the amino acids around this dipeptide are conserved only within a particular glycosidase category, i.e. galactosidase vs glucuronidase vs mannosidase. From this we can assign Glu504 as the catalytic nucleophile.

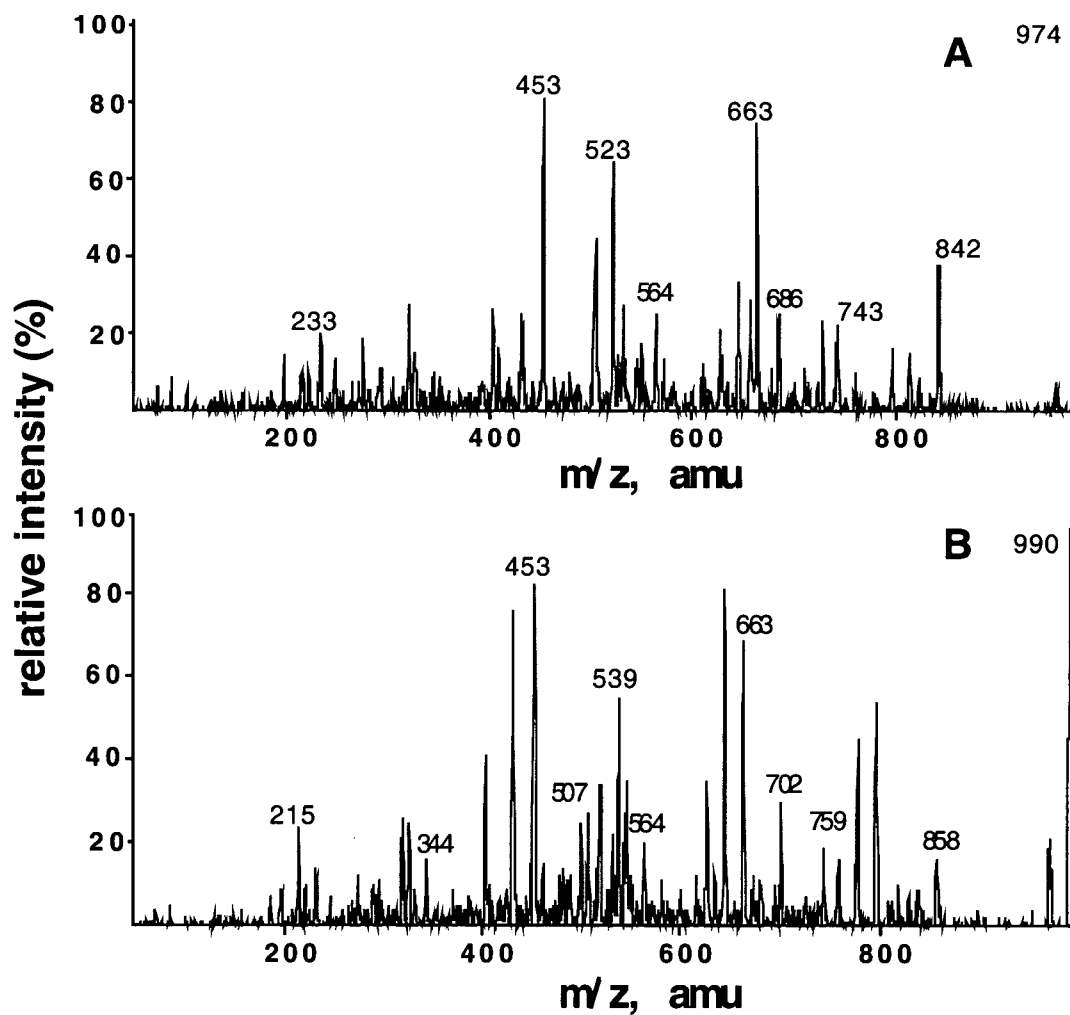
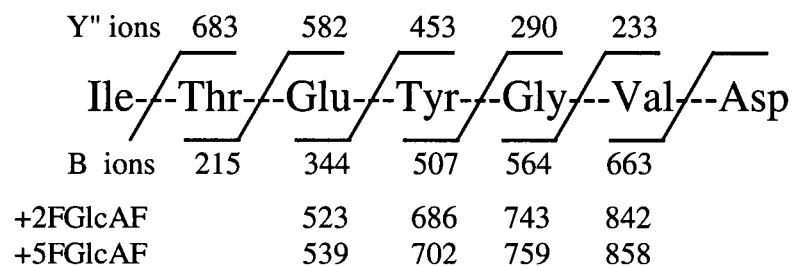


Figure 2.27: Electrospray tandem MS daughter ion spectrum of labeled peptides. A, Observed fragments for peptide labelled with 2FGlcAF. B, Observed fragments for peptide labelled with 5FGlcAF. The sizes of the observed B and Y'' series fragments are shown above.

2.5.3 Conclusion

The novel compound 5-fluoro- β -D-glucopyranosyluronic acid fluoride was shown to be an effective mechanism-based inactivator of the β -glucuronidase from *E. coli*. The reagent functions via the formation of a stable, catalytically competent 5-fluoroglucopyranosyluronic acid-enzyme intermediate. Proteolysis of this labelled enzyme coupled with tandem mass spectrometric analysis revealed the labeled residue as Glu504 within the sequence ₅₀₂ITEYGVD₅₀₈.

Table 2.5: Conserved active site residues of Family 2 glycosidases. The enzymes are grouped according to substrate specificity.

Group	Sequence	Species
galactosidases	507 PRIICE EY AHAM	<i>Escherichia coli</i> alpha-subunit
	520 PYISCE EY MHSM	<i>Clostridium acetobutylicum</i>
	532 PLILCE EY AHAM	<i>Escherichia coli</i>
	539 PLILCE EY AHAM	<i>Klebsiella pneumoniae</i>
	546 PLILCE EY GHAM	<i>Kluyveromyces lactis</i>
	526 PFISV EY AHAM	<i>Lactobacillus delbrueckii</i>
	529 PFLNCE EY MHDM	<i>Leuconostoc lactis</i>
	640 PYISCE EY MHTM	<i>Streptococcus thermophilus</i>
	457 PYLVTE EY NGHM	<i>Thermoanaerobacter thermosulfurogenes</i>
glucuronidases	534 PIIQSE EY GAET	<i>Canis familiaris</i>
	499 PIIITE EY GVDT	<i>Escherichia coli</i>
	535 PIIQSE EY GAET	<i>Homo sapiens</i>
	531 PIIQSE EY GADA	<i>Mus musculus</i>
	531 PIIQSE EY GADA	<i>Rattus norvegicus</i>
mannosidases	549 ARFVSE EY GYQS	<i>Bos taurus</i>
	549 ARFVSE EY GYQS	<i>Capra hircus</i>
	549 ARFASE EY GYQS	<i>Homo sapiens</i>
	554 PRCASE EY GVQS	<i>Caenorhabditis elegans</i>

2.6 Studies employing HBG

2.6.1 Stereochemistry of HBG hydrolysis

Prior to the inhibitor studies with the 2-deoxy-2-fluoro-glycosides, we wished to demonstrate that HBG does indeed hydrolyze its substrates with retention of anomeric configuration. To do this, we employed a NMR spectroscopic experiment.

The use of proton NMR in the determination of the stereochemical course of enzyme catalyzed glycoside hydrolyses has been demonstrated previously.^{79,80} Chemical shifts and coupling constants of the anomeric protons of α - and β -glycosides, and the product hemiacetals are distinct and readily observed. When sufficient enzyme is used to complete the hydrolysis quickly (typically <2 minutes), the initially formed anomer is detected before mutarotation has occurred to any significant extent. Figure 2.28 illustrates the experiment performed using HBG. Fig. 2.28A shows the anomeric proton region of pNPGlcA prior to the addition of enzyme. The multiplet centred at δ 5.18-5.28 ppm arises from the axial anomeric proton of the β -glycoside substrate and the large resonance at δ 4.7 is from HOD. Figures 2.28B, 2.28C, and 2.28D were recorded at time intervals after addition of the enzyme. As can be seen (Figure 2.28B), the enzymatic hydrolysis was essentially complete after 1.5 minutes since the resonance at δ 5.18-5.28 ppm has almost disappeared. Simultaneously, a new resonance has appeared at δ 4.58 (J = 7.9 Hz). The chemical shift and coupling constant identify this as the axial anomeric proton of β -D-glucuronic acid. After 4 minutes, a new doublet has appeared at δ 5.18 (J

= 3.6 Hz) (Figure 2.28C). This corresponds to the equatorial anomeric proton of α -D-glucuronic acid resulting from mutarotation of the initial β -D-glucuronic acid product. After 20 minutes, the product D- glucuronic acid has converted via mutarotation to the equilibrium ratio of anomers (34:66 α/β) (Figure 2.28D). The data unequivocally demonstrate that hydrolysis catalyzed by HBG proceeds with net retention of anomeric configuration, presumably via a double displacement mechanism.

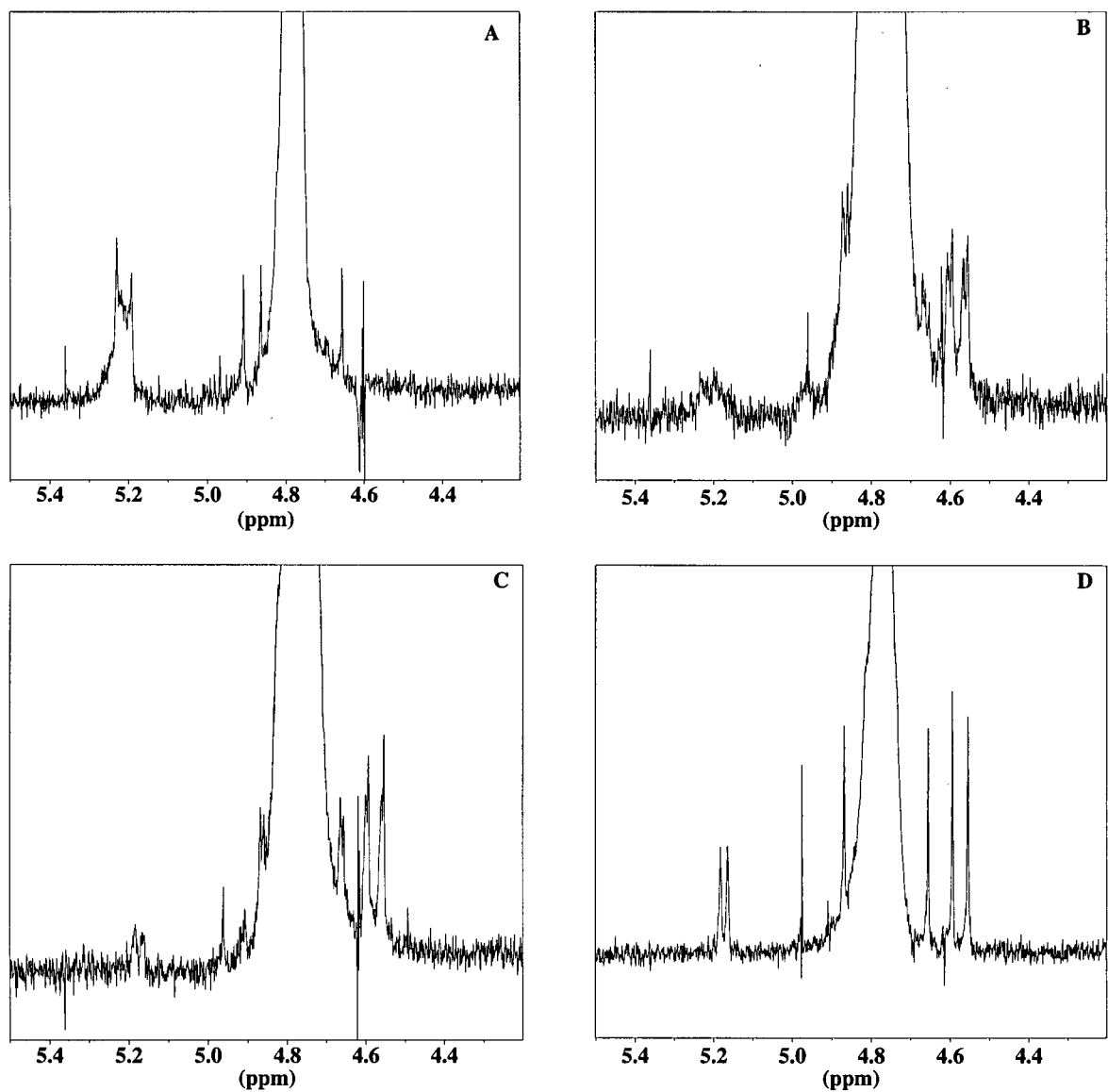


Figure 2.28: Proton NMR spectra showing the stereochemical course of hydrolysis of pNPGlcA by HBG. Spectra are for the anomeric proton region of the substrate at different time intervals relative to addition of HBG: A) 0 min. B) 1.5 min. C) 4 min. D) 20 min. The large peak at ~4.7 ppm is due to HOD.

2.6.2 Inactivation Kinetics using 2FGlcAF and 2FManAF

Incubation of HBG with 2FGlcAF resulted in inactivation of the enzyme in a time dependent manner according to pseudo first order kinetics (Figure 2.29A). However, no saturation was observed, even at the highest inactivator concentrations studied (Figure 2.29B). Yet higher concentrations could not be investigated due to the rapidity of inactivation, which precluded accurate sampling. Reliable values for the inactivation rate constant (k_i) or the reversible dissociation constant (K_i) could not, therefore, be determined. However, a reliable second order rate constant of $k_i/K_i = 0.19 \pm 0.01 \text{ min}^{-1} \text{ mM}^{-1}$ was calculated for the slope of the plot of k_{obs} vs [2FGlcAF].

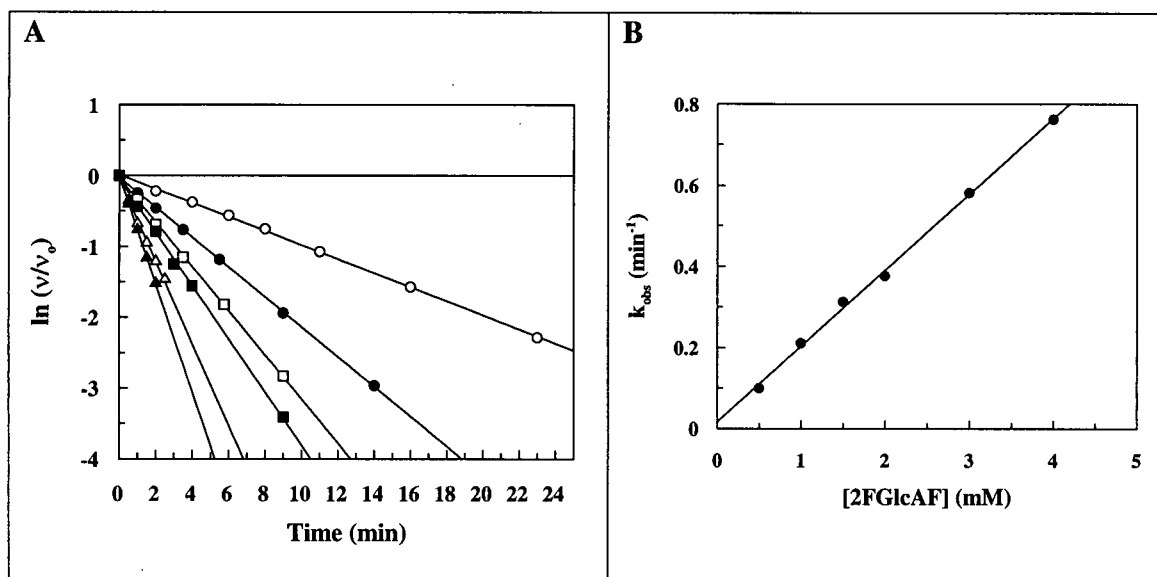


Figure 2.29: Inactivation of HBG by 2FGlcAF. A, semilogarithmic plot of residual activity versus time at the indicated inactivator concentrations: 0.5 mM (○), 1 mM (●), 1.5 mM (□), 2 mM (■), 3 mM (△), and 4 mM (▲). B, replot of the first-order rate constants from A.

We also tested 2FManAF with HBG. Similarly, a value of $k_i/K_i = 0.56 \pm 0.01 \text{ min}^{-1} \text{ mM}^{-1}$ was calculated for the slope of the plot of k_{obs} vs [2FManAF] (Figure 2.30).

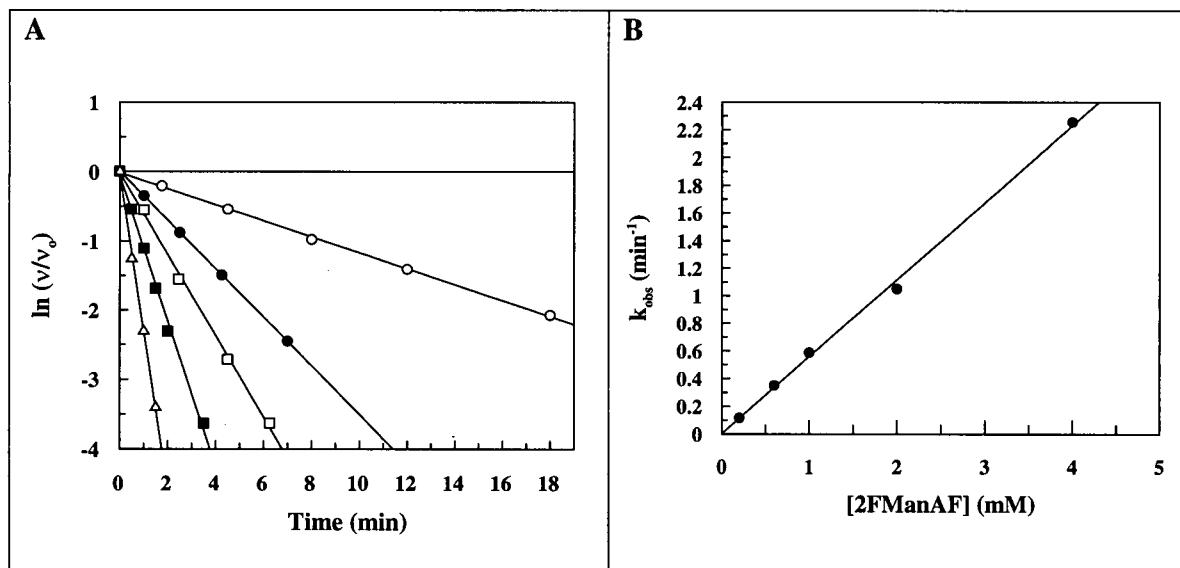


Figure 2.30: Inactivation of HBG by 2FManAF. A, semilogarithmic plot of residual activity versus time at the indicated inactivator concentrations: 0.2 mM (○), 0.6 mM (●), 1 mM (□), 2 mM (■), and 4 mM (△). B, replot of the first-order rate constants from A.

Incubation of the enzyme with 2FGlcAF (150 μM) in the presence of the competitive inhibitor D-saccharic acid 1,4-lactone (0.68 μM , $K_i = 0.23 \mu\text{M}$) resulted in a two-phase reaction (Figure 2.31). This behaviour is due to the slow binding of the inhibitor to the enzyme. The initial inactivation rate constant was calculated to be 0.054 min^{-1} , nearly identical to the apparent inactivation rate constant of 0.057 min^{-1} obtained in the absence of the lactone. The final inactivation rate constant was calculated to be 0.019 min^{-1} . This observed protection from inactivation in the presence of the lactone is consistent with 2FGlcAF being active site directed. These results suggest that inactivation is a

consequence of accumulation of a stable covalent 2-deoxy-2-fluoro- α -D-glucopyranosyluronic acid-enzyme intermediate, a conclusion that is supported by the mass spectral analysis of the inactivated enzyme.

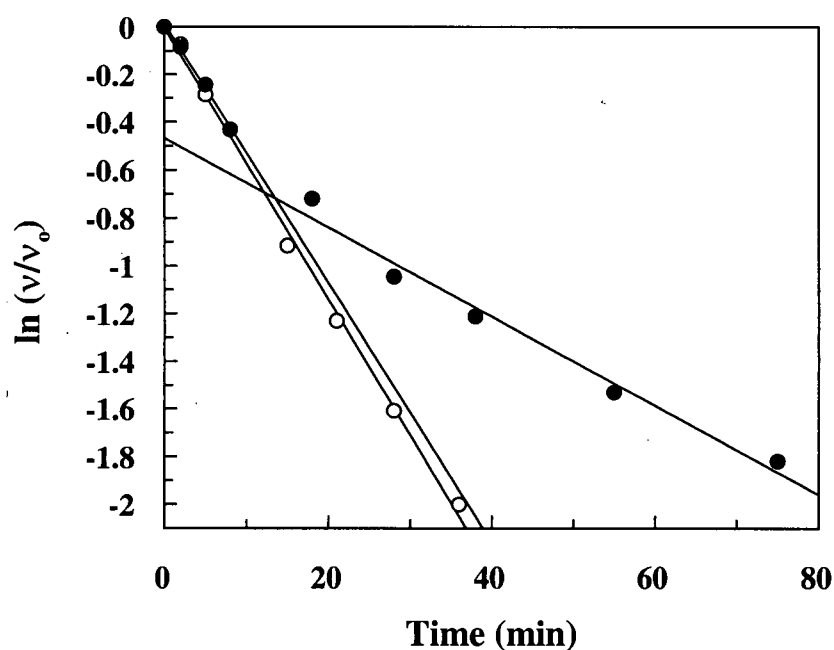


Figure 2.31: Inactivation with 150 μ M 2FGlcAF in the absence (○) and presence (●) of 0.68 μ M D-saccharic acid 1,4-lactone.

Catalytic Competence

Further evidence supporting the existence of a covalent 2F-glucopyranosyluronic acid-enzyme arises from demonstration of the catalytic competence of the trapped intermediate. Following removal of excess inactivator from the labeled enzyme, the sample was incubated at 37°C in the presence of buffer alone, with 50 mM chitobiose or with 50 mM *N*-acetyl-glucosamine, and the recovery of activity associated with the regeneration of the free enzyme was monitored. Reactivation kinetics of the 2F-

glucopyranosyluronic acid-enzyme in buffer alone followed a first order process with an apparent rate constant of $k_{re} = 0.0040 \text{ hr}^{-1}$ ($t_{1/2} = 173 \text{ hr}$) (Figure 2.32). Rate constants for reactivation by transglycosylation (k_{trans}) were found to be 0.0033 hr^{-1} ($t_{1/2} = 210 \text{ hr}$) with *N*-acetyl-glucosamine and 0.0072 hr^{-1} ($t_{1/2} = 96 \text{ hr}$) with chitobiose. The higher enzyme reactivation rate observed in the presence of chitobiose (2 fold higher than the spontaneous reactivation rate) suggests that reactivation is accelerated by transglycosylation to an acceptor sugar. That chitobiose functions as a transglycosylation acceptor is not surprising since the natural substrates of HBG are the glycosaminoglycans, oligosaccharides composed of alternating glucuronic acid and *N*-acetyl-glucosamine residues, and chitobiose is a GlcNAc(β 1-4)GlcNAc disaccharide. However, the fact that *N*-acetyl-glucosamine apparently slows the rate of reactivation indicates that it may be binding to the enzyme in a non-productive fashion, i.e. the active site of HBG most likely has more than one binding site to accommodate the aglycone portion of its natural substrate and the *N*-acetyl-glucosamine is binding in a site non-adjacent to the bound inactivator. This would preclude another nucleophile, such as water, from entering the active site and cleaving the bound 2-fluorosugar to reactivate the enzyme.

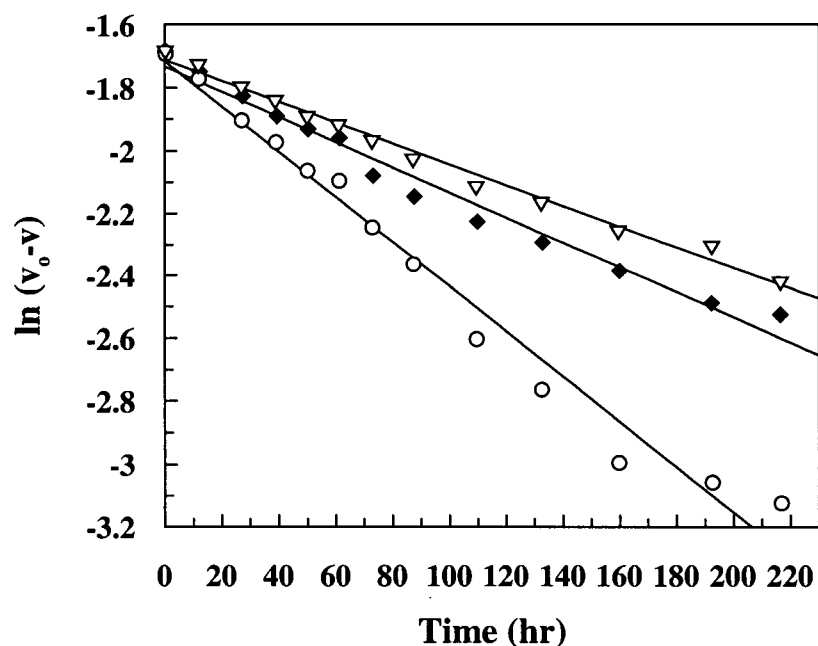


Figure 2.32: Reactivation of 2F-glucopyranosyluronic acid glucuronidase. Semilogarithmic plot of activity vs. time in buffer alone (◆), with 50 mM chitobiose (○), or with 50 mM *N*-acetyl-glucosamine (▽).

2.6.3 Identification of the catalytic nucleophile by electrospray MS

Peptic hydrolysis of native HBG or 2F-glucopyranosyluronic acid-enzyme resulted in a mixture of peptides which were separated by reverse-phase HPLC using the ESMS as detector. When scanned in the normal LC/MS mode the total ion chromatograms (TIC) showed a large number of peaks, each corresponding to one or more peptides in the digest mixture (Figures 2.33A and 2.33C). The masses under each peak in the labeled sample were compared with the masses of the corresponding peptides in the native sample, searching for a peptide present only in the labeled sample that was 178 Da greater than a peptide present only in the unlabelled sample. Only one pair of peaks satisfied this requirement of difference in mass by that of the attached label, these being a

peak with m/z 756 in the native digest which was not observed in the labeled digest (Figure 2.33B) and a peak with m/z 934 in the labeled digest which was not observed in that of the native enzyme (Figure 2.33D). The mass difference between these two peaks is 178, which corresponds exactly to the mass of the 2F-glucopyranosyluronic acid label. The labeled parent ion (m/z 934) and the unlabelled intact peptide (m/z 756) thus appear as singly charged species.

Candidate peptides with a mass of 756 ± 2 Da were then identified by inspection of the amino acid sequence of the enzyme and searching for all possible peptides with this mass. Twenty such peptides were identified but of these, all but five were eliminated because their sequences did not contain either an aspartate or a glutamate residue. Precedent with all retaining glycosidases to date would predict that the nucleophile should be one of these two amino acids. The candidate peptides are $_{257}\text{KLEVRL}_{262}$, $_{60}\text{EEQWY}_{64}$, $_{318}\text{DFYTL P}_{323}$, $_{484}\text{NSNYAAD}_{490}$, and $_{539}\text{SEYGAET}_{545}$. The peptide was then unambiguously identified by peptide sequencing using MS/MS.

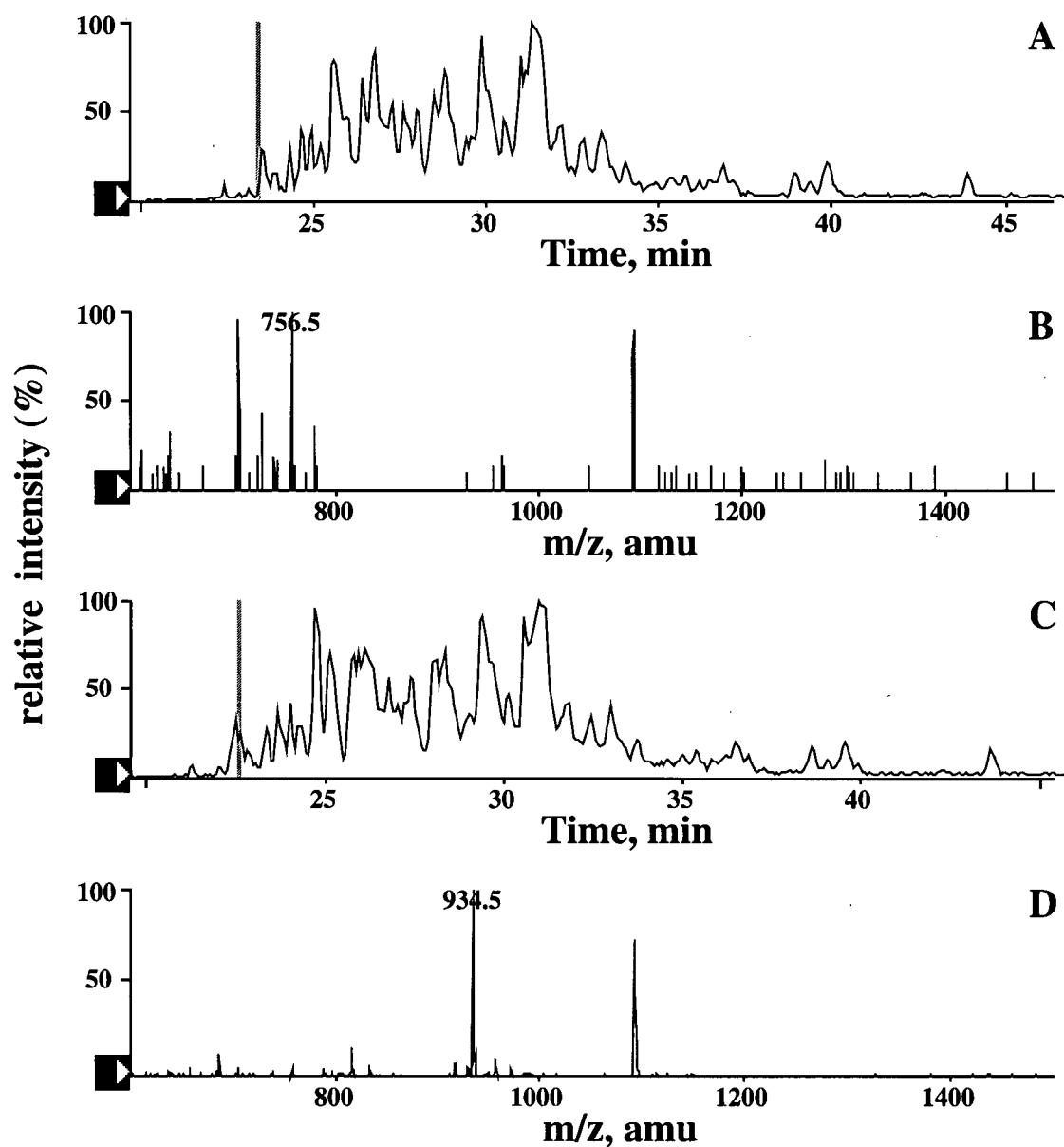


Figure 2.33: ESMS experiments on a peptic digest of human β -glucuronidase. A) unlabelled enzyme, TIC in normal MS mode. B) peptides at 23.5 min in A. C) enzyme labeled with 2FGlcAF, TIC in normal MS mode. D) peptides at 22.7 min in C.

Peptide Sequencing

Information on the sequence was obtained by additional fragmentation of the peptide of interest (m/z 934) in the daughter ion scan mode (Figure 2.34). The parent ion of interest

(m/z 934) was selected in the first quadrupole and subjected to collision-induced fragmentation, and then the masses of the daughter ions were detected in the third quadrupole. Peaks resulting from Y⁺ ions correspond to fragments ET (m/z 249), AET (m/z 320), GAET (m/z 378), YGAET (m/z 540), and EYGAET (m/z 669). Peaks arising from B ions bearing the label include SE (m/z 395), SEY (m/z 558), SEYG (m/z 616), SEYGA (m/z 687), and SEYGAE (m/z 816). Because the B ions bearing the label include SE (m/z 395) we can infer that the label is linked to either Ser539 or Glu540. This information, in conjunction with the mass of the labeled peptide and the primary sequence of the enzyme, permits identification of the peptide containing the active site nucleophile as ${}_{539}\text{SEYGAET}_{545}$ (Figure 2.35).

As with EBG, comparison of the isolated peptide sequence with those of the other Family 2 glycosidase sequences reveals the conserved dipeptide EY (Table 2.5). Within the glucuronidases, we note that the sequence SEYGA is almost completely conserved (only *E. coli*'s enzyme has a slightly different sequence – TEYGV). From this we can assign Glu540 as the catalytic nucleophile of HBG.

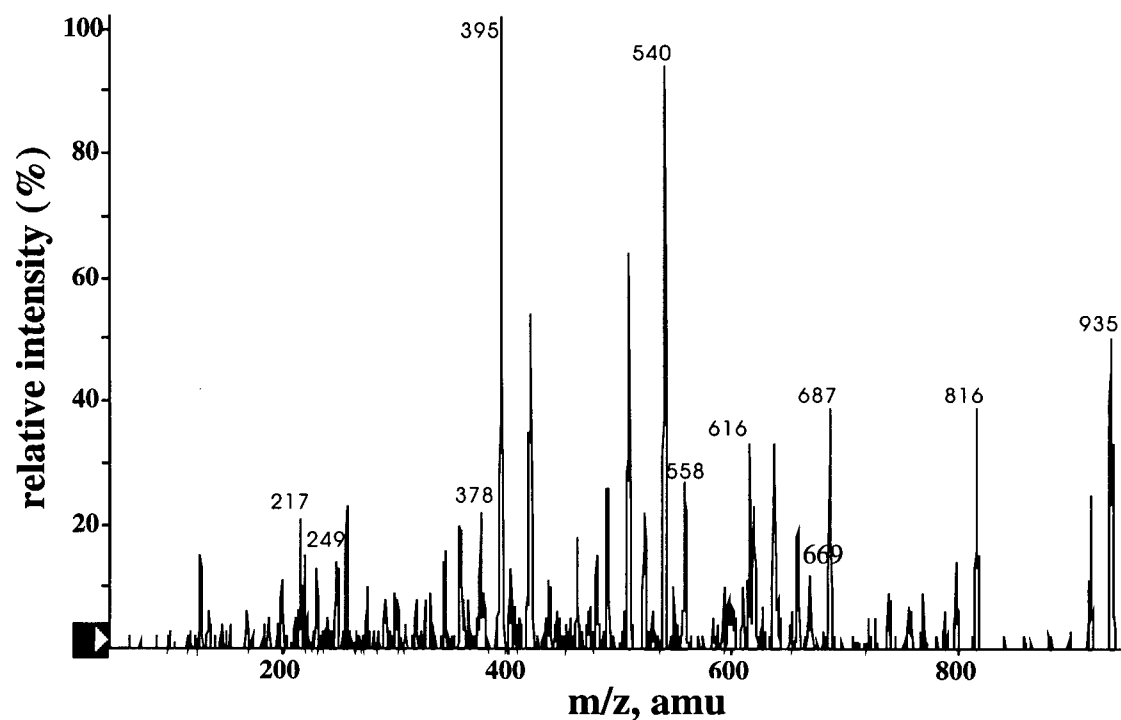


Figure 2.34: ESMS/MS daughter ion spectrum of the 2F-glucopyranosyluronic acid peptide (m/z 934, in the singly charged state).

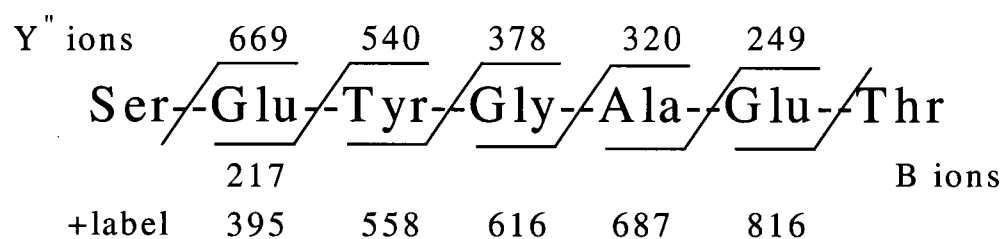


Figure 2.35: Sequence of the 2FGlcA-HBG peptide. Observed B and Y'' series fragments are shown below and above the peptide sequence, respectively.

2.6.4 Conclusion

Both 2FGlcAF and 2FManAF were found to be good time-dependent inactivators of HBG, with the *manno* compound having a second order rate constant three times larger than that of the *gluco* compound (0.56 and $0.19 \text{ min}^{-1} \text{ mM}^{-1}$, respectively). This could be a consequence of 2FManAF being inherently more reactive than 2FGlcAF, a view supported by the spontaneous hydrolysis data for these inactivators ($t_{1/2}$ (2FManAF) = 0.019 min^{-1} vs $t_{1/2}$ (2FGlcAF) = 0.0075 min^{-1}).

Aside from a mechanistic interest in comparing 2FGlcAF and 2FManAF, our interest in the latter compound stems from the fact that a ^{18}F -radiolabelled version of it may be useful as a positron emission tomography agent. The *manno* compound would be rapidly accessible via electrophilic fluorination with ^{18}F -fluorine of the glycol of glucuronic acid, while the synthesis of the *gluco* compound would be much more time-consuming. The radiolabelled compound could be used to temporarily label HBG which, when administered to a patient, would allow for the localization of the enzyme *in vivo*. The radiolabelling of a glycosidase *in vitro* has previously been demonstrated using a ^{18}F -radiolabelled 2-deoxy-2-fluoro- β -D-mannosyl fluoride.⁸¹

Doubts have been expressed previously concerning the identity of the catalytic nucleophile of HBG. In particular, on the basis of the three-dimensional crystal structure, it had been suggested that Asp207 might well serve in that role.⁹ Further, the fact that EBGal is a metalloenzyme, requiring a Mg^{2+} bound at the active site for catalytic activity whereas HBG has no such requirement causes concerns about parallels drawn between

the two enzyme active sites. These are further heightened by the fact that HBG cleaves a substrate containing a carboxylic acid, thus a different active site composition may be required to accommodate this additional charge. However, the assignment of Glu540 as the catalytic nucleophile of HBG removes any ambiguity concerning the identity of this residue and is completely consistent with expectations on the basis of sequence similarity.¹

2.7 Studies employing IDUA

Note: these studies were performed in collaboration with Catharine E. Nieman and are included here for completeness.

2.7.1 Previous studies using 5FIdoAF

5FIdoAF was tested as both an inactivator and a reversible competitive inhibitor of IDUA.⁶⁵ No time-dependent inactivation was found; rather, enzyme activity dropped immediately to a constant level with the amount of decrease depending on the concentration of 5FIdoAF, indicating competitive inhibition. An assay of enzyme activity in the presence of 50 μM MUI (4-methylumbelliferyl- α -L-idopyranosiduronic acid, $K_m = 15 \mu\text{M}$ and $V_{\max} = 12 \mu\text{mol}/(\text{min}\cdot\text{mg})$) and varying concentrations of 5FIdoAF yielded a linear plot of $1/V$ versus $[5\text{FIdoAF}]$. A value of $K_i' = 1.2 \mu\text{M}$ was determined from this data. Such a low value for K_i' is most likely explained by the fact that 5FIdoAF is acting as a slow substrate. Indeed, the author found that this was the case when

fluoride release was monitored using a fluoride electrode. To show that turnover of 5FIdoAF proceeded via a covalent glycosyl-enzyme intermediate, IDUA was treated with the compound, proteolytically digested and the peptide fragments subjected to LC/MS analysis. A doubly charged labelled peptide found only in the treated enzyme mix was determined to have the sequence $_{291}\text{ADTPIYNDEADPLVG}_{305}$ with $m/z = 893 \pm 1$. Further MS/MS fragmentation of this peptide narrowed the location of the label to either Asp298 or Glu299. While no peptide fragments were observed that point to the label being on Asp298, the labelled fragment EADPLVG, with $m/z = 895$, was found (at low intensities), indicating that the label is on Glu299. However, there was some ambiguity in the identification. To this end, we attempted to confirm Glu299's role as the nucleophilic residue through the use of the alternate inactivator 2-deoxy-2-fluoro- α -L-idopyranosyluronic acid fluoride (2FIdoAF).

2.7.2 Inactivation kinetics using 2FIdoAF

When 2FIdoAF was tested as a time-dependent inactivator of IDUA, similar results were obtained as with 5FIdoAF, i.e. no time-dependent inactivation was found; instead, enzyme activity dropped immediately to a constant level with the amount of decrease depending on the concentration of 2FIdoAF (Figure 2.36).

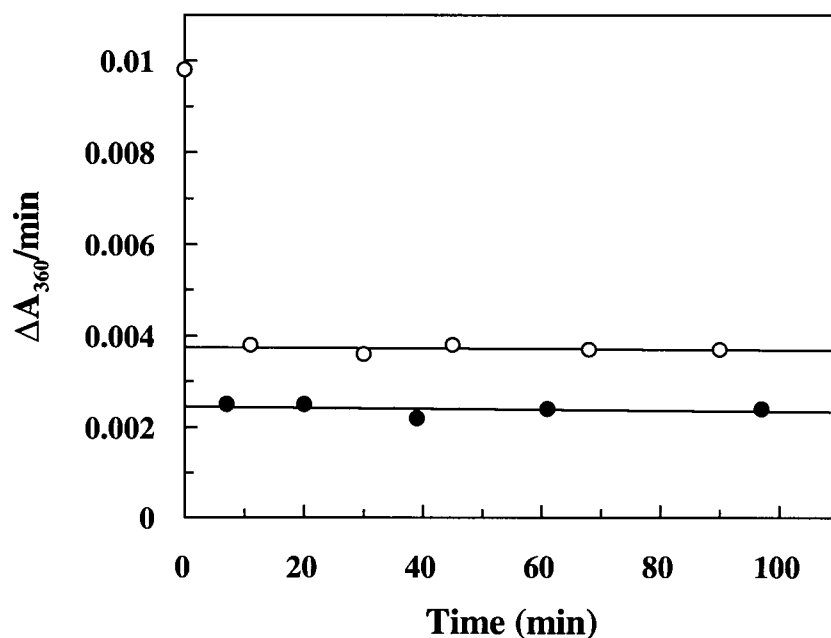


Figure 2.36: Testing of 2FIdoAF as a time-dependent inactivator of IDUA. Plot of residual activity versus time at the indicated inactivator concentrations: 1 mM (○) and 4 mM (●).

2FIdoAF was then tested as a reversible competitive inhibitor of IDUA. To do this, the kinetic parameters K_m and V_{max} were first determined for the substrate of choice (pNPIdoA). They were found to be 53 μM and 4.4 $\mu\text{mol}/(\text{min}\cdot\text{mg})$, respectively. An assay of enzyme activity in the presence of 119 μM pNPIdoA and varying concentrations of 2FIdoAF yielded a linear plot of $1/V$ versus [2FIdoAF] described by the equation $y = 215x + 1009$. Intersection of this line with $y = 1/V_{max}$ yielded a value of $K_i' = 4.6 \mu\text{M}$ (Figure 2.37).

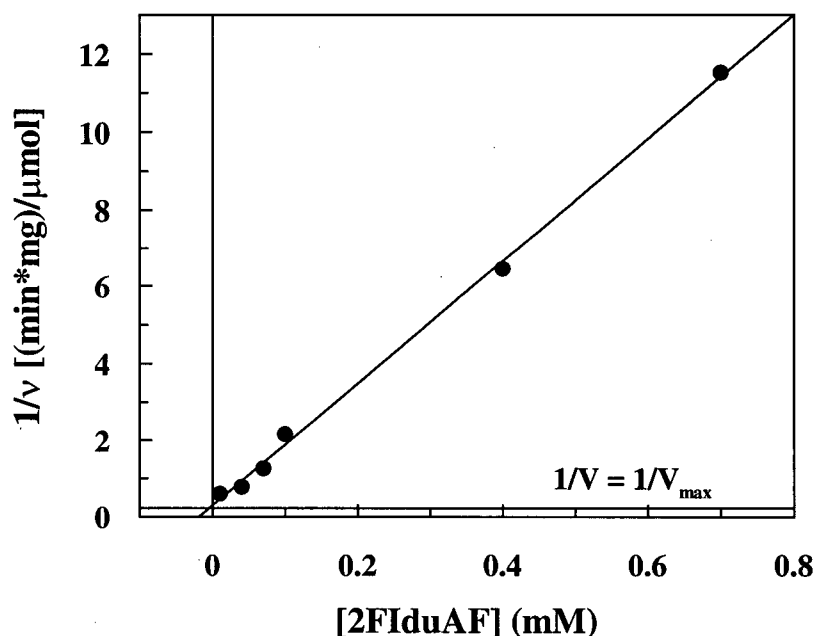


Figure 2.37: Reversible K_i' for 2FIdoAF with IDUA determined under steady-state conditions. The plot of $1/V$ versus $[2FIdoAF]$ intersects a line given by $1/V_m$ at $-K_i'$.

2.7.3 Identification of the catalytic nucleophile by electrospray MS

Assuming that IDUA does form a covalent glycosyl-enzyme intermediate with 2FIdoAF, we attempted to label the enzyme and to identify its catalytic nucleophile. These experiments were carried out in an analogous fashion to those for EBG and HBG. IDUA was treated with 2FIdoAF, then proteolytically digested and the subsequent peptide mixture analyzed by LC/MS.

Comparison of the masses of the peptides under each peak of the TIC for the labelled sample versus those for the unlabelled sample revealed a peptide of $m/z = 1769$ present

only in the labelled sample (Figure 2.38). Furthermore, a peak corresponding to a peptide fragment of $m/z = 885$ was also noted. This is most likely the doubly charged species of the peptide with $m/z = 1769$. Based on the mass of the 2F-idopyranosyluronic acid moiety (179), the parent peptide fragment thus has a molecular weight of 1590.

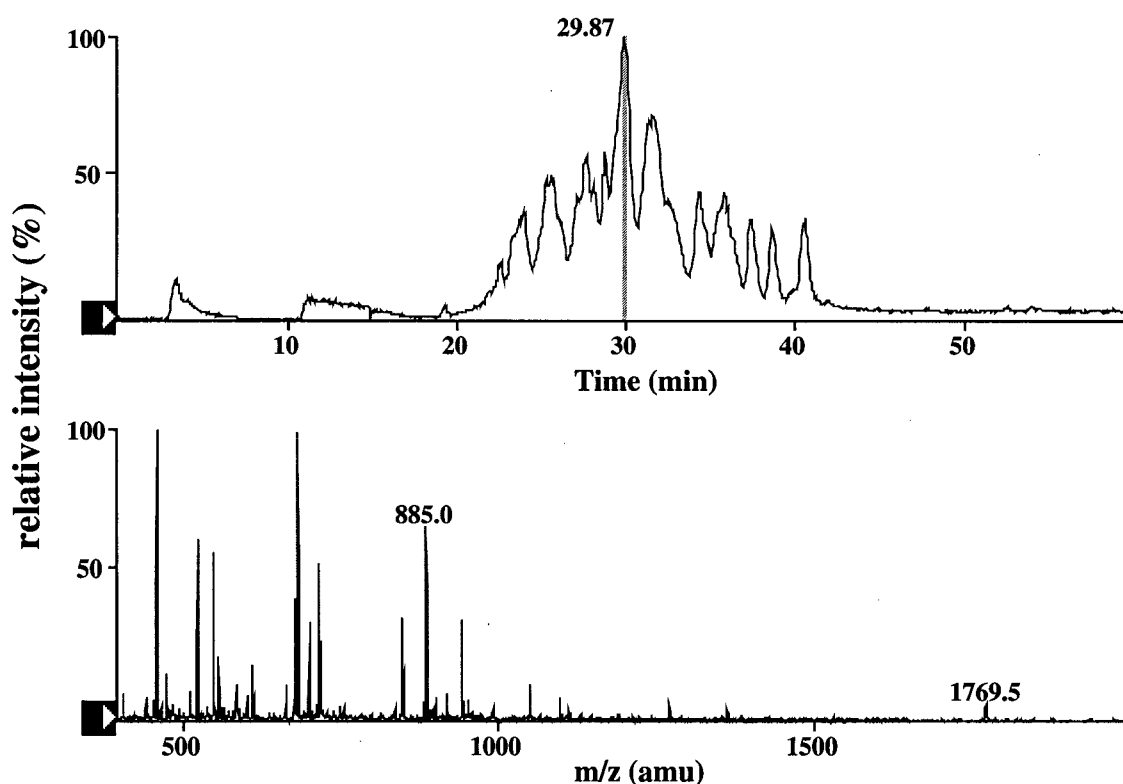


Figure 2.38: Electrospray mass spectrometry experiment on labelled IDUA proteolytic digest. The upper trace shows the total ion chromatogram (TIC) of IDUA labelled with 2FIdoAF. The lower trace shows the mass spectrum of peptides at 29.87 min with the unique peptide having $m/z = 1769$ (singly charged) and $m/z = 885$ (doubly charged) indicated.

Candidate peptides with a mass of 1590 ± 1 Da were then identified by inspection of the amino acid sequence of the enzyme and searching for all possible peptides with this mass. Seventeen such peptides were identified but of these, all but six were eliminated

because their sequences did not contain either an aspartate or a glutamate residue, or contained more than one basic residue (this would then give rise to a triply charged species). Precedent with all retaining glycosidases to date would predict that the nucleophile should be an aspartate or a glutamate residue. The candidate peptides are ¹²²RENQLLPGFELMGS₁₃₅, ²⁴⁵TNFFTGEAGVRLDY₂₅₈, ²⁹¹ADTPIYNDEADPLVG₃₀₅, ²⁹³TPIYNDEADPLVGW₃₀₆, ⁴⁰¹LWAEVSQAGTVLDSN₄₉₀, and ⁶⁰⁵FVFSPDTGAVSGSYR₆₁₉. The peptide was then unambiguously identified by peptide sequencing using MS/MS.

Peptide Sequencing

Information on the sequence was obtained by additional fragmentation of the peptide of interest ($m/z = 885$) in the daughter ion scan mode (Figure 2.39A). The parent ion of interest ($m/z = 885$) was selected in the first quadrupole and subjected to collision-induced fragmentation, and then the masses of the daughter ions were detected in the third quadrupole. Peaks resulting from Y'' and B ions are tabulated (Table 2.6). This information, in conjunction with the mass of the labeled peptide and the primary sequence of the enzyme, permits identification of the peptide containing the active site nucleophile as ²⁹¹ADTPIYNDEADPLVG₃₀₅ (Figure 2.40).

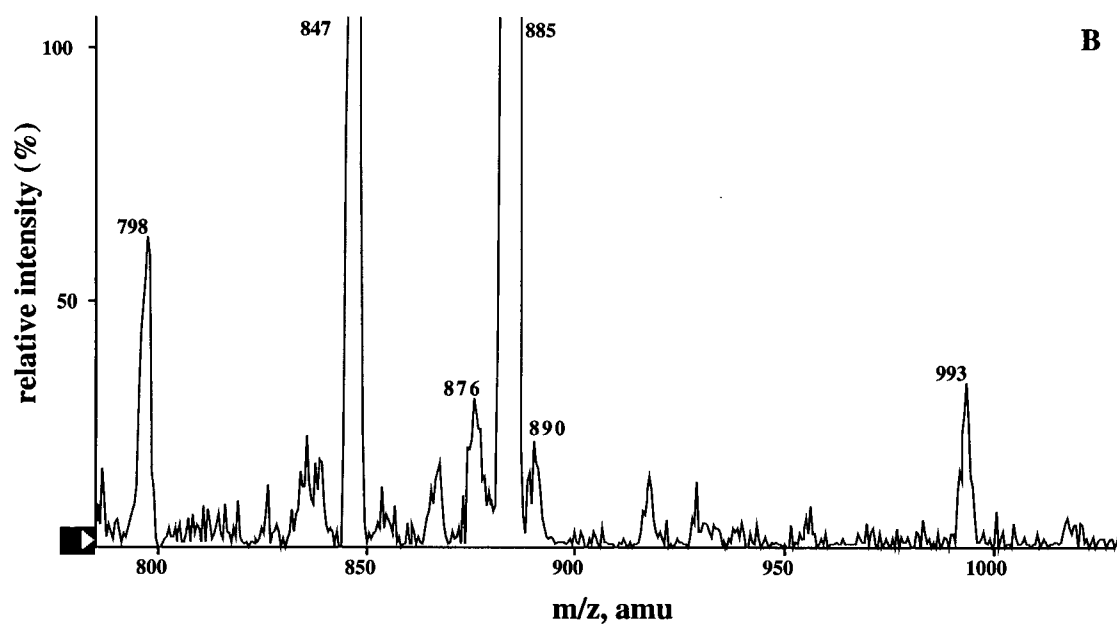
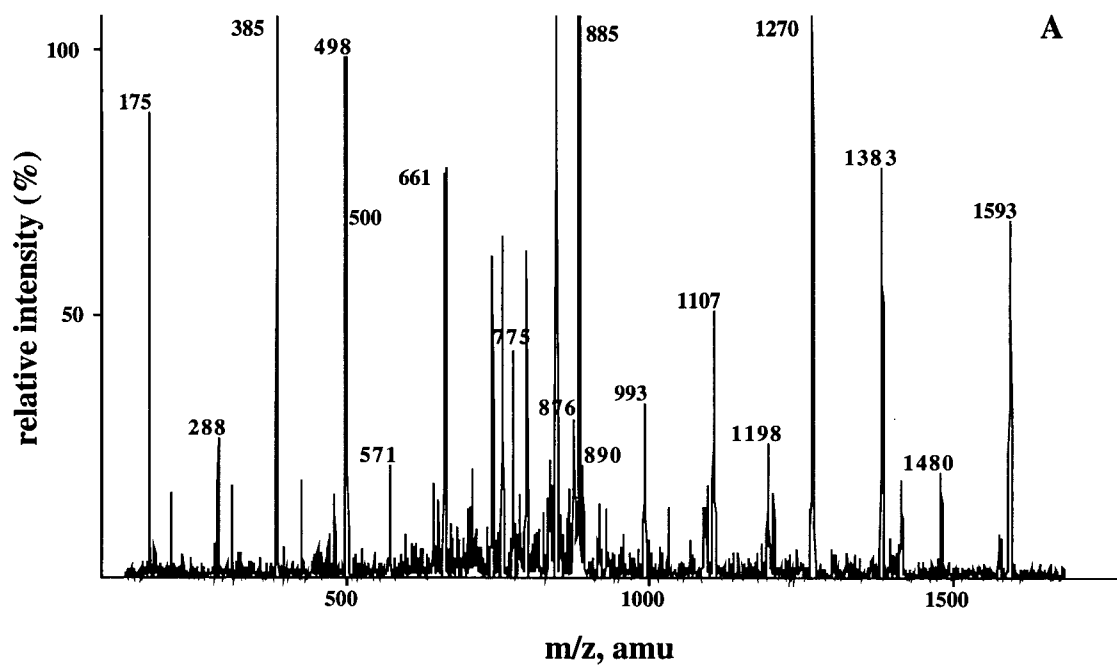


Figure 2.39: ESMS/MS daughter ion spectrum of the 2F-iduronyl peptide (m/z 885). **A)** Original trace with selected peaks labeled. **B)** Expansion of region around parent peptide peak (m/z 885).

Table 2.6: Observed peptide fragments resulting from fragmentation of the labelled parent peptide ($m/z = 885$). Bolded sequences contain the 2FIdoA label.

Fragment m/z	Ion type	Corresponding Sequence
175	Y	VG
288	B or Y	ADT or LVG
385	B or Y	ADTP or PLVG
498	B	ADTPI
500	Y	DPLVG
571	Y	ADPLVG
663	B	ADTPIY
775	B	ADTPIYN
885	Parent ion (doubly charged)	ADTPIYNDEADPLVG
890	B	ADTPIYND
993	Y	DEADPLVG
1108	Y	NDEADPLVG
1198	B	ADTPIYNDE
1270	Y	YNDEADPLVG
1383	B or Y	ADTPIYNDEAD or IYNDEADPLVG
1480	B or Y	ADTPIYNDEADP or PIYNDEADPLVG
1593	B	ADTPIYNDEADPL

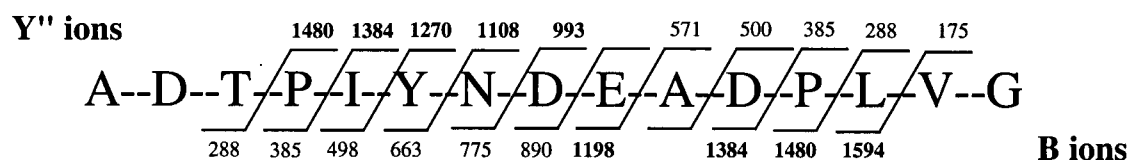


Figure 2.40: Sequence of the 2FIIdA-IDUA peptide. Observed B and Y'' ion fragment masses are shown below and above the parent peptide sequence, respectively. Bolded numbers indicate a labelled fragment.

While the identity of the peptide is quite clear, the site of attachment remains to be determined. Previous data had narrowed the possibilities to Asp298 or Glu299, thus we had hoped to identify a peptide containing the sugar and only one of these two residues. From the tabulated data, it is immediately obvious that the peak corresponding to the

labelled daughter ion fragment ${}_{299}\text{EADPLVG}_{305}$ is missing from the list. This labelled fragment would have $m/z = 878$, a value close to the parent peptide's $m/z = 885$. Expansion of the region around the parent peptide (Figure 2.39B) reveals a fragment of $m/z = 876$. While this might indeed be the labelled peptide of interest, assuming that the uncertainty in the mass would be ± 2 units, the fact that the rest of the peaks observed have masses matching the calculated values casts doubt upon this hypothesis. However, other indirect evidence does support the idea that Glu299 is the labelled residue. Firstly, the observed peak with $m/z = 890$ corresponds to the unlabelled peptide fragment ADTPIYND. The labelled version of this peptide would have a mass of 1068, and this is not observed in the mass spectrum. The counterargument to this would be that the labelled peptide lost the 2-deoxy-2-fluoro- α -L-idopyranosyluronic acid moiety during the fragmentation experiment and thus would not be observed. However, while this is certainly a possibility, the unlabelled counterparts of the observed labelled fragments were not found. One would expect that if one labelled fragment could lose its label, then certainly the other labelled peptides' ester linkage to the 2-deoxy-2-fluoro- α -L-idopyranosyluronic acid moiety would cleave as well. Based upon these arguments, and previous findings by Nieman, we conclude that Glu299 is indeed the labelled residue and hence the catalytic nucleophile.

2.7.4 Conclusion

2FI α AF was not a time dependent inactivator of IDUA, as was hoped. Instead, it acts as a slow substrate, in a similar fashion to 5FI α AF. However, in both cases, the turnover

of the glycosyl-enzyme intermediate was slow enough to allow for the proteolysis of the labelled protein and the isolation of a labelled peptide fragment. This fragment had the same sequence in both cases, ${}_{291}\text{ADTPIYNDEADPLVG}_{305}$ and based on the MS/MS data obtained from collision induced fragmentation of this peptide, the catalytic nucleophile was shown in both cases to be Glu299. This is in agreement with amino acid sequence similarity predictions and dispels doubts about iduronidase's assignment to Family 39.

One wonders why 2FIdoAF did not inactivate IDUA in a time-dependent fashion. However, this is not necessarily surprising in the light of previous attempts at labelling α -glycosidases with 2-deoxy-2-fluoro- α -D-glucosyl fluoride (2F α GF). It was proposed that the 2-deoxy-2-fluoro- β -D-glucosyl-enzyme species that is formed on an α -glucosidase is inherently less stable compared to its 2-deoxy-2-fluoro- α -D-glucosyl-enzyme counterpart. Evidence supporting this theory came from comparison of the spontaneous hydrolysis data for 2-deoxy-2-fluoro- β -D-glucosyl fluoride versus β -D-glucosyl fluoride ($t_{1/2}$ 15 h versus 0.5 h) and for 2-deoxy-2-fluoro- α -D-glucosyl fluoride versus α -D-glucosyl fluoride ($t_{1/2}$ 2900 h versus 19 h).⁷⁶ These data point to a smaller electronic effect of fluorine substitution on the hydrolysis rate for the 2-deoxy-2-fluoro- β -D-glucosyl-enzyme species, suggesting a lesser degree of oxocarbenium ion character at this transition state. This would be consistent with the smaller α -secondary deuterium isotope effects seen with β -methyl glucoside and β -glucosyl fluoride relative to the α anomers.^{18,82}

The 2-deoxy-2-fluoro- α -L-idopyranosyluronic acid fluoride and the 5-fluoro- α -L-idopyranosyluronic acid fluoride might be expected to have 1C_4 conformations. If this is the case and iduronidase binds these compounds in this manner, then reaction of the catalytic nucleophile with these compounds would occur as shown in Figure 2.41.

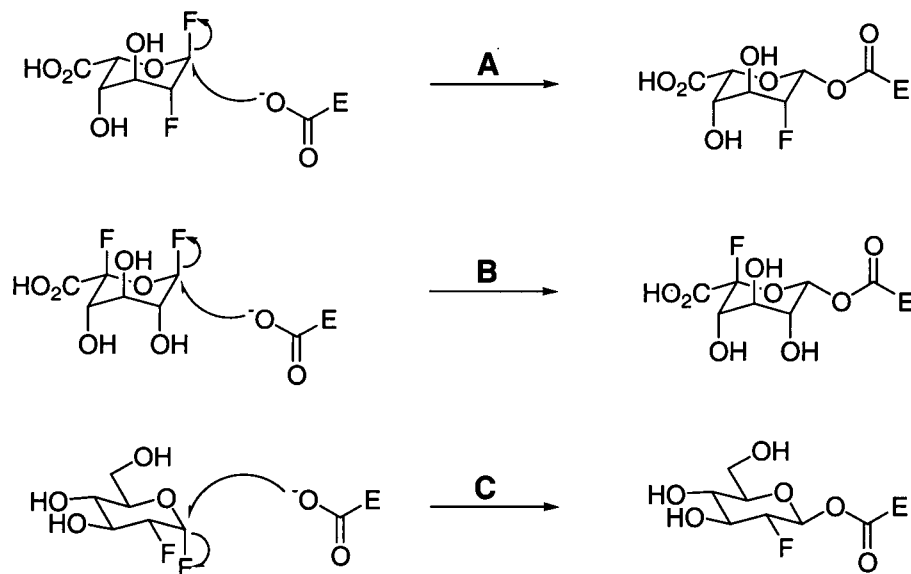


Figure 2.41: Proposed reactions of different fluoro-sugar inactivators with an enzyme active site nucleophilic carboxylate residue. A) 2FIdoAF in a 1C_4 conformation. B) 5FIdoAF in a 1C_4 conformation. C) 2F α GF in a 4C_1 conformation.

In each case, the new bond formed is in an equatorial position on the ring and would thus be inherently unstable.

In the above scheme, the reaction of 5FIdoAF with an enzymic nucleophile was included. Would we expect 5FIdoAF and 2FIdoAF to react in a manner similar to IDUA? The following table lists the values of k_{re} (the rate constant for spontaneous reactivation) or

k_{cat} , and K_i' (the reversible inhibition constant) obtained for 2F α GF, 5F α GF, 2FI α AF and 5FI α AF.

Table 2.7: Values of k_{re} and K_i' obtained for 2F α GF and 5F α GF (yeast α -glucosidase), and 2FI α AF and 5FI α AF (EBG and IDUA)

Compound	k_{re} or k_{cat} (min^{-1})	K_i' (mM)
2F α GF (yeast α -glucosidase)	96 ^a	4.8
5F α GF (yeast α -glucosidase)	6.6 ^a	0.0014
2FI α AF (EBG)	0.0023 \pm 0.0003	1.5
5FI α AF (EBG)	0.0010 \pm 0.0001	4.6
2FI α AF (IDUA)	-	0.0046
5FI α AF (IDUA)	50 ^b	0.0012

^a taken from ref. 76

^b obtained from fluoride release measurements using a fluoride electrode⁶⁵

One notes that in the case of yeast α -glucosidase, k_{re} decreased 15-fold when 2F α GF was switched to 5F α GF. However, only a 2-fold difference was observed between 2FI α AF and 5FI α AF with EBG. While we did not measure a k_{re} value for 2FI α AF with IDUA, the fact that both 2FI α AF and 5FI α AF behave in similar fashion, i.e. slow substrates, leads one to believe that it will be similar to k_{re} for 5FI α AF. Assuming that the inactivators for yeast α -glucosidase bind in a ⁴C₁ conformation, this would lead one to suspect that both 2FI α AF and 5FI α AF may bind in a conformation other than a chair to counteract the difference in electronic effects between a C-2 fluorine and a C-5 fluorine.

Recently, two crystal structures of family 11 xylanases were obtained showing a 2-deoxy-2-fluoro-xylose moiety bound at the -1 subsite in a boat (${}^{2,5}\text{B}$) conformation.^{12,83} This would be highly unusual for D-sugars possessing a hydroxymethyl group or a carboxylate at C-5 where the preferred conformation is ${}^4\text{C}_1$. In a ${}^{2,5}\text{B}$ conformation, the C-5 substituent would be forced into a pseudo-axial orientation causing destabilizing interactions with the C-2 hydrogen. Xylose has no C-5 substituent, and can thus adopt this conformation. α -L-Iduronic acid is a sugar that can adopt a number of different conformations. If it adopted a ${}^{2,5}\text{B}$ conformation, the C-5 carboxylate would be pseudo-equatorial and thus there would be no destabilizing flagpole interactions.

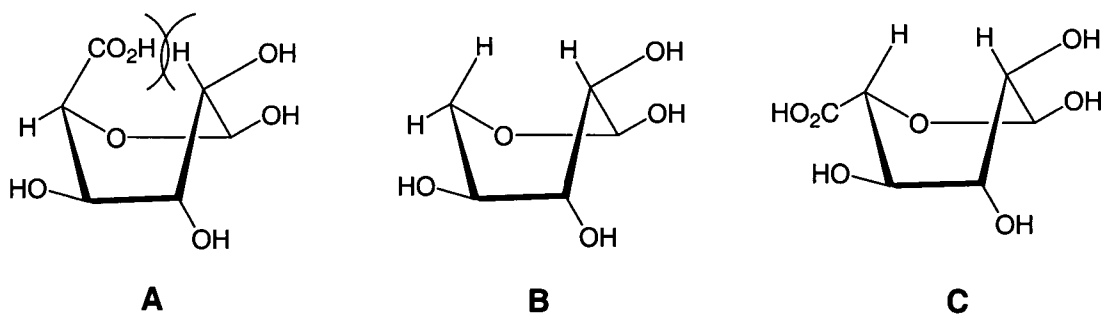


Figure 2.42: ${}^{2,5}\text{B}$ conformations of different pyranose sugars. A) β -D-glucuronic acid; B) D-xylose; C) α -L-iduronic acid.

If both 2FIdoAF and 5FIdoAF were to adopt this conformation in the active site, then perhaps it would minimize the difference in electronic effect between a C-2 and a C-5 fluorine.

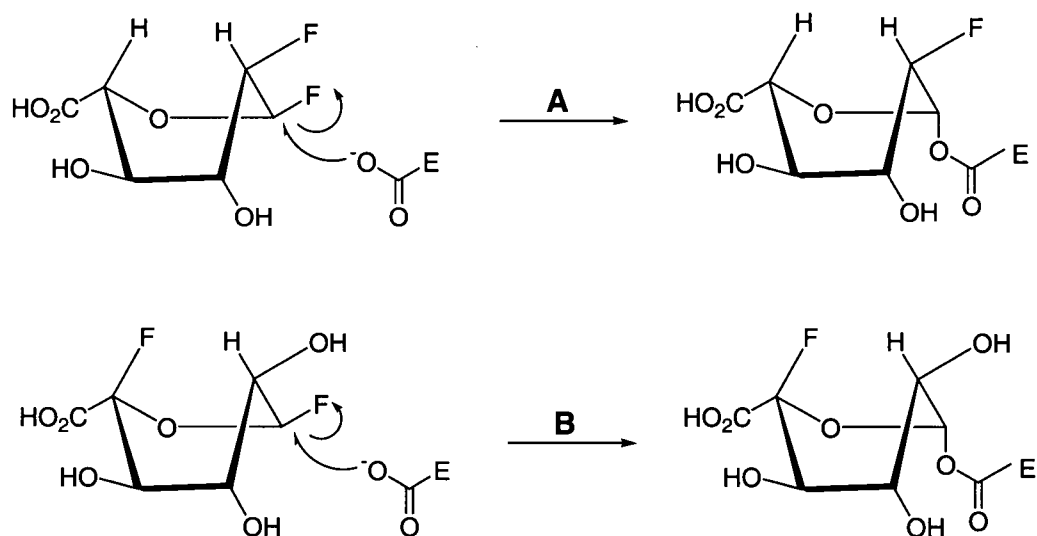


Figure 2.43: Proposed reactions of 2FidoAF and 5FidoAF with IDUA. Both sugars are shown in a ^{2,5}B conformation. A) 2FidoAF; B) 5FidoAF.

Currently, efforts at crystallizing IDUA are underway.⁸⁴ Once the protein has been crystallized, it would indeed be interesting to eventually attempt to soak in one of these inactivators and observe the bound sugar's conformation.

Chapter 3 Attempted Radiolabelling of Glucocerebrosidase

3.1 Introduction

Glucocerebrosidase (GCase) is an exoglycosidase involved in the breakdown of glucosylceramide.

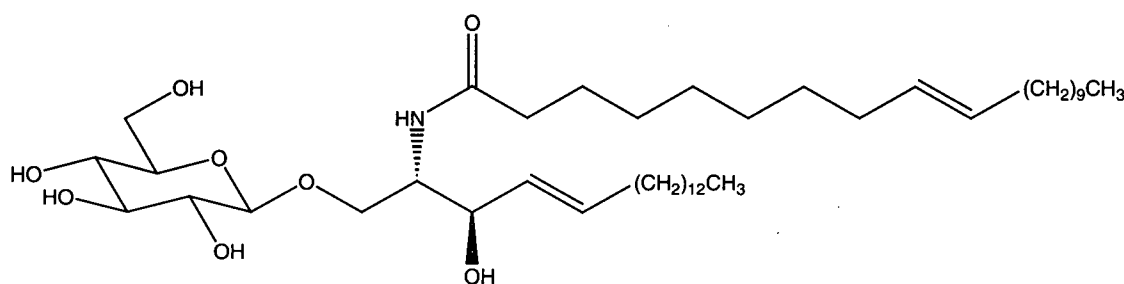


Figure 3.1: Structure of glucosyl ceramide

This glycosidase is a 497 amino acid membrane-associated glycoprotein of 59-67 kDa, depending on the state of glycosidic processing, containing both high mannose and complex oligosaccharides.^{42,85,86} The crucial role of GCase in glycolipid catabolism has been established by the disruption of the GCase gene in mice, such mice dying within hours of birth.⁸⁷ Various point mutations of the human enzyme result in variants of the lysosomal disorder Gaucher disease.⁸⁸ This is the most common of the lysosomal storage disorders, with estimates of 10000-20000 Americans being affected and frequencies of 1 in 57000 (Australia) and 1.16 in 100000 (Netherlands) being reported.⁸⁹⁻⁹¹ The clinical manifestations of this disorder include anemia, thrombocytopenia, leukopenia, hepatosplenomegaly, pulmonary dysfunction, and weakening and undermineralization of bones, leading to spontaneous fractures and painful infarctions. Patients exhibiting these symptoms without signs of central nervous

system involvement (nonneuronopathic) are classified as type I Gaucher disease sufferers. The rarer (neuronopathic) type II Gaucher disease results in hepatosplenomegaly and severe, rapidly progressing brain damage in infancy. A third phenotype, type III Gaucher disease, leads to symptoms as exhibited by type I patients with slow, progressive brain involvement. This is summarized in the following table:

Table 3.1: The clinical manifestations of the three types of Gaucher disease.

Clinical Features	Type I	Type II	Type III
Clinical Onset	Childhood/Adulthood	Infancy	Childhood
Hepatosplenomegaly	+	+	+
Hematologic Complications	+	+	+
Skeletal Involvement	+	-	+
Neurologic Involvement	-	+	+
Survival	Variable	< 2 yrs	2nd - 4th decade
Ethnic Predilection	Ashkenazic Jewish	Panethnic	Northern Swedish

Currently, treatment of patients with type I Gaucher disease has been possible through the use of enzyme replacement therapy.^{92,93} This involves the intravenous administration of recombinant human GCase to the patient. While this is the only lysosomal enzyme in regular use for enzyme replacement therapy, other such proteins being tested in trials include α -L-iduronidase (mucopolysaccharidosis I) and α -galactosidase (Fabry disease). Targetting of administered enzyme is usually investigated via invasive techniques, i.e. tissue biopsy or animal sacrifice.^{94,95} Both diagnosis of the presence and the severity of the disease, as well as the monitoring of treatment would benefit from new non-invasive methods of quantitating and localizing enzyme *in vivo*. Selective covalent inhibitors of

these glycosidases that can be detected by positron emission tomography would be valuable in this regard.

3.1.1 Positron emission tomography (PET)

Positron emission tomography (PET) is a medical imaging technique based on the labelling of biologically active molecules with a short-lived positron-emitting isotope. The location and quantitation of regional concentrations of the administered compound is achieved by computed tomography.⁹⁶

The radionuclides commonly incorporated into biologically active compounds include ^{11}C , ^{13}N , ^{15}O and ^{18}F . Their instability is due to an excessive number of protons in their nuclei and a positive charge. Positron emission stabilizes the nucleus by removing a positive charge through the conversion of a proton into a neutron. Because the positron is the anti-matter equivalent of an electron, a collision with an electron in the surrounding environment leads to mutual annihilation with the simultaneous emission of two high energy (511 keV) photons 180° apart. These coincident photons can then be detected using a ring of detectors surrounding the patient.

Of the four radionuclides commonly in use, ^{18}F is the most convenient to use since it has the longest half-life (110 minutes), thus allowing for flexibility in the type of chemical reaction used to introduce the radioisotope. As well, the energy of the emitted positron is the lowest of the radionuclides (maximum $E(\beta^+) = 0.64 \text{ MeV}$) with a maximum range

travelled of 2.4 mm, allowing for the sharpest imaging with a high-resolution PET detector.⁹⁷

PET studies range from standard image displays that provide indices of physiological function to complex kinetic analysis methods for absolute quantification. Depending on their biochemical properties, PET radiotracers may be divided into two categories.

The first category includes non-specific radiotracers following a biochemical pathway and allowing for measurement of tissue extraction or metabolism. Radiotracers from the first category include: ^{15}O -water which is a freely diffusable inert tracer used for cerebral blood flow measurement; and ^{18}F -deoxyfluoroglucose which follows the initial phases of glucose metabolism but does not enter the Krebs cycle after phosphorylation and therefore is effectively trapped in the cells to allow tissue glucose metabolism measurement.

The second category includes specific radioligands involved in an interaction with a receptor transporter or a receptor site. Radiotracers from this category include ^{11}C -labelled analogues of cocaine used in the study of the dopamine transporter complex. As well, radioligands which covalently modify their target enzymes have also been reported. Examples include deprenyl and clorgyline (monoamine oxidase) and α -fluoromethyl-6-fluoro-L-dopa (L-amino acid decarboxylase).^{98,99}

3.1.2 Earlier Studies using ^{18}F -labelled glycosidase inactivators

Excellent carbohydrate inactivator candidates for the incorporation of ^{18}F are 2-deoxy-2-fluoro- β -D-glycopyranosyl fluorides. Such reagents have been shown to function as specific mechanism-based inactivators of 'retaining' β -glycosidases via formation of a relatively stable 2-deoxy-2-fluoro- α -D-glycopyranosyl-enzyme intermediate.^{43,100} Therefore, by use of a 2-deoxy-2- ^{18}F -fluoroglycopyranosyl fluoride it should be possible to radiolabel all functional glycosidases of that class and then localize them using a PET tomograph.

In an earlier approach to this problem 2-deoxy-2- ^{18}F -fluoro- β -D-mannopyranosyl fluoride was synthesized and shown to covalently derivatize *Agrobacterium* sp. β -glucosidase.⁸¹ Furthermore, it was shown that the trapped species was catalytically competent since it was capable of 'turnover' with release of 2-deoxy-2-fluoro-mannose and native enzyme. Unfortunately tests of this derivative *in vivo* revealed that hydrolysis occurred with formation of 2-deoxy-2-fluoro-mannose which then underwent metabolic conversion resulting in metabolic labelling that obscures the PET signal.

The choice of the synthesized 2-deoxy-2-fluoro- β -D-mannopyranosyl fluoride was a consequence of the relative simplicity and speed of its synthesis in radiolabelled form via electrophilic addition of ^{18}F -fluorine gas to D-glucal. A better, more specific, analogue would appear to be 2-deoxy-2- ^{18}F -fluoro- β -D-glucopyranosyl fluoride. However, rapid synthesis of this derivative in the desired β -anomeric form is non-trivial. Further, should

spontaneous hydrolysis occur, the released 2-deoxy-2-fluoro-glucose would become rapidly phosphorylated and trapped in the cell's glycolytic pathway, obliterating any image from the labelled glycosidase. A possible solution to both problems involves incorporation of ^{18}F at the 6-position since the replacement of the 6-hydroxyl group with fluorine prohibits possible phosphorylation and offers a simpler means of radiolabelling using higher specific activity ^{18}F -fluoride. Earlier studies had demonstrated the tolerance of glycosidases for modifications of the substrate at the 6-position.¹⁰¹

3.2 Specific Aims

Initially, the synthesis of 2,6-dideoxy-2,6-difluoro- β -D-glucopyranosyl fluoride **30** will be carried out and kinetic studies performed on both *Agrobacterium* sp. β -glucosidase (Abg) and on human glucocerebrosidase (GCase). Then the synthesis of 2,6-dideoxy-2-fluoro-6- ^{18}F -fluoro- β -D-glucopyranosyl fluoride **32** will be performed using ^{18}F -fluoride. Finally the radiolabelling of GCase using **32** will be attempted.

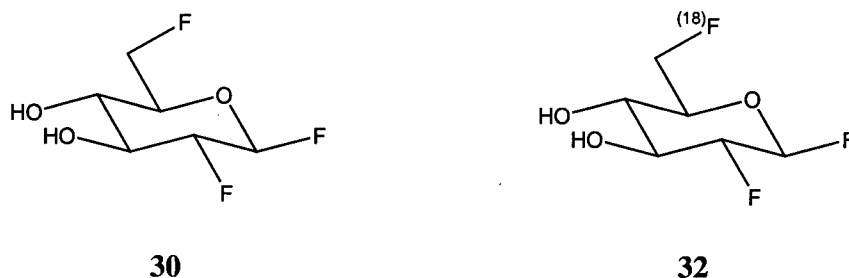


Figure 3.2: Structures of 2,6-dideoxy-2,6-difluoro- β -D-glucopyranosyl fluoride and 2,6-dideoxy-2-fluoro-6- ^{18}F -fluoro- β -D-glucopyranosyl fluoride.

3.3 Results and Discussion

3.3.1 Synthesis

In order to determine whether the proposed 2,6-dideoxy-2,6-difluoro- β -D-glucopyranosyl fluoride would be a good inactivator of GCCase, we had to first synthesize it. The route we chose is illustrated in the following scheme.

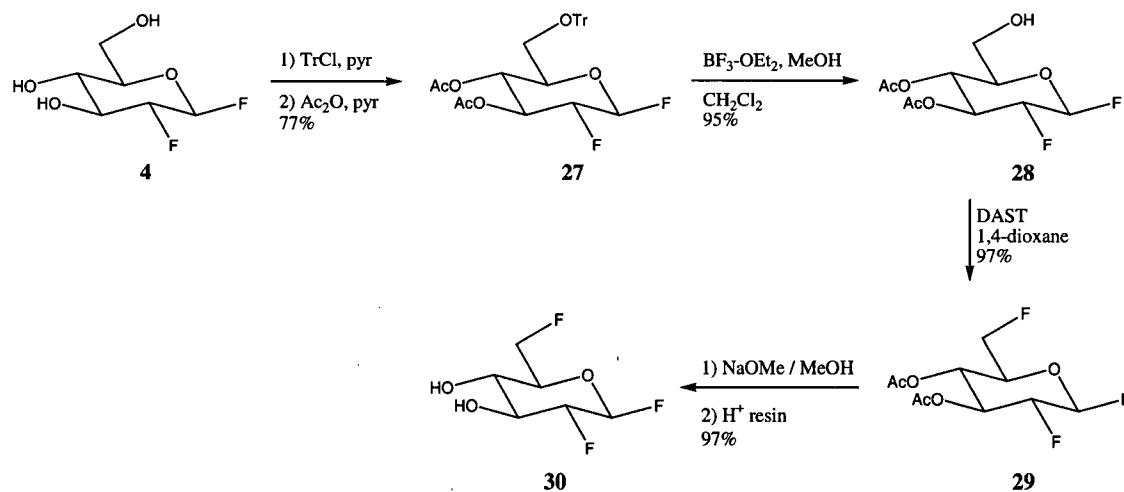


Figure 3.3: Synthetic scheme of 2,6-dideoxy-2,6-difluoro- β -D-glucopyranosyl fluoride **30**.

Selective triphenylmethylation of **4**,¹⁰² followed by acetylation yielded compound **27**. Removal of the trityl group was easily accomplished using boron trifluoride etherate to

afford the alcohol **28**.¹⁰³ This was then treated with diethylaminosulfur trifluoride followed by Zemplén deacetylation to yield the desired product **30**.

3.3.2 Radiosynthesis

Because of the short half-life of ^{18}F , it is essential to have as few chemical steps as possible after the label is introduced. Fortunately for our purposes, we already had in hand a precursor (**28**) that required only activation of the C-6 OH toward nucleophilic displacement with ^{18}F -fluoride. Once a good leaving group was installed at C-6, all that would be required is the actual displacement step and deprotection/purification of the labelled intermediate.

For our purposes, we chose to activate C-6 as the trifluoromethanesulfonic ester because its use is well established in PET chemistry, i.e. with FDG (fluorodeoxyglucose) synthesis. The synthesis of the triflate **31** was relatively straightforward – treatment of **28** with trifluoromethanesulfonic anhydride and 2,6-di-*t*-butylpyridine gave the triflate in 70% yield.

2,6-Dideoxy-2-fluoro-6- ^{18}F -fluoro- β -D-glucopyranosyl fluoride was synthesized via displacement of a good leaving group installed at C-6 with ^{18}F -fluoride.

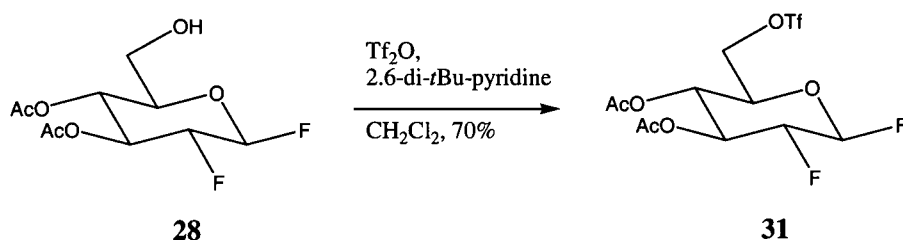


Figure 3.4: Synthetic scheme of 3,4-di-O-acetyl-6-O-trifluoromethanesulfonyl-2-deoxy-2-fluoro- β -D-glucopyranosyl fluoride **31**.

In the proposed radiolabelling experiment, the [^{18}F]-fluoride is normally isolated from the ^{18}O -water after it has been produced, by passing the solution through an anion exchange Sep-Pak. The fluoride is then eluted off the Sep-Pak using a solution of Kryptofix 222, an aminopolyether, and potassium carbonate in acetonitrile/water. Azeotropic distillation with acetonitrile removes the water. The fluoride is then ready to be used as the nucleophile in a displacement reaction. Before attempting to use [^{18}F]-fluoride to displace the C-6 triflate, a test reaction was run using the same procedure that would be used in the radiolabelling experiment, only the fluoride source was potassium fluoride instead of [^{18}F]-fluoride. Using one equivalent of KF, 2,6-dideoxy-2,6-difluoro- β -D-glucopyranosyl fluoride was obtained in 30% isolated yield.

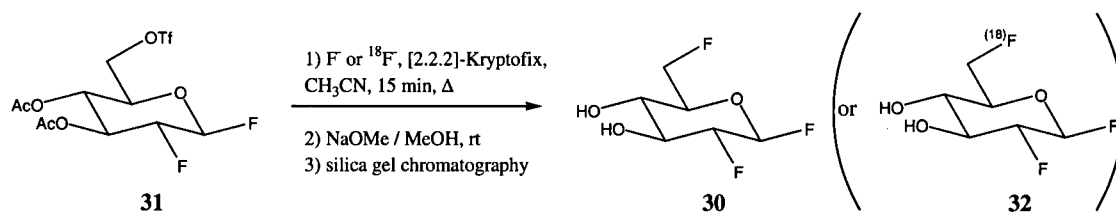


Figure 3.5: Synthetic scheme of 2,6-dideoxy-2,6-difluoro- β -D-glucopyranosyl fluoride **3.1** and 2,6-dideoxy-2-fluoro-6- ^{18}F -fluoro- β -D-glucopyranosyl fluoride **3.2** using fluoride anion.

The radiolabelling experiment was then performed using the same procedure, only [^{18}F]-fluoride, produced by the irradiation of ^{18}O -water with a proton beam, was used. Although the final product could not be analyzed using spectroscopic techniques, thin layer chromatography demonstrated that the purified product had the same R_f value (0.35, 1:1 ethyl acetate:hexanes) as the non-radiolabelled 2,6-dideoxy-2,6-difluoro- β -D-glucopyranosyl fluoride. The overall radiochemical yield for the reaction and purification steps was 9% (corrected for radioactive decay).

To calculate the theoretical amount of radiolabelled compound at the time of purification, we first need to know the specific activity per mole of ^{18}F . For ^{18}F , this number is 1.71×10^9 Ci/mol.⁹⁷

Assuming all of the activity of the purified compound is attributed to ^{18}F , then the number of moles of compound produced can be calculated by dividing the compound's activity by the specific activity of ^{18}F ($0.00415 \text{ Ci} / (1.71 \times 10^9 \text{ Ci/mol})$) to give 2.42×10^{-12} mol. In practice, one never obtains such a high specific activity due to the unavoidable presence of the non-radioactive isotope. Usually, the specific activity is ~5000-fold lower, or 3.42×10^5 Ci/mol.⁹⁷ If we use this number, then the actual amount of compound produced was 1.2×10^{-8} mol.

3.3.3 Kinetic analysis of the reaction of 2,6diFGF with Abg and GCase

Incubation of Abg with 2,6diFGF resulted in inactivation of the enzyme in a time dependent manner according to pseudo first order kinetics (Figure 3.6A). The first order rate constants were plotted versus time (Figure 3.6B). Higher concentrations could not be investigated due to the rapidity of inactivation, which precluded accurate sampling. Values for the inactivation rate constant (k_i) and the reversible dissociation constant (K_i) were determined to be $3.8 \pm 0.5 \text{ min}^{-1}$ and $58.8 \pm 8.4 \text{ mM}$.

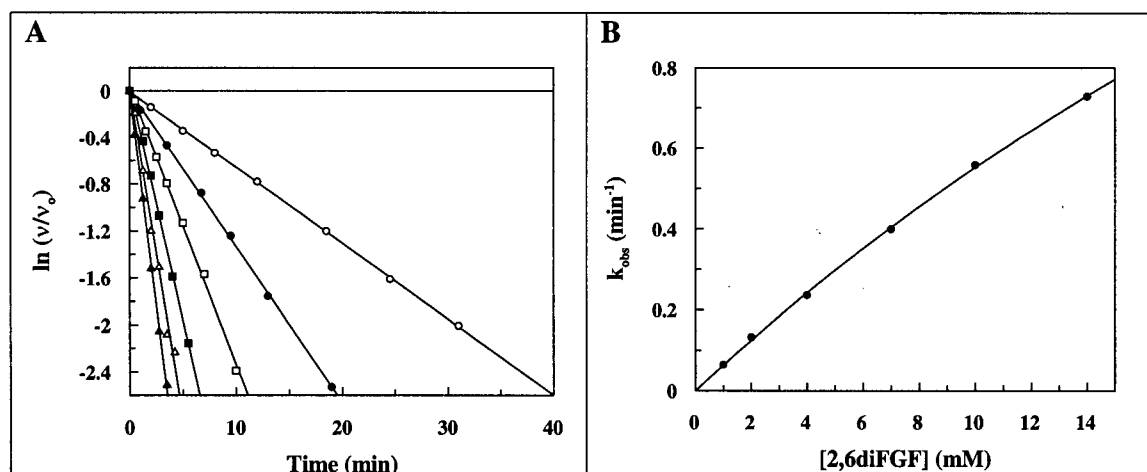


Figure 3.6: Inactivation of *Agrobacterium* sp. β -glucosidase by 2,6diFGF. A, semilogarithmic plot of residual activity versus time at the indicated inactivator concentrations: 1 mM (\circ), 2 mM (\bullet), 4 mM (\square), 7 mM (\blacksquare), 10 mM (\triangle), and 14 mM (\blacktriangle). B, replot of the first-order rate constants from A.

Incubation of Abg with 2,6diFGF (4 mM) in the presence of the competitive inhibitor castanospermine ($3.8 \mu\text{M}$, $K_i = 2.8 \mu\text{M}$) reduced k_{obs} , the pseudo-first order inactivation rate constant, from $0.24 \pm 0.01 \text{ min}^{-1}$ to $0.10 \pm 0.01 \text{ min}^{-1}$ (Figure 3.7). This observed protection from inactivation is consistent with 2,6diFGF being active site directed. These

results suggest that inactivation is a consequence of accumulation of a stable covalent 2,6-dideoxy-2,6-difluoro- α -D-glucopyranosyl-enzyme intermediate.

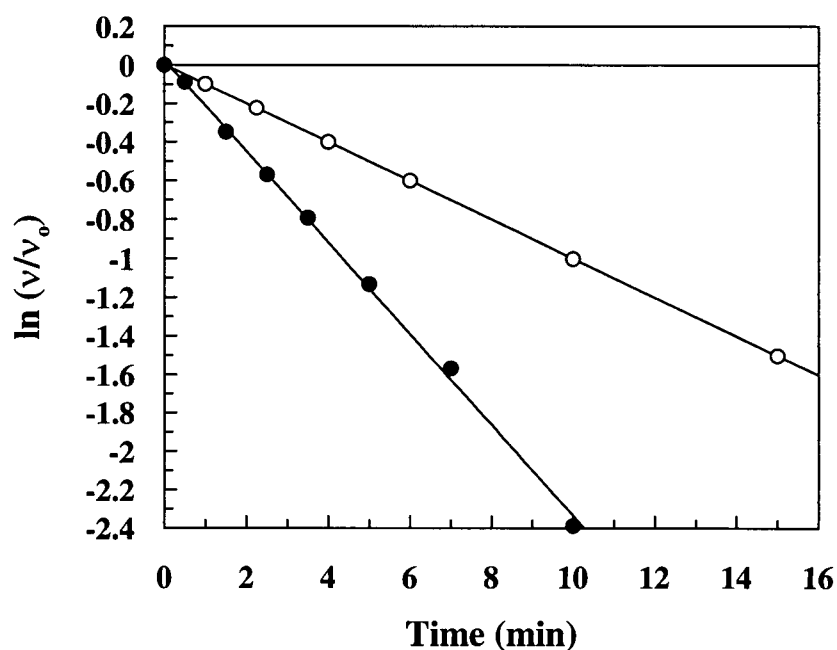


Figure 3.7: Inactivation of Abg with 4 mM 2,6diFGF in the absence (●) and the presence (○) of 3.8 μ M castanospermine.

Inactivation of GCase by 2,6diFGF also occurred according to pseudo first order kinetics (Figure 3.8). Values for the inactivation rate constant (k_i) and the reversible dissociation constant (K_i) were determined to be $0.17 \pm 0.01 \text{ min}^{-1}$ and $101 \pm 17 \text{ mM}$. Incubation of the enzyme with 2,6diFGF (200 mM) in the presence of the competitive inhibitor castanospermine (8.0 μ M, $K_i = 7 \mu\text{M}$) reduced k_{obs} , the pseudo-first order inactivation rate constant by the expected amount, from $0.10 \pm 0.01 \text{ min}^{-1}$ to $0.07 \pm 0.01 \text{ min}^{-1}$ (Figure 3.9).

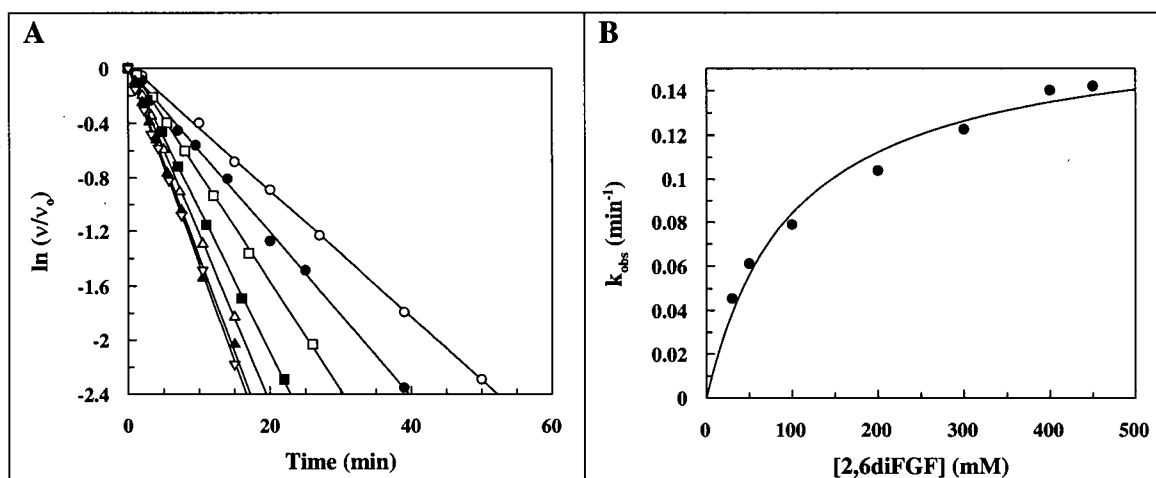


Figure 3.8: Inactivation of human glucocerebrosidase by 2,6diFGF. A, semilogarithmic plot of residual activity versus time at the indicated inactivator concentrations: 30 mM (○), 50 mM (●), 100 mM (□), 200 mM (■), 300 mM (△), 400 mM (▲), and 450 mM (▽). B, replot of the first-order rate constants from A.

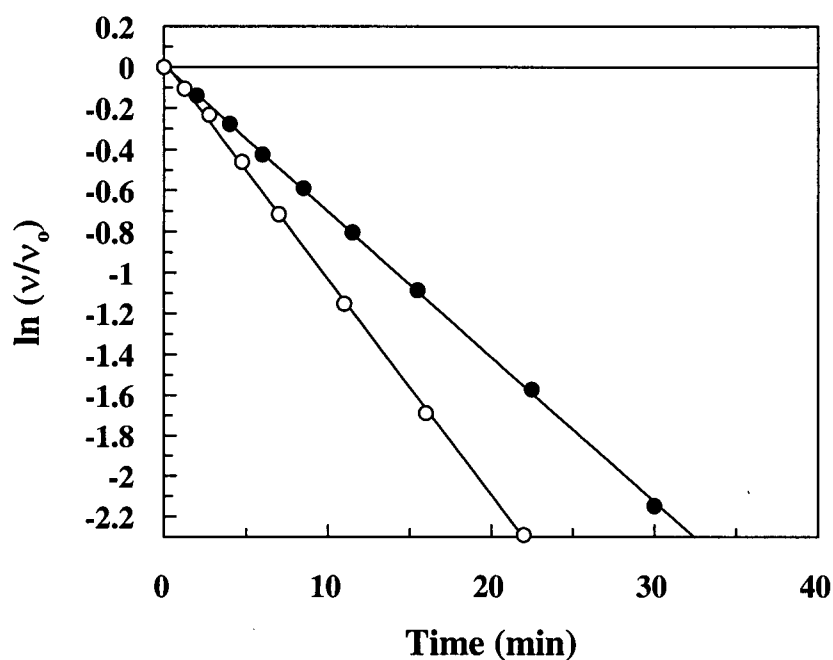


Figure 3.9: Inactivation of GCase with 200 mM 2,6diFGF in the absence (○) and the presence (●) of 8.0 μM castanospermine.

Kinetic parameters for inactivation of Abg and GCase by 2,6-dideoxy-2,6-difluoro- β -D-glucopyranosyl fluoride (2,6diFGF), 2-deoxy-2-fluoro- β -D-glucopyranosyl fluoride (2F β GF) and 2-deoxy-2-fluoro- β -D-mannopyranosyl fluoride (2F β MF) are provided in the following table.

Table 3.2: Kinetic parameters determined for the inactivation of Abg and GCase by 2,6-dideoxy-2,6-difluoro- β -D-glucopyranosyl fluoride (2,6diFGF). For comparison, values previously reported using 2-deoxy-2-fluoro- β -D-glucopyranosyl fluoride (2F β GF) and 2-deoxy-2-fluoro- β -D-mannopyranosyl fluoride (2F β MF) are also shown.^{43,76}

Kinetic parameters	Abg			GCase		
	2,6diFGF	2F β GF	2F β MF	2,6diFGF	2F β GF	2F β MF
k_i (min ⁻¹)	3.8 \pm 0.5	5.9	5.6	0.17 \pm 0.01	-	-
K_i (mM)	58.8 \pm 8.4	0.4	1.2	101 \pm 17	-	-
k_i / K_i (min ⁻¹ mM ⁻¹)	0.065 \pm 0.018	14.75	4.7	0.0017 \pm 0.0004	0.0227	0.0019

Catalytic Competence

Further evidence supporting the existence of a covalent 2,6-dideoxy-2,6-difluoro- α -D-glucopyranosyl-enzyme arises from demonstration of the catalytic competence of the trapped intermediate. Following removal of excess inactivator from the labeled Abg, the sample was incubated at 37 °C in the presence of 20 mM isopropyl- β -D-thioglucoiside, and the recovery of activity associated with the regeneration of the free enzyme was monitored. Reactivation kinetics of the labelled Abg followed a first order process with an apparent rate constant of $k_{re} = 0.0010 \pm 0.0001 \text{ min}^{-1}$ ($t_{1/2} = 693 \text{ min}$) (Figure 3.10A). For GCase, the labelled enzyme, freed of excess inactivator, was incubated in buffer

alone. An apparent rate constant of $k_{re} = 0.00052 \pm 0.00004 \text{ min}^{-1}$ ($t_{1/2} = 1333 \text{ min}$) was obtained (Figure 3.10B).

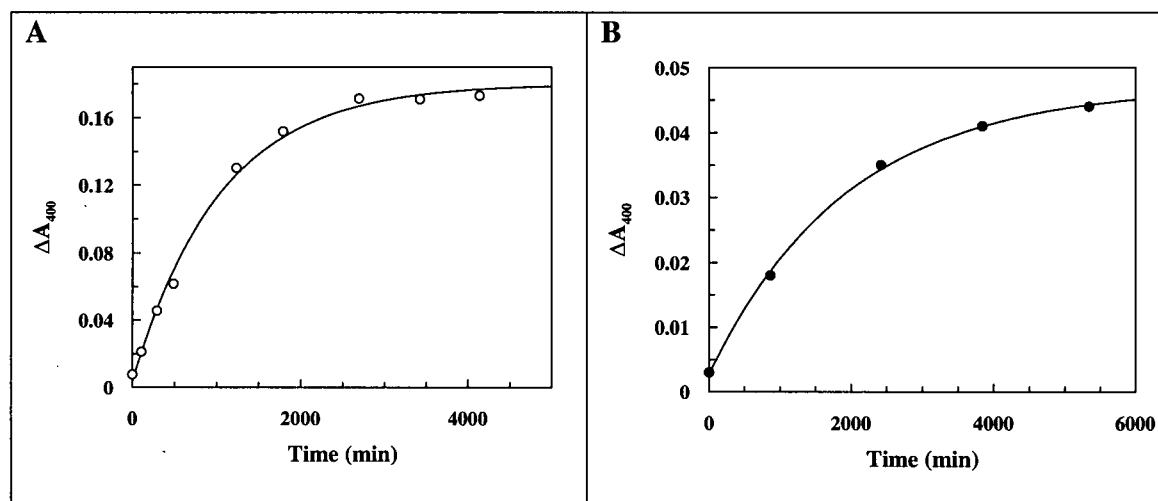


Figure 3.10: A) Reactivation of inactivated *Agrobacterium* sp. β -glucosidase. Shown is a plot of residual activity versus time in the presence of 20 mM isopropyl- β -D-thioglucoiside. B) Reactivation of inactivated human glucocerebrosidase. Shown is a plot of residual activity versus time in buffer alone.

3.3.4 Attempted radiolabelling of GCase

Once the radiolabelled 2,6diFGF was made and purified, it was then added to a sample of glucocerebrosidase (60 U, 3.6 mg, 5.3×10^{-8} mol) and incubated at 37°C. After the elapsed time, the enzyme was freed from the low molecular weight compounds present using two Pharmacia Hi-Trap desalting columns (Sephadex G-25 Superfine) connected in series. Fractions eluted were assayed for radioactivity and, after allowing a sufficient period of time for the radioactivity present to decay to background levels, were assayed for enzymatic activity. In all cases, the initial fractions eluted off the size exclusion column possessed enzymatic activity but no radioactivity while the later fractions were

initially radioactive but did not possess enzymatic activity. Results for a typical experiment are shown in the table below.

Table 3.3: Presence (+) or absence (-) of both enzymatic activity and radioactivity of eluted fractions obtained from purification of GCCase radiolabelling experiment using a Hi-Trap desalting column.

Fraction	Enzymatic activity	Radioactivity
1	+	-
2	+	-
3	-	-
4	-	+
5	-	+
6	-	+

Why did the experiment not work? A couple of explanations come to mind. The first is that the main byproduct in the ^{18}F -fluoride displacement reaction arises from the hydrolysis of the triflate to give 3,4-di-O-acetyl-2-deoxy-2-fluoro- β -D-glucopyranosyl fluoride. After deprotection, the silica gel purification step may not have fully separated the more polar 2-deoxy-2-fluoro- β -D-glucopyranosyl fluoride from the radiolabelled material. If this is the case, then GCCase would be inactivated preferentially by the difluoro-sugar, thus no radioactivity would be incorporated.

Another explanation is that the total concentration of purified, radiolabelled inactivator is far below that of K_i (10^{-2} mM), and hence only a very tiny amount of enzyme would be labelled in the amount of time used to incubate the enzyme and inactivator together. The estimated amount of the purified inactivator (calculated from 4.15 mCi) was $\sim 1.2 \times 10^{-8}$

mol. Under the experimental conditions used, the final concentration of compound was 1.2×10^{-4} M, or 8×10^3 -fold lower than K_i . Another way of looking at this is to determine the ratio of enzyme concentration to K_i . In our case, the concentration of GCase was 5.3×10^{-4} M, thus the calculated ratio would be ~ 0.005 . This is far lower than what has been suggested previously, that the ratio of enzyme concentration to K_i should be at least 4 for an agent to be useful for imaging low-capacity sites with PET.¹⁰⁴ The simplest way of remedying this would be to make an inactivator whose K_i is much lower than that for 2,6diFGF. The natural substrate of GCase, glucosyl ceramide, has a K_m of 0.08 mM and a k_{cat} of 700 min^{-1} , while the fluorescent substrate 4-methylumbelliferyl β -D-glucopyranoside has a K_m of 4.17 mM and a k_{cat} of $6.14 \times 10^3 \text{ min}^{-1}$.¹⁰⁵ Thus, the enzyme definitely has a binding site for the ceramide moiety. Replacement of 2,6diFGF's anomeric fluoride with ceramide should lower K_i . However, the rate of inactivation would certainly be compromised as the ceramide moiety is a poorer leaving group compared to the fluoride anion. In the above example, replacement of the ceramide moiety with a 4-methylumbelliferyl group caused a ~ 9 -fold increase in k_{cat} . While ceramide may not be the best choice as a replacement for the anomeric fluoride of 2,6diFGF, further investigations are required in order to determine what the best compromise is in terms of k_i and K_i .

3.3.5 Conclusions

We have shown that 2,6-dideoxy-2,6-difluoro- β -D-glucopyranosyl fluoride is an inactivator of glucocerebrosidase, with a value of k_i/K_i comparable to that of 2-deoxy-2-

fluoro- β -D-mannopyranosyl fluoride. We have also shown that 2,6-dideoxy-2-fluoro-6-[^{18}F]-fluoro- β -D-glucopyranosyl fluoride can be made albeit in a relatively low radiochemical yield. However, no labelling experiments to date have yielded a radiolabelled glycosyl-glucocerebrosidase intermediate. Two possible reasons for this result are:

- 1) the radiolabelled compound was not completely purified from contaminating 2-deoxy-2-fluoro- β -D-glucopyranosyl fluoride side product which would out-compete the former for GCCase
- 2) the radiolabelled compound was not in sufficiently high enough concentration to inactivate the enzyme in the time used in the experiments

Although these results are disappointing, we believe that further experiments are necessary before the idea of labelling a glucocerebrosidase with a radioinactivator is ruled unfeasible. For example, attempts at improving the radiochemical yield of the ^{18}F -labelling step could be made. Also, the inactivator could be altered to make it resemble GCCase's natural substrate, i.e. replace the fluoride leaving group with a ceramide moiety.

Chapter 4 Materials and Methods

4.1 Synthetic Procedures

4.1.1 Analytical methods

^1H NMR spectra were recorded on the following Bruker instruments at the indicated field strengths: AC-200 at 200 MHz, AV-300 at 300 MHz or a WH-400 at 400 MHz. ^{19}F NMR spectra were recorded on a Bruker AC-200 or AV-300 multinuclear spectrometers operating at frequencies of 188 MHz and 282 MHz, respectively. ^1H NMR spectra chemical shifts are internally referenced to CDCl_3 or MeOH and for samples dissolved in D_2O , the spectra are externally referenced to 2,2-dimethyl-2-silapentane-5-sulfonate ($\delta = 0.015$ ppm). ^{19}F NMR shifts are referenced to CFCl_3 , although the samples were externally referenced to trifluoroacetic acid ($\delta = -76.53$ ppm).

Thin layer chromatography (TLC) was performed using plates (silica gel 60 F₂₅₄, Merck) with visualization under UV light or after charring with 10% H_2SO_4 in MeOH or ammonium molybdate- H_2SO_4 solution in MeOH. Column chromatography was performed under elevated pressure using Kieselgel 60 (230-400 mesh).

Microanalyses were performed by Mr. Peter Borda in the microanalytical laboratory at the Department of Chemistry, University of British Columbia. Samples that were extremely hygroscopic were dried over phosphorous pentoxide until the elemental composition was constant, and the difference between the expected values and the values

determined by Mr. Borda accounted for by assuming the compound remained hydrated (however, no independent confirmation of this was obtained).

4.1.2 Solvents and reagents

Solvents and reagents were either of reagent, certified, spectral, or HPLC grade. Dry solvents were prepared as follows. Acetonitrile, carbon tetrachloride, dichloromethane, pyridine and toluene were distilled over calcium hydride. Diethyl ether and tetrahydrofuran were distilled over sodium and benzophenone. Dimethylformamide was predried over 4 Å molecular sieves overnight and stored over 4 Å molecular sieves. Methanol was distilled over magnesium with iodine.

4.1.3 General work-up procedure

Unless otherwise stated, the following work-up procedure was employed. To the reaction mixture was added dichloromethane, and the organic layer was washed with saturated aqueous sodium bicarbonate until the washings remained basic, then washed with brine. The organic layer was dried over magnesium sulfate for 10 minutes, suction-filtered, and the solvents evaporated *in vacuo* using a rotary evaporator. The residual oil or solid was purified by flash chromatography using the solvent systems indicated for the individual compounds.

4.1.4 Synthesis of 2-deoxy-2-fluoro- β -D-glucopyranosyluronic acid fluoride (2FGlcAF) **5**

1,3,4,6-Tetra-O-acetyl-2-deoxy-2-fluoro- β -D-glucopyranose 2

To a solution of tri-O-acetyl-D-glucal **1** (10.4 g, 38 mmol) in acetic anhydride (150 mL) was added acetic acid (40 mL, 700 mmol). The solution was warmed to and maintained at 70°C. To this was added Selectfluor™ (14.9 g, 42 mmol) portionwise then the reaction was stirred for 2 hours at 70°C. The bulk of the acetic anhydride was removed by evaporation and the concentrated mixture then diluted with 200 mL water and extracted with CH₂Cl₂ (2x150 mL). The organic phase was washed with water and saturated aqueous sodium bicarbonate, dried over magnesium sulfate, and concentrated *in vacuo*. Silica gel chromatography (7:2 petroleum ether-ethyl acetate) yielded 3.1 g of the desired *gluco* epimer (23%) and 4.2 g of the *manno* epimer (31%). The ¹H NMR spectra were identical to those previously reported.¹⁰⁶

2-Deoxy-2-fluoro- β -D-glucopyranosyl fluoride 4

The fluoride was prepared by dissolving the tetra-acetate **2** (3 g, 8.6 mmol) in 45% HBr/glacial acetic acid (10 mL) and stirring at room temperature for 2 hours. The mixture was then diluted with water (200 mL) and extracted with CH₂Cl₂ (2x150 mL). The organic phase was washed with water and saturated sodium bicarbonate, dried over magnesium sulfate, and concentrated *in vacuo*. The resulting syrup was dissolved in HPLC grade acetonitrile (30 mL), silver fluoride (2.17 g, 17.1 mmol) was added, and the suspension was allowed to stir overnight in the dark. The silver salts were then filtered

off through a silica gel plug, using ethyl acetate as the eluent and the solvents were evaporated *in vacuo*. The syrup was dissolved in anhydrous methanol (30 mL), then sodium methoxide (46 mg, 0.86 mmol) was added to the solution. After stirring at room temperature for 30 minutes, the reaction mixture was neutralized with Amberlite IR-120 (H^+) resin and evaporated *in vacuo*. Silica gel chromatography (27:2:1 ethyl acetate-methanol-water) yielded a white solid (1.34 g, 85%). The 1H NMR spectrum was identical to that previously reported.¹⁰⁶

Phenacyl (2-Deoxy-2-fluoro- β -D-glucopyranosyl fluoride)uronate 6

To a stirred solution of the 2-deoxy-fluoro- β -D-glucosyl fluoride **4** (19.5 mg, 0.106 mmol) in water (0.5 mL) was added sodium bromide (3.3 mg, 0.032 mmol) and TEMPO (0.5 mg, 0.0032 mmol). After cooling to 0 °C, 5.25% v/v bleach (3 mL, 2.1 mmol), already cooled to 0 °C, was added slowly, followed by enough 1 N NaOH to maintain the mixture at pH 10 and the reaction mixture was stirred at 0 °C for 2 hours. It was then acidified with 1 M HCl and the water evaporated *in vacuo*. The residue was suspended in DMF (1 mL). To this was added 2-bromoacetophenone (phenacyl bromide) (24.1 mg, 0.121 mmol), followed by triethylamine (16 μ L, 0.115 mmol). After stirring for 1 hour at room temperature the mixture was diluted with 1 M HCl (10 mL) and extracted with ethyl acetate (4 \times 10 mL). The organic phase was dried over magnesium sulfate and concentrated *in vacuo*. Silica gel chromatography (3:1 ethyl acetate-petroleum ether) yielded a yellowish gum (10.0 mg, 33%). 1H NMR data (200 MHz, $CDCl_3$): δ 7.87-8.00 (m, 2 H, H-2', H-6'), 7.64-7.68 (m, 1 H, H-4'), 7.45-7.56 (m, 2 H, H-3', H-5'), 5.90 (d, 1 H, $J = 16.6$ Hz, OCH-H), 5.40 (ddd, 1 H, $J_{1,2} = 6.2$ Hz, $J_{1,F1} = 51.6$ Hz, $J_{1,F2} = 4.4$ Hz, H-

1), 5.28 (d, 1 H, $J = 16.6$ Hz, OCH-*H*), 4.48 (dddd, 1 H, $J_{2,1} = 6.2$ Hz, $J_{2,F1} = 12.2$ Hz, $J_{2,3} = 8.1$ Hz, $J_{2,F2} = 50.6$ Hz, H-2), 4.20 (d, 1 H, $J_{5,4} = 9.3$ Hz, H-5), 3.86-4.05 (m, 2 H, H-3, H-4). ^{19}F NMR (188 MHz, CDCl_3): δ -64.93 (dt, 1 F, $J_{F,1} = 51.6$ Hz, $J_{F,2} = 12.2$ Hz, F-1), -126.42 (dt, 1 F, $J_{F,2} = 50.6$ Hz, $J_{F,1} = 4.4$ Hz, F-2).

2-Deoxy-2-Fluoro- β -D-Glucopyranosyluronic acid Fluoride 5

The phenacyl ester **6** (10.0 mg, 0.032 mmol) was dissolved in 4:1 methanol-water (1 mL). To the solution was added a spatula tip full of 10% Pd-C and the suspension stirred at room temperature for six hours under an atmosphere of hydrogen. The catalyst was removed via filtration through Celite 545 and the solvent was evaporated *in vacuo*. Silica gel chromatography (27:2:1 ethyl acetate-methanol-water) yielded a gum (5.5 mg, 87%).

^1H NMR data (200 MHz, D_2O): δ 5.46 (ddd, 1 H, $J_{1,2} = 7.0$ Hz, $J_{1,F1} = 52.9$ Hz, $J_{1,F2} = 3.4$ Hz, H-1), 4.33 (dddd, 1 H, $J_{2,1} = 7.0$ Hz, $J_{2,F1} = 13.7$ Hz, $J_{2,3} = 8.9$ Hz, $J_{2,F2} = 51.5$ Hz, H-2), 3.81 (d, 1 H, $J_{5,4} = 9.5$ Hz, H-5), 3.80 (dt, 1 H, $J_{3,2} = 8.9$ Hz, $J_{3,4} = 9.5$ Hz, $J_{3,F2} = 15.9$ Hz, H-3), 3.81 (t, 1 H, $J_{4,3} = J_{4,5} = 9.5$ Hz, H-4). ^{19}F NMR (188 MHz, D_2O): δ -67.84 (dt, 1 F, $J_{F,1} = 52.9$ Hz, $J_{F,2} = 13.7$ Hz, F-1), -126.42 (dt, 1 F, $J_{F,2} = 51.5$ Hz, $J_{F,1} = 3.4$ Hz, F-2). HR-LSIMS (M-H) $^-$ calcd 197.0259; found 197.0257.

4.1.5 Synthesis of 2-deoxy-2-fluoro- β -D-mannopyranosyluronic acid fluoride (2FManAF) **8**

*Phenacyl (2-Deoxy-2-fluoro- β -D-mannopyranosyl fluoride)uronate **9***

To a stirred solution of the 2-deoxy-2-fluoro- β -D-mannosyl fluoride **7** (400 mg, 2.17 mmol) in water (0.5 mL) was added sodium bromide (6.7 mg, 0.065 mmol) and TEMPO (1.0 mg, 0.0064 mmol). After cooling to 0 °C, 5.25% v/v bleach (6 mL, 4.2 mmol), already cooled to 0 °C, was added slowly, followed by enough 1 N NaOH to maintain the mixture at pH 10 and the reaction mixture was stirred at 0 °C for 1 hour¹. It was then acidified with 1 M HCl and the water evaporated *in vacuo*. The residue was suspended in DMF (4 mL). To this was added 2-bromoacetophenone (phenacyl bromide) (51.9 mg, 2.61 mmol), followed by triethylamine (360 μ L, 2.58 mmol) already dissolved in ethyl acetate (10 mL). After stirring over night at room temperature the mixture was diluted with 1 M HCl (20 mL) and extracted with ethyl acetate (4 \times 10 mL). The organic phase was dried over magnesium sulfate and concentrated *in vacuo*. Silica gel chromatography (3:1 ethyl acetate-petroleum ether) yielded a yellowish gum (199 mg, 29%). **¹H NMR data** (400 MHz, CDCl₃): δ 7.88-7.96 (m, 2 H, H-2', H-6'), 7.64-7.68 (m, 1 H, H-4'), 7.48-7.56 (m, 2 H, H-3', H-5'), 5.86 (d, 1 H, J = 16.6 Hz, OCH- H), 5.42 (dd, 1 H, $J_{1,F1}$ = 47.4 Hz, $J_{1,F2}$ = 16.1 Hz, H-1), 5.32 (d, 1 H, J = 16.6 Hz, OCH- H), 4.95 (ddd, 1 H, $J_{2,3}$ = 2.7 Hz, $J_{2,F1}$ = 3.6 Hz, $J_{2,F2}$ = 51.0 Hz, H-2), 4.62 (s, 1 H, -OH), 4.20 (t, 1 H, $J_{4,5}$ = 9.2 Hz, H-4), 4.09 (d, 1 H, $J_{5,4}$ = 9.2 Hz, H-5), 3.84 (ddd, 1 H, $J_{3,F1}$ = 1.7 Hz, $J_{3,4}$ = 9.2 Hz, $J_{3,F2}$ = 26.6 Hz, H-3). **¹⁹F NMR** (188 MHz, CDCl₃): δ -72.02 (dd, 1 F, $J_{F,H1}$ = 47.4 Hz, $J_{F1,F2}$ = 12.2 Hz, F-1), -146.49 (m, 1 F, F-2).

2-Deoxy-2-Fluoro- β -D-Mannopyranosyluronic acid Fluoride 8

The phenacyl ester **9** (20.0 mg, 0.064 mmol) was dissolved in 4:1 methanol-water (1 mL). To the solution was added a spatula tip full of 10% Pd-C and the suspension stirred

at room temperature for six hours under an atmosphere of hydrogen. The catalyst was removed via filtration through Celite 545 and the solvent was evaporated *in vacuo*. Silica gel chromatography (27:2:1 ethyl acetate-methanol-water) yielded a gum (11.3 mg, 90%). This was then dissolved in minimal ddH₂O and eluted through a column of Bio-Rad AG 1X-8 resin (H⁺ form) using ddH₂O as the eluant. Fractions obtained were lyophilized to yield a white foam (10.5 mg, 84%). **¹H NMR data.** (400 MHz, CDCl₃): δ 5.47 (dd, 1 H, $J_{1,F1} = 47.4$ Hz, $J_{1,F2} = 17.5$ Hz, H-1), 4.85 (ddd, 1 H, $J_{2,3} = 2.4$ Hz, $J_{2,F1} = 3.0$ Hz, $J_{2,F2} = 51.9$ Hz, H-2), 3.63-3.78 (m, 3 H, H-3, H-4, H-5). **¹⁹F NMR** (188 MHz, D₂O): δ -73.48 (1 F, $J_{F,H1} = 47.4$ Hz, $J_{F1,F2} = 10.2$ Hz, F-1), -147.33 (m, 1 F, F-2). **Anal.** Calcd. for C₆H₈O₅F₂·½H₂O: C, 34.79; H, 4.38; Found: C, 34.90; H, 4.25.

4.1.6 Synthesis of 2-deoxy-2-fluoro-α-L-idopyranosyluronic acid fluoride (2FIdoAF) 14

Phenacyl (3,4-di-O-acetyl-2-deoxy-2-fluoro-β-D-glucopyranosyl fluoride)uronate 10

Phenacyl (2-deoxy-2-fluoro-β-D-glucopyranosyl fluoride)uronate **6** (1.49 g, 4.71 mmol) was dissolved in dry dichloromethane (15 mL). To the solution was added acetyl chloride (1.0 mL, 14.1 mmol, 3 eq) followed by triethylamine (1.4 mL, 9.89 mmol, 2.1 eq). After stirring at room temperature for 3 hours, the solution was washed with 1 N HCl followed by saturated sodium bicarbonate, dried over magnesium sulfate and concentrated *in vacuo*. Silica gel chromatography (2:1 petroleum ether-ethyl acetate) yielded a white foam (1.51 g, 80%). **¹H NMR data** (400 MHz, CDCl₃): δ 7.83-7.88 (m, 2 H, H-2', H-6'), 7.57-7.64 (m, 1 H, H-4'), 7.43-7.48 (m, 2 H, H-3', H-5'), 5.55 (dt, 1 H, $J_{1,2} = 5.3$ Hz, $J_{1,F1} = 51.2$ Hz, H-1), 5.45 (t, $J_{4,3} = 9.1$ Hz, $J_{4,5} = 8.5$ Hz, H-4), 5.34-5.42

(m, 3 H, 2 x OCH-H, H-3), 4.58 (dddd, 1 H, $J_{2,1} = 5.3$ Hz, $J_{2,F1} = 10.3$ Hz, $J_{2,3} = 7.2$ Hz, $J_{2,F2} = 49.2$ Hz, H-2), 4.48 (d, 1 H, $J_{5,4} = 8.5$ Hz, H-5), 2.10-2.30 (2 s, 6 H, 2 x -(CO)CH₃). ¹⁹F NMR (188 MHz, CDCl₃): δ -61.92 (dt, 1 F, $J_{F,H1} = 51.2$ Hz, $J_{F,H2} = 10.3$ Hz, $J_{F1,F2} = 14.2$ Hz, F-1), -123.65 (m, 1 F, F-2).

Phenacyl (5-bromo-3,4-di-O-acetyl-2-deoxy-2-fluoro-β-D-glucopyranosyl fluoride)uronate 11

Phenacyl (3,4-di-O-acetyl-2-deoxy-2-fluoro-β-D-glucopyranosyl fluoride)uronate **10** (1.51 g, 3.77 mmol) was dissolved in dry CCl₄ (40 mL), recrystallized N-bromosuccinimide (1.00 g, 1.5 eq) added, and the mixture irradiated with two 200 W light bulbs. After 45 minutes, the resulting orange mixture was filtered through glass wool and the solvent evaporated. The crude material was purified by flash chromatography using 1:3 ethyl acetate:petroleum ether to yield a gum (0.93g, 51%). ¹H NMR data (400 MHz, CDCl₃): δ 7.83-7.90 (m, 2 H, H-2', H-6'), 7.58-7.64 (m, 1 H, H-4'), 7.43-7.50 (m, 2 H, H-3', H-5'), 5.84 (ddd, 1 H, $J_{1,2} = 7.2$ Hz, $J_{1,F1} = 51.3$ Hz, $J_{1,F2} = 4.7$ Hz, H-1), 5.65 (dd, $J_{3,2} = 9.3$ Hz, $J_{3,4} = 9.3$ Hz, $J_{3,F2} = 23.0$ Hz, H-3), 5.39-5.49 (m, 2 H, 2 x OCH-H, H-4), 4.63 (dddd, 1 H, $J_{2,1} = 7.2$ Hz, $J_{2,F1} = 13.9$ Hz, $J_{2,3} = 9.3$ Hz, $J_{2,F2} = 50.6$ Hz, H-2), 2.09 (s, 6 H, 2 x -(CO)CH₃). ¹⁹F NMR (188 MHz, CDCl₃): δ -75.01 (dt, 1 F, $J_{F,H1} = 51.3$ Hz, $J_{F,H2} = 13.9$ Hz, $J_{F1,F2} = 15.1$ Hz, F-1), -118.35 (m, 1 F, F-2).

Phenacyl (3,4-di-O-acetyl-2-deoxy-2-fluoro-α-L-idopyranosyl fluoride)uronate 12

Phenacyl (5-bromo-3,4-di-O-acetyl-2-deoxy-2-fluoro-β-D-glucopyranosyl fluoride)uronate **11** (0.93 g, 1.9 mmol) was dissolved in dry toluene (20 mL), tributyltin

hydride added (1.0 mL, 3.9 mmol, 2 eq), and the solution boiled at reflux for 2 hours. The solvent was then removed *in vacuo*, 20 mL acetonitrile added, and the mixture extracted with petroleum ether (4x20 mL). The acetonitrile layer was concentrated *in vacuo* and the residue was purified by flash chromatography using 1:3 ethyl acetate:petroleum ether to yield a white needles (0.235g, 30%). Also, the *gluco* epimer was obtained (0.226 g, 29%). Both products were re-chromatographed to remove residual tributyltin compounds. The *ido* product was recrystallized from ethyl acetate:petroleum ether to yield white needles suitable for X-ray crystallography. **¹H NMR data** (300 MHz, CDCl₃): δ 7.83-7.89 (m, 2 H, H-2', H-6'), 7.57-7.62 (m, 1 H, H-4'), 7.45-7.52 (m, 2 H, H-3', H-5'), 5.87 (dd, 1 H, $J_{1,F2} = 7.2$ Hz, $J_{1,F1} = 47.4$ Hz, H-1), 5.53 (d, 1 H, OCH-*H*), 5.34 (d, 1 H, OCH-*H*), 5.33 (m, 1 H, H-4), 5.20-5.28 (m, 1 H, H-3), 5.11 (d, 1 H, $J_{5,4} = 1.7$ Hz, H-5), 4.44-4.64 (m, 1 H, H-2), 2.20 (s, 3 H, -(CO)CH₃), 2.14 (s, 1 H, -(CO)CH₃). **¹⁹F NMR** (282 MHz, CDCl₃): δ -62.89 (dd, 1 F, $J_{F,H1} = 47.4$ Hz, $J_{F1,F2} = 14.0$ Hz, F-1), -118.08 (dddd, 1 F, $J_{F2,H1} = 7.2$ Hz, $J_{F2,H3} = 9.6$ Hz, $J_{F1,F2} = 14.0$ Hz, $J_{F2,H2} = 42.8$ Hz, F-2).

3,4-Di-O-acetyl-2-deoxy-2-fluoro-α-L-idopyranosiduronic acid fluoride 13

Phenacyl (3,4-di-O-acetyl-2-deoxy-2-fluoro-α-L-idopyranosyl fluoride)uronate **12** (0.216 g, 0.540 mmol) was dissolved in 1:1 ethyl acetate: methanol (8 mL), 10% Pd-C (0.060 g, 0.1 eq) added, and the suspension stirred at room temperature under an atmosphere of hydrogen gas for 3 hours. The suspension was then filtered through a plug of Celite 545 and the filtrate concentrated *in vacuo*. The crude material was purified by flash chromatography using initially ethyl acetate, followed by 1:1 ethyl acetate:methanol to

yield a white solid (0.134 g, 88%). **¹H NMR data** (400 MHz, CD₃OD): δ 5.58 (dd, 1 H, $J_{1,F2} = 8.3$ Hz, $J_{1,F1} = 48.6$ Hz, H-1), 5.25 (s, 1 H, H-4), 5.21 (d, 1 H, $J_{3,F2} = 10.5$ Hz, H-3), 4.70 (s, 1 H, H-5), 4.60 (d, 1 H, $J_{2,F2} = 43.3$ Hz, H-2), 2.12 (s, 3 H, -(CO)CH₃), 2.03 (s, 1 H, -(CO)CH₃).

2-Deoxy-2-fluoro- α -L-idopyranosyluronic acid fluoride 14

3,4-Di-O-acetyl-2-deoxy-2-fluoro- α -L-idopyranosyluronic acid fluoride **13** (0.134 g, 0.48 mmol) was dissolved in dry methanol (10 mL) and cooled to 0°C under argon. Anhydrous ammonia was then bubbled through the solution until it was saturated. After stirring at room temperature for 2 hours, the reaction was still incomplete so 10 drops of 0.1 M NaOMe/MeOH was added and the reaction mixture stirred for a further 30 minutes. Silica gel (230-400 mesh) was added to the solution, the solvent removed *in vacuo*, and the silica gel layered atop a flash column. Ethyl acetate was used as the initial eluant, followed by 7:2:1 ethyl acetate:methanol:water, and finally 5:2:1 ethyl acetate:methanol:water. Fractions containing the desired product were concentrated, re-dissolved in ddH₂O, filtered through a 0.22 micron filter and passed through a column of Bio-Rad AG 50WX-8 resin (H⁺ form) using ddH₂O as the eluant. Fractions obtained were lyophilized to yield a white foam (0.070 g, 74%). However, the sample proved to be impure by NMR spectroscopy.

Repurification of 2-deoxy-2-fluoro- α -L-idopyranosyluronic acid fluoride 14

The impure 2-deoxy-2-fluoro- α -L-idopyranosyluronic acid fluoride **14** (0.070 g, 0.35 mmol) was dissolved in dimethyl formamide (0.5 mL) and ethyl acetate (1 mL). To the

stirring solution was added phenacyl bromide (0.141 g, 2 eq), followed by a solution of triethylamine (59 μ L, 1.2 eq) pre-dissolved in ethyl acetate (2mL). After stirring overnight, the mixture was washed with water, dried over magnesium sulfate and concentrated *in vacuo*. The crude material was purified by flash chromatography using 1:1 ethyl acetate:petroleum ether to yield a white solid (0.037 g, 33%). The ester was then dissolved in ethyl acetate (5 mL), methanol (5 mL) and 10% Pd-C (0.020 g, 0.18 eq) added, and the suspension stirred at room temperature under an atmosphere of hydrogen gas for 2.5 hours. The suspension was then filtered through a plug of Celite 545 and the filtrate concentrated *in vacuo*. The crude material was purified by flash chromatography using initially ethyl acetate, followed by 1:1 ethyl acetate:methanol, then 1:2 ethyl acetate:methanol, and finally 1:3 ethyl acetate:methanol. Fractions containing the desired product were concentrated, re-dissolved in ddH₂O, filtered through a 0.22 micron filter and passed through a column of Bio-Rad AG 50WX-8 resin (H⁺ form) using ddH₂O as the eluant. Fractions obtained were lyophilized to yield a white foam (0.019 g, 95%). ¹H NMR data (300 MHz, D₂O): δ 5.75 (dd, 1 H, $J_{1,F2} = 8.6$ Hz, $J_{1,F1} = 48.0$ Hz, H-1), 4.78 (s, 1 H, H-5), 4.52 (d, 1 H, $J_{2,F2} = 43.0$ Hz, H-2), 4.00-4.10 (m, 2 H, H-3, H-4). ¹⁹F NMR (282 MHz, D₂O): δ -61.50 (dd, 1 F, $J_{F,H1} = 48.0$ Hz, $J_{F1,F2} = 10.0$ Hz, F-1), -117.22 (m, 1 F, F-2). **Anal.** Calcd. for C₆H₈O₅F₂·½H₂O: C, 34.79; H, 4.38; Found: C, 35.16; H, 4.32.

4.1.7 Syntheses of 5-fluoro-glycopyranosyluronic fluorides (5FGlcAF and 5FIdoAF) 25 and 26

1,2,3,4-Tetra-O-acetyl- β -D-glucuronic acid 17

D-Glucuronic acid **16** (20 g, 103 mmol) was suspended in 200 mL acetonitrile. To it was added acetic anhydride (60 mL, 636 mmol, 6.2 eq) and concentrated sulfuric acid (1 mL). The mixture was stirred at room temperature for 16 hours. The solvent was then removed *in vacuo* and the remaining acetic acid was removed by co-evaporation with toluene. To the concentrated syrup was added 100 mL of water and the mixture stirred at room temperature for 2 hours. The resulting white solids were filtered off, rinsed with water and dried over P₂O₅ under vacuum. The yield of the product was 23 g (62%). **¹H-NMR data** (CD₃OD, 200 MHz): δ 5.89 (d, 1 H, $J_{1,2}$ = 8.0 Hz, H-1), 5.39 (t, 1 H, $J_{3,2}$ = 9.0 Hz, $J_{3,4}$ = 9.4 Hz, H-3), 5.19 (t, 1 H, $J_{4,3}$ = 9.4 Hz, $J_{4,5}$ = 9.6 Hz, H-4), 5.06 (t, 1 H, $J_{2,1}$ = 8.0 Hz, $J_{2,3}$ = 9.0 Hz, H-2), 4.35 (d, 1 H, $J_{5,4}$ = 9.6 Hz, H-5), 1.97-2.09 (4 s, 12 H, -OAc).

Phenacyl 2,3,4-tri-O-acetyl-D-glucopyranuronate 18

1,2,3,4-Tetra-O-acetyl-D-glucuronic acid **17** (7.59 g, 20.9 mmol) was dissolved in 70 mL HPLC grade acetonitrile. To this solution was added hydrazine acetate (3.86 g, 41.8 mmol, 2 eq). The resulting suspension was warmed until most of the solid had dissolved and the solution then stirred at room temperature for 15 minutes. The reaction was quenched with the addition of 100 mL 0.5 M HCl, the acetonitrile was evaporated *in vacuo* and the aqueous layer extracted with ethyl acetate (8 x 50 mL). The organic layer was dried over magnesium sulfate, filtered, and evaporated. The crude gum was dissolved in 100 mL ethyl acetate and 2-bromoacetophenone (4.62 g, 23.2 mmol, 1.1 eq) followed by triethylamine (4 mL, 28.7 mmol, 1.4 eq) was added. After stirring at room temperature overnight, the mixture was washed with 1 M HCl and saturated sodium bicarbonate, dried with magnesium sulfate, filtered, and evaporated. The crude material

was purified by flash chromatography using 1:1 ethyl acetate:petroleum ether to yield a white solid (4.3 g, 47% over 2 steps). **¹H-NMR data** (CD₃OD, 400 MHz): δ 7.82-7.90 (m, 2 H, H-2', H-6'), 7.56-7.62 (m, 1 H, H-4'), 7.42-7.51 (m, 2 H, H-3', H-5'), 5.57-5.63 (m, 2 H, H-1, H-3), 5.41 (d, 1 H, *J* = 16.4 Hz, -CH-*H*-), 5.35 (d, 1 H, *J* = 16.4 Hz, -CH-*H*-), 5.29 (dd, 1 H, *J*_{4,3} = 9.5 Hz, *J*_{4,5} = 10.0 Hz, H-4), 4.94 (dd, 1 H, *J*_{2,1} = 3.5 Hz, *J*_{2,3} = 10.1 Hz, H-2), 4.80 (d, 1 H, *J*_{5,4} = 10.0 Hz, H-5), 3.60 (s, -OH), 1.98-2.10 (3 s, 9 H, -OAc).

Phenacyl (2,3,4-tri-O-acetyl-β-D-glucopyranosyl fluoride)uronate 19

Phenacyl 2,3,4-tri-O-acetyl-glucopyranuronate **18** (4.3 g, 9.8 mmol) was dissolved in 100 mL dry dichloromethane, cooled to -30°C under N₂, then DAST (2.5 mL, 18.9 mmol, 1.9 eq) was added dropwise to the stirring solution. After the addition, the solution was allowed to warm gradually to room temperature. When the reaction was complete, as determined by TLC, the solution was cooled to 0°C and methanol (5 mL) was added dropwise and the solution stirred for 15 minutes. The mixture was then worked up according to the general procedure. The crude material was passed through a silica gel plug using 1:1 ethyl acetate:petroleum ether. The β-anomer was selectively crystallized using dichloromethane and petroleum ether to yield white needles (2.41 g, 56%). **¹H-NMR data** (CDCl₃, 200 MHz): δ 7.82-7.92 (m, 2 H, H-2', H-6'), 7.56-7.68 (m, 1 H, H-4'), 7.42-7.53 (m, 2 H, H-3', H-5'), 5.54 (t, 1 H, *J* = 1.1 Hz, *J* = 8.6 Hz, *J* = 9.2 Hz), 5.48 (dd, 1 H, *J*_{H1-F} = 51.0 Hz, *J*_{1,2} = 4.9 Hz, H-1), 5.42 (s, 2 H, -CH₂-), 5.26 (t, 1 H, *J*_{3,2} = 7.1 Hz, *J* = 8.5 Hz, H-3), 5.13 (ddd, 1 H, *J*_{2,1} = 5.0 Hz, *J*_{2,3} = 7.1 Hz, *J*_{2,F} = 9.4 Hz, H-2), 4.49

(d, $J_{5,4} = 9.0$ Hz, H-5), 2.00-2.18 (3 s, 9 H, OAc). **^{19}F -NMR data** (CDCl_3 , 188 MHz): δ -57.87 (dd, 1 F, $J_{\text{H1-F}} = 51.1$ Hz, $J_{\text{H2-F}} = 9.4$ Hz, F-1).

Phenacyl (5-bromo-2,3,4-tetra-O-acetyl- β -D-glucopyranosyl fluoride)uronate 20

Phenacyl (2,3,4-tri-O-acetyl- β -D-glucopyranosyl fluoride)uronate **19** was suspended in dry CCl_4 (50 mL), recrystallized N-bromosuccinimide (3.23 g, 4 eq) added, and the mixture irradiated with two 200 W light bulbs. After 2 hours, the resulting orange mixture was filtered through glass wool, washed with saturated sodium bicarbonate, dried with magnesium sulfate, filtered, and evaporated. The crude material was purified by flash chromatography using 1:5 ethyl acetate:petroleum ether to yield a gum (1.02 g, 43%). **^1H -NMR data** (CDCl_3 , 200 MHz): δ 7.82-7.92 (m, 2 H, H-2', H-6'), 7.56-7.68 (m, 1 H, H-4'), 7.42-7.53 (m, 2 H, H-3', H-5'), 5.70 (dd, 1 H, $J_{1,2} = 7.5$ Hz, $J_{1,\text{F}} = 51.3$ Hz, H-1), 5.38-5.54 (m, 4 H, H-3, H-4, -CH₂-), 5.26 (ddd, 1 H, $J_{2,1} = 7.5$ Hz, $J_{2,3} = 2.3$ Hz, $J_{2,\text{F}} = 13.5$ Hz, H-2), 1.94-2.08 (3 s, 9 H, -OAc). **^{19}F -NMR data** (CDCl_3 , 188 MHz): δ -74.42 (dd, 1 F, $J_{\text{H1,F}} = 51.3$ Hz, $J_{\text{H2,F}} = 13.5$ Hz, F-1).

Phenacyl (5-fluoro-2,3,4-tri-O-acetyl- β -D-glucopyranosyl fluoride)uronate 21

Phenacyl (2,3,4-tri-O-acetyl-5-bromo- β -D-glucopyranosyl fluoride)uronate **20** (0.176 g, 0.339 mmol) was dissolved in dry diethyl ether (3.5 mL) and cooled to 10°C. To this solution was added silver tetrafluoroborate (0.166 g, 0.850 mmol, 2.5 eq). After stirring the mixture at room temperature in the dark for 1 hour, the mixture was diluted with ethyl acetate (10 mL) and washed with water. The aqueous phase was extracted once more with ethyl acetate. Then the organic phase was washed with brine, dried with magnesium

sulfate, filtered, and evaporated. The crude material was purified by flash chromatography using 1:3 ethyl acetate:petroleum ether to yield a white solid (0.0192 g, 12%). Also obtained was **22** as a gum (0.050 g, 31%). **¹H-NMR data** (CDCl₃, 400 MHz): δ 7.82-7.90 (m, 2 H, H-2', H-6'), 7.58-7.64 (m, 1 H, H-4'), 7.44-7.51 (m, 2 H, H-3', H-5'), 5.81 (dd, 1 H, $J_{4,3} = 9.4$ Hz, $J_{4,F5} = 22.4$ Hz, H-4), 5.72 (dd, 1 H, $J_{1,2} = 5.7$ Hz, $J_{1,F1} = 51.7$ Hz, H-1), 5.53 (d, 1 H, $J = 16.1$ Hz, -CH-*H*-), 5.43 (dd, 1 H, $J_{3,2} = 6.8$ Hz, $J_{3,4} = 9.4$ Hz, H-3), 5.39 (d, 1 H, $J = 16.1$ Hz, -CH-*H*-), 5.27 (ddd, 1H, $J_{2,1} = 5.7$ Hz, $J_{2,3} = 6.8$ Hz, $J_{2,F1} = 10.6$ Hz, H-2), 2.00-2.21 (3 s, 9 H, -OAc). **¹⁹F-NMR data** (CDCl₃, 188 MHz): δ -51.11 (dd, 1 F, $J_{F5,H4} = 22.4$ Hz, $J_{F5,F1} = 9.4$ Hz, F-5), -64.67 (dt, 1 F, $J_{F1,H1} = 51.7$ Hz, $J_{F1,H2} = 10.6$ Hz, $J_{F1,F5} = 9.4$ Hz, F-1).

*Phenacyl (5-fluoro-2,3,4-tri-O-acetyl- α -L-idopyranosyl fluoride)uronate **22***

Phenacyl (2,3,4-tri-O-acetyl-5-bromo- β -D-glucopyranosyl fluoride)uronate **20** (0.322 g, 0.619 mmol) was dissolved in 5 mL dry acetonitrile. To this solution was added silver fluoride (0.236 g, 1.86 mmol, 3 eq). After stirring the mixture at room temperature overnight, the mixture was filtered through a plug of silica gel and the solvent evaporated. The crude material was purified by flash chromatography using 2:5 ethyl acetate:petroleum ether to yield a gum (0.092 g, 32%). **¹H-NMR data** (CDCl₃, 400 MHz): δ 7.83-7.89 (m, 2 H, H-2', H-6'), 7.57-7.62 (m, 1 H, H-4'), 7.44-7.51 (m, 2 H, H-3', H-5'), 5.75 (d, 1 H, $J_{1,F1} = 50.1$ Hz, H-1), 5.61-5.67 (m, 1 H, H-4), 5.58 (d, 1 H, $J = 16.1$ Hz, -CH-*H*-), 5.39 (d, 1 H, $J = 16.1$ Hz, -CH-*H*-), 5.31-5.36 (m, 1 H, H-3), 5.21-5.29 (m, 1 H, H-2), 2.05-2.20 (3 s, 9 H, -OAc). **¹⁹F-NMR data** (CDCl₃, 188 MHz): δ -30.40

(dd, 1 F, $J_{F5,H4} = 9.4$ Hz, $J_{F5,F1} = 15.6$ Hz, F-5), -47.77 (ddd, 1 F, $J_{F1,H1} = 50.1$ Hz, $J_{F1,H2} = 9.1$ Hz, $J_{F1,F5} = 15.6$ Hz, F-1).

5-Fluoro-2,3,4-tri-O-acetyl- β -D-glucopyranosyluronic acid fluoride 23

Phenacyl (2,3,4-tri-O-acetyl-5-fluoro- β -D-glucopyranosyl fluoride)uronate **21** (0.050 g, 0.109 mmol) was dissolved in 4:1 methanol:water (5 mL). To this solution was added a spatula tip of 10% Pd/C. The mixture was stirred under an atmosphere of hydrogen gas at room temperature for 1 hour. The suspension was then filtered through a plug of Celite 545 and the filtrate concentrated *in vacuo*. The crude material was purified by flash chromatography using initially 1:1 ethyl acetate:petroleum ether, followed by 4:1 ethyl acetate:methanol to yield a gum (0.033 g, 90%). **¹H-NMR data** (CD₃OD, 400 MHz): δ 5.69 (dd, 1 H, $J_{1,2} = 6.6$ Hz, $J_{1,F1} = 53.0$ Hz, H-1), 5.69 (dd, 1 H, $J_{4,3} = 9.8$ Hz, $J_{4,F5} = 22.0$ Hz, H-4), 5.35 (t, 1 H, $J_{3,2} = 8.7$ Hz, $J_{3,4} = 9.8$ Hz, H-3), 5.23 (ddd, 1 H, $J_{2,1} = 6.6$ Hz, $J_{2,3} = 8.7$ Hz, $J_{2,F1} = 12.6$ Hz, H-2), 1.96-2.12 (3 s, 9 H, -OAc).

5-Fluoro-2,3,4-tri-O-acetyl- α -L-idopyranosyluronic acid fluoride 24

Phenacyl (2,3,4-tri-O-acetyl-5-fluoro- α -L-idopyranosyl fluoride)uronate **22** (0.086 g, 0.188 mmol) was dissolved in 4:1 methanol:water (5 mL). To this solution was added a spatula tip of 10% Pd/C. The mixture was stirred under an atmosphere of hydrogen gas at room temperature for 1 hour. The suspension was then filtered through a plug of Celite 545 and the filtrate concentrated *in vacuo*. The crude material was purified by flash chromatography using 27:2:1 ethyl acetate:methanol:water to yield a gum (0.057 g, 90%). **¹H-NMR data** (CD₃OD, 400 MHz): δ 5.83 (dd, 1 H, $J_{1,2} = 2.8$ Hz, $J_{1,F} = 52.4$ Hz,

H-1), 5.58 (t, 1 H, $J_{3,2} = 6.8$ Hz, $J_{3,4} = 8.8$ Hz, H-3), 5.49 (dd, 1 H, $J_{4,3} = 8.8$ Hz, $J_{4,F5} = 11.1$ Hz, H-4), 5.24 (ddd, 1 H, $J_{2,1} = 2.8$ Hz, $J_{2,3} = 6.8$ Hz, $J_{2,F1} = 12.3$ Hz, H-2), 2.00-2.10 (3 s, 9 H, -OAc).

5-Fluoro- β -D-glucopyranosyluronic acid fluoride 25

5-Fluoro-2,3,4-tri-O-acetyl- β -D-glucopyranosyluronic acid fluoride **23** (0.033 g, 0.097 mmol) was dissolved in 5 mL dry methanol and cooled to 0°C. Anhydrous ammonia was bubbled through the solution until it was saturated. The solution was allowed to warm to room temperature and stirred for 30 minutes. The solution was then concentrated *in vacuo*. The crude material was purified by flash chromatography using 17:2:1 ethyl acetate:methanol:water to yield a gum (0.019 g, 90%). This was then dissolved in minimal ddH₂O and eluted through a column of Bio-Rad AG 1X-8 resin (H⁺ form) using ddH₂O as the eluant. Fractions obtained were lyophilized to yield a white powder (0.016 g, 85%). **¹H-NMR data** (D₂O, 400 MHz): δ 5.48 (dd, 1 H, $J_{1,2} = 7.3$ Hz, $J_{1,F1} = 53.9$ Hz, H-1), 3.95 (dd, 1 H, $J_{4,3} = 9.6$ Hz, $J_{4,F5} = 22.8$ Hz, H-4), 3.76 (t, 1 H, $J_{3,2} = 9.4$ Hz, $J_{3,4} = 9.6$ Hz, H-3), 3.67 (ddd, 1 H, $J_{2,1} = 7.3$ Hz, $J_{2,3} = 9.4$ Hz, $J_{2,F1} = 14.8$ Hz, H-2). **¹⁹F-NMR data** (D₂O, 188 MHz): δ -30.40 (dd, 1 F, $J_{F5,H4} = 22.8$ Hz, $J_{F5,F1} = 15.6$ Hz, F-5), -47.77 (ddd, 1 F, $J_{F1,H1} = 53.9$ Hz, $J_{F1,H2} = 14.8$ Hz, $J_{F1,F5} = 15.6$ Hz, F-1). **Anal.** Calcd. for C₆H₈O₆F₂·½H₂O: C, 32.30; H, 4.07; Found: C, 32.33; H, 4.09.

5-fluoro- α -L-idopyranosyluronic acid fluoride 26

5-Fluoro-2,3,4-tri-O-acetyl- α -L-idopyranosyluronic acid fluoride **24** (0.249 g, 0.732 mmol) was dissolved in 10 mL dry methanol and cooled to 0°C. Anhydrous ammonia

was bubbled through the solution until it was saturated. The solution was allowed to warm to room temperature and stirred for 30 minutes. The solution was then concentrated *in vacuo*. The crude material was purified by flash chromatography using 17:2:1 ethyl acetate:methanol:water to yield a gum. This was then dissolved in minimal ddH₂O and eluted through a column of Bio-Rad AG 1X-8 resin (H⁺ form) using ddH₂O as the eluant. Fractions obtained were lyophilized to yield a white powder (0.133 g, 85%). **¹H-NMR data** (D₂O, 400 MHz): δ 5.70 (ddd, 1 H, $J_{1,2} = 4.0$ Hz, $J_{1,F1} = 55.0$ Hz, $J_{1,F5} = 1.6$, H-1), 3.98 (ddd, 1 H, $J_{4,2} = 1.0$ Hz, $J_{4,3} = 7.5$ Hz, $J_{4,F5} = 13.2$ Hz, H-4), 3.92 (m, 1 H, H-2), 3.82 (t, 1 H, $J_{3,4} = 7.5$ Hz, $J_{3,2} = 7.4$, H-3). **¹⁹F-NMR data** (D₂O, 188 MHz): δ -26.09 (t, 1 F, $J_{F5,H4} = 13.2$ Hz, $J_{F5,F1} = 12.7$ Hz, F-5), -48.59 (dt, 1 F, $J_{F1,H1} = 55.0$ Hz, $J_{F1,H2} = 9.1$ Hz, $J_{F1,F5} = 12.7$ Hz, F-1). **Anal.** Calcd. for C₆H₈O₆F₂·H₂O: C, 31.04; H, 4.34; Found: C, 31.01; H, 4.32.

4.1.8 Synthesis of 2,6-dideoxy-2,6-trifluoro- β -D-glucopyranosyl fluoride (2,6diFGF) 30

3,4-Di-O-acetyl-6-O-triphenylmethyl-2-deoxy-2-fluoro- β -D-glucopyranosyl fluoride 27

2-Deoxy-2-fluoro- β -D-glucopyranosyl fluoride **4** (1.19 g, 6.45 mmol) was dissolved in 20 mL dry pyridine, and triphenylmethyl chloride (1.98 g, 1.1 eq) then added. After stirring at room temperature overnight, acetic anhydride (4 mL, 42 mmol, 6.6 eq) was added and the reaction mixture was allowed to stir at room temperature for 2 hours. The mixture was evaporated *in vacuo* and the resulting syrup diluted with methylene chloride. The resultant solution was washed with 1 N HCl, saturated sodium bicarbonate; dried

over anhydrous magnesium sulfate, filtered and evaporated *in vacuo*. The crude material was purified by flash chromatography using 1:2 ethyl acetate:petroleum ether to yield a white foam (2.54 g, 77%). The foam was crystallized by dissolving in minimal dichloromethane and adding petroleum ether, yielding white crystals (2.06 g, 63%). **¹H NMR data** (400 MHz, CDCl₃): δ 7.35-7.45 (m, 6 H, H-2', H-6'), 7.15-7.35 (m, 9 H, H-3', H-4', H-5'), 5.40 (ddd, 1 H, $J_{1,2} = 6.2$ Hz, $J_{1,F1} = 52.3$ Hz, $J_{1,F2} = 3.8$ Hz, H-1), 5.18-5.30 (m, 2 H, H-3, H-4), 4.50 (dddd, 1 H, $J_{2,1} = 6.2$ Hz, $J_{2,F1} = 11.5$ Hz, $J_{2,F2} = 50.5$ Hz, $J_{2,3} = 8.2$ Hz, H-2), 3.72 (ddd, 1 H, $J_{5,4} = 9.4$ Hz, $J_{5,6a} = 2.7$ Hz, $J_{5,6b} = 4.3$ Hz, H-5), 3.36 (dd, 1 H, $J_{6a,5} = 2.7$ Hz, $J_{6a,6b} = 10.7$ Hz, H-6a), 3.11 (dd, 1 H, $J_{6b,5} = 4.3$ Hz, $J_{6b,6a} = 10.7$ Hz, H-6b), 2.15 (s, 3 H, OAc), 1.75 (s, 3 H, OAc). **¹⁹F-NMR data** (CDCl₃, 188 MHz): δ -64.27 (ddd, 1 F, $J_{F1,H1} = 52.3$ Hz, $J_{F1,H2} = 11.5$ Hz, $J_{F1,F2} = 16.1$ Hz, F-1), -124.68 (ddd, 1 F, $J_{F2,H1} = 3.8$ Hz, $J_{F2,H2} = 50.5$ Hz, $J_{F1,F2} = 16.1$ Hz, F-2).

3,4-Di-O-acetyl-2-deoxy-2-fluoro-β-D-glucopyranosyl fluoride 28

3,4-Di-O-acetyl-6-O-triphenylmethyl-2-deoxy-2-fluoro-β-D-glucopyranosyl fluoride **27** (2.00 g, 3.91 mmol) was dissolved in 40 mL anhydrous methylene chloride, then dry methanol (1.6 mL, 10 eq) and boron trifluoride-diethyl etherate (0.48 mL, 1 eq) were added. After stirring at room temperature for 15 minutes, the solution was diluted with methylene chloride, washed twice with water, washed once with saturated sodium bicarbonate, dried over anhydrous magnesium sulfate, filtered and evaporated *in vacuo*. The crude material was purified by flash chromatography using 1:1 ethyl acetate:petroleum ether to yield a white foam (0.99 g, 95%). **¹H NMR data** (400 MHz, CDCl₃): δ 5.42 (ddd, 1 H, $J_{1,2} = 6.3$ Hz, $J_{1,F1} = 52.2$ Hz, $J_{1,F2} = 3.8$ Hz, H-1), 5.30-5.42

(m, 1 H, H-3), 5.09 (t, 1 H, $J_{4,3} = 9.4$ Hz, $J_{4,5} = 9.6$ Hz, H-4), 4.45 (dddd, 1 H, $J_{2,1} = 6.3$ Hz, $J_{2,F1} = 11.5$ Hz, $J_{2,F2} = 50.3$ Hz, $J_{2,3} = 8.3$ Hz, H-2), 3.74-3.82 (m, 1 H, H-6a), 3.69 (ddd, 1 H, $J_{5,4} = 9.6$ Hz, $J_{5,6a} = 4.5$ Hz, $J_{5,6b} = 2.3$ Hz, H-5), 3.58-3.65 (m, 1 H, H-6b), 2.00-2.10 (2 s, 6 H, OAc). **^{19}F -NMR data** (CDCl_3 , 188 MHz): δ -64.31 (dt, 1 F, $J_{F1,H1} = 52.2$ Hz, $J_{F1,H2} = 11.5$ Hz, $J_{F1,F2} = 15.6$ Hz, F-1), -124.83 (ddd, 1 F, $J_{F2,H1} = 3.8$ Hz, $J_{F2,H2} = 50.3$ Hz, $J_{F1,F2} = 15.6$ Hz, F-2).

3,4-Di-O-acetyl-2,6-dideoxy-2,6-difluoro- β -D-glucopyranosyl fluoride 29

3,4-Di-O-acetyl-2-deoxy-2-fluoro- β -D-glucopyranosyl fluoride **28** (0.202 g, 0.75 mmol) was dissolved in 3 mL anhydrous 1,4-dioxane followed by diethylaminosulfur trifluoride (0.30 mL, 3 eq). The solution was stirred at 100°C for 9 minutes, then cooled to 4°C and 1 mL MeOH added dropwise. The mixture was then worked up according to the general procedure. The crude material was purified by flash chromatography using 1:2 ethyl acetate:petroleum ether to yield a yellowish solid (0.198 g, 97%). **^1H NMR data** (400 MHz, CDCl_3): δ 5.42 (ddd, 1 H, $J_{1,2} = 5.8$ Hz, $J_{1,F1} = 51.9$ Hz, $J_{1,F2} = 4.3$ Hz, H-1), 5.31 (dd, 1 H, $J_{3,2} = 7.8$ Hz, $J_{3,4} = 8.9$ Hz, $J_{3,F2} = 15.8$ Hz, H-3), 5.12 (t, 1 H, $J_{4,3} = 8.9$ Hz, $J_{4,5} = 9.6$ Hz, H-4), 4.36-4.61 (m, 3 H, H-2, H-6a, H-6b), 3.90 (dddd, 1 H, $J_{5,4} = 9.6$ Hz, $J_{5,6a} = 2.9$ Hz, $J_{5,6b} = 4.5$ Hz, $J_{5,6F} = 21.0$ Hz, H-5), 2.00-2.14 (2 s, 6 H, OAc). **^{19}F NMR** (188 MHz, D_2O): δ -63.30 (1 F, dt, $J_{F,H1} = 51.9$ Hz, $J_{F,H2} = 13.7$ Hz, F-1), -124.21 (dt, 1 F, $J_{F,H1} = 4.3$ Hz, $J_{F,H2} = 49.9$ Hz, $J_{F,H3} = 15.8$ Hz, F-2), -156.01 (dt, 1 F, $J_{F,H5} = 21.0$ Hz, $J_{F,H6} = 46.8$ Hz, F-6).

2,6-Dideoxy-2,6-difluoro- β -D-glucopyranosyl fluoride 30

3,4-Di-O-acetyl-2,6-dideoxy-2,6-difluoro- β -D-glucopyranosyl fluoride **29** (0.40 g, 1.5 mmol) was dissolved in 20 mL anhydrous MeOH followed by 1 M NaOMe in MeOH (1 mL, 0.67 eq). After stirring at room temperature for 15 minutes, the solution was neutralized with Rexyn 101 (H^+) resin, filtered and evaporated *in vacuo*. The crude material was purified by flash chromatography using 2:1 ethyl acetate:petroleum ether to yield a white solid (0.271 g, 97%). **1H NMR data** (400 MHz, D_2O): δ 5.55 (ddd, 1 H, $J_{1,2} = 7.0$ Hz, $J_{1,F1} = 52.8$ Hz, $J_{1,F2} = 3.4$ Hz, H-1), 5.31 (dd, $J_{3,2} = 7.8$ Hz, $J_{3,4} = 8.9$ Hz, $J_{3,F2} = 15.8$ Hz, H-3), 5.12 (t, 1 H, $J_{4,3} = 8.9$ Hz, $J_{4,5} = 9.6$ Hz, H-4), 4.36-4.61 (m, 3 H, H-2, H-6a, H-6b), 4.65-4.85 (m, 2 H, H-6a, H-6b), 4.38 (dddd, 1 H, $J_{2,1} = 7.0$ Hz, $J_{2,F1} = 13.6$ Hz, $J_{2,F2} = 51.3$ Hz, $J_{2,3} = 8.9$ Hz, H-2), 3.88 (dt, 1 H, $J_{3,2} = 8.9$ Hz, $J_{3,4} = 9.3$ Hz, $J_{3,F2} = 15.5$ Hz, H-3), 3.80 (ddt, 1 H, $J_{5,4} = 9.9$ Hz, $J_{5,6} = 2.7$ Hz, $J_{5,F6} = 25.8$ Hz, H-5), 3.86 (t, $J_{4,3} = 9.3$ Hz, $J_{4,5} = 9.9$ Hz, H-4). **^{19}F NMR** (188 MHz, D_2O): δ -67.44 (1 F, dt, $J_{F,H1} = 52.8$ Hz, $J_{F,H2} = 13.6$ Hz, $J_{F1,F2} = 15.8$ Hz, F-1), -126.14 (1 F, dt, $J_{F,H2} = 51.3$ Hz, $J_{F,H3} = 15.8$ Hz, $J_{F2,F1} = 15.8$ Hz, F-2), -159.00 (dt, 1 F, $J_{F,H5} = 25.8$ Hz, $J_{F,H6} = 47.2$ Hz, F-6). Anal. Calcd. for $C_6H_9O_3F_3$: C, 38.72; H, 4.87; Found: C, 38.75; H, 4.85.

3,4-Di-O-acetyl-6-O-trifluoromethanesulfonyl-2-deoxy-2-fluoro- β -D-glucopyranosyl fluoride 31

3,4-Di-O-acetyl-2-deoxy-2-fluoro- β -D-glucopyranosyl fluoride **28** (0.63 g, 2.34 mmol) was dissolved in 5 mL anhydrous dichloromethane followed by a solution of 2,6-di-*t*-butylpyridine (0.74 mL, 1.4 eq) and trifluoromethanesulfonic anhydride (0.55 mL, 1.4 eq) in 5 mL anhydrous dichloromethane. After stirring at room temperature for 1 hour under nitrogen, the solution was diluted with dichloromethane and washed with ice-cold

saturated sodium bicarbonate. The aqueous phase was re-extracted with dichloromethane. The combined organic layers were washed twice with cold water, dried over anhydrous magnesium sulfate, filtered and evaporated *in vacuo*. The crude material was purified by flash chromatography using 1:3 ethyl acetate:petroleum ether to yield a faint yellow solid (0.66 g, 70%). **¹H NMR data** (400 MHz, CDCl₃): δ 5.49 (ddd, 1 H, $J_{1,2} = 5.4$ Hz, $J_{1,F1} = 51.3$ Hz, $J_{1,F2} = 4.3$ Hz, H-1), 5.29-5.39 (m, 1 H, H-3), 5.10 (t, 1 H, $J_{4,3} = 9.0$ Hz, $J_{4,5} = 9.1$ Hz, H-4), 4.51-4.60 (m, 2 H, H-6a, H-6b), 4.50 (dddd, 1 H, $J_{2,1} = 5.4$ Hz, $J_{2,F1} = 9.6$ Hz, $J_{2,F2} = 48.9$ Hz, $J_{2,3} = 7.1$ Hz, H-2), 4.00-4.10 (m, 1 H, H-5), 2.00-2.10 (2 s, 6 H, OAc). **¹⁹F-NMR data** (CDCl₃, 188 MHz): δ 1.78 (s, 3 F, -CF₃), -61.60 (ddd, 1 F, $J_{F1,H1} = 51.3$ Hz, $J_{F1,H2} = 9.6$ Hz, $J_{F1,F2} = 15.6$ Hz, F-1), -122.90 (dt, 1 F, $J_{F2,H1} = 4.3$ Hz, $J_{F2,H2} = 48.9$ Hz, $J_{F1,F2} = 15.6$ Hz, F-2).

4.1.9 Radiosynthesis of 2,6-dideoxy-6-¹⁸F-2-fluoro-β-D-glucopyranosyl fluoride 32

Using the facilities at TRIUMF, 1 mL of H₂¹⁸O was irradiated with a 13 MeV proton beam for 15 minutes. The water was then passed through a QMA Sep-Pak conditioned with 5 mL deionized water followed by 5 mL saturated sodium bicarbonate. Radioactivity count using a Capintec, Inc. CRC-35R dose calibrator was determined to be 131 mCi. A solution of Kryptofix 2.2.2 (4 mg) and potassium carbonate (1.8 mg) dissolved in 0.7 mL acetonitrile and 1.5 mL deionized water was used to elute the fluoride-18 off the Sep-Pak into a conical glass tube. The solvent was boiled off and acetonitrile (2x1.5 mL) was used to remove residual water via azeotropic distillation.

To the ^{18}F -fluoride residue was added a solution of 3,4-di-O-acetyl-6-O-trifluoromethanesulfonyl-2-deoxy-2-fluoro- β -D-glucopyranosyl fluoride **31** (10 mg) dissolved in 2 mL acetonitrile and the resulting mixture boiled at 80°C. Additional volumes of acetonitrile were added as the solvent decreased in volume during this period. After 15 minutes, the solvent was boiled off and the residue cooled to room temperature, then 0.5 mL of 0.1 M NaOMe/MeOH was added and the solution allowed to sit at room temperature for 15 minutes. The solution was loaded directly onto a silica gel column using 1:1 ethyl acetate:hexanes as the eluant. Fractions containing the desired product (as determined by TLC) were pooled and concentrated *in vacuo*. Radioactivity count was 4.15 mCi (after 2 hours 43 minutes). After correcting for radioactive decay, the radiochemical yield was 8.8%.

4.2 Spontaneous Hydrolysis of Glycosyl Fluorides

Solutions of the 2-deoxy-2-fluoro- and the 5-fluoro-glycosyl fluorides were prepared in 50 mM sodium phosphate buffer, pH 6.8, containing 1 M NaClO₄. Samples (0.5 mL) were incubated at 50°C in parafilm 1.5 mL screw-top plastic vials with O-ring seals, and aliquots (50 μL) were removed at different time intervals and diluted fourfold into the same buffer, frozen immediately, and the fluoride concentrations determined at the end of the experiment using a fluoride electrode. In cases where the hydrolysis had gone essentially to completion, the rate of fluoride release was determined by plotting the concentration of fluoride versus time and fitting the data to a first-order rate equation. If the reaction was slow, so that only partial hydrolysis was observed over the assay period

(~7 days), the rate constant was determined by a linear fit of the initial rate of hydrolysis. Values of k refer to glycosyl fluoride consumed. Thus for initial rate determinations of the 2-deoxy-2-fluoro sugars, $k = \text{rate}/[\text{F}]$; for the 5-fluoro sugars, $k = \frac{1}{2}(\text{rate}/[\text{F}])$.

4.3 Enzyme Kinetics

4.3.1 General Materials and Methods

Buffer chemicals and reagents for kinetic measurements were obtained from the BDH, Boehringer Mannheim or Sigma-Aldrich chemical companies. All kinetics studies were carried out on a UNICAM 8700 UV-visible spectrophotometer equipped with a circulating water bath. Quartz or plastic cuvettes with a pathlength of 1 cm were used. A continuous spectrophotometric assay based on the hydrolysis of an appropriate nitrophenyl glycoside was used to monitor enzyme activity by measurement of the rate of nitrophenolate release upon hydrolysis. Enzyme concentrations and reaction times were chosen so that less than 10% of the total substrate was hydrolyzed to ensure linear kinetics.

Human glucocerebrosidase (GCase) was kindly provided by Dr. Lorne Clarke of the British Columbia Research Institute for Children's and Women's Health, Vancouver, British Columbia, Canada. The protein was a commercial product obtained from Genzyme Corporation. Human β -glucuronidase (HBG) was kindly provided by Mr. J. H. Grubb and Dr. W. S. Sly of E.A. Doisy Department of Biochemistry and Molecular Biology, St. Louis University School of Medicine, St. Louis, Missouri, USA. The protein

was purified as described previously.^{107,108} *E. coli* β -glucuronidase (EBG) was purchased from Sigma Chemical Company in lyophilized form. Human α -L-iduronidase (IDUA) was kindly provided by Dr. John J. Hopwood of the Centre for Medical Genetics at the Women's and Children's Hospital, Adelaide, Australia and Dr. Lorne Clarke of the British Columbia Research Institute for Children's and Women's Health, Vancouver, Canada. The protein was purified as described previously and stored in pH 7.0 phosphate buffer containing 0.5 M NaCl.¹⁰⁹ Kinetic studies with these enzymes were performed using the conditions listed in the following table:

Enzyme	Buffer conditions	Substrate used	Assay wavelength (λ)	Released phenolate extinction coefficient ($\times 10^{-3} \text{ M}^{-1}\text{cm}^{-1}$)
HBG	100 mM sodium acetate buffer, pH 4.8 at 37°C	<i>p</i> -nitrophenyl β -D-glucuronide	360	2.25
EBG	100 mM potassium phosphate buffer, pH 6.8 at 37°C	<i>p</i> -nitrophenyl β -D-glucuronide	400	7.28
IDUA	100 mM 3,3-dimethylglutarate, pH 4.5 at 37°C	<i>p</i> -nitrophenyl α -L-iduronide	360	2.53
GCase	20 mM sodium citrate, 60 mM sodium phosphate buffer, pH 5.5 containing 4 mM mercaptoethanol, 0.25% (v/v) Triton X-100, and 0.25% taurocholate at 37°C	2,4-dinitrophenyl- β -D-glucoside	400	10.7

Michaelis-Menten parameters for *p*-nitrophenyl β -D-glucuronide, previously undetermined with HBG and EBG, were $K_m = 1.50$ mM and $k_{cat} = 1860$ s⁻¹; and $K_m = 87$ μ M and $k_{cat} = 226$ s⁻¹, respectively.

4.3.2 Time-dependent inactivation

The kinetic parameters for the inactivation of the various glycosidases by different inhibitors were determined as follows. The enzyme was incubated in the appropriate buffer with various concentrations of the inhibitor. Aliquots (5 or 10 μ l) were removed at different time intervals and diluted into assay cells containing a large volume (700 μ L) of substrate (at saturating concentrations, $7 \times K_m$, or at least $\sim K_m$). This effectively stops the inactivation both by dilution of the inhibitor and by competition with an excess of substrate. The residual enzymatic activity was determined from the rate of hydrolysis of substrate, which is directly proportional to the amount of active enzyme. The process was monitored until the enzymatic activity had decreased by 80-90%. Pseudo first-order inactivation rate constants (k_{obs}) for each inactivator concentration were calculated from the slopes of the plots of the natural logarithm of the residual enzymatic activity versus time or by fitting plots of the residual enzymatic activity versus time to a single exponential equation using the program GraFit (Leatherbarrow, R. J. *GraFit Version 3.09b*; Erithacus Software Ltd.: Staines, U.K., 1996). If inactivation was not complete and a significant steady-state rate was observed, these data were fitted to a single exponential equation plus offset. Values of k_i and K_i were determined from these k_{obs} values by fitting to the equation

$$k_{obs} = \frac{k_i[I]}{K_i + [I]}$$

If, however, due to very large values of K_i or rapidity of inactivation, saturation was not observed, a value of k_i/K_i , was calculated according to

$$k_{obs} = \frac{k_i[I]}{K_i}$$

where $[I] \ll K_i$. In this case, k_i/K_i is determined from the initial slope of a plot of k_{obs} against inactivator concentration.

4.3.3 Protection against inactivation

Protection against inactivation was investigated by incubating samples of enzyme in the appropriate buffer containing the inhibitor and in the absence or presence of a competitive inhibitor (at a concentration of $\sim K_i$ or higher). The same procedures used in the time-dependent inactivation experiments were then followed.

4.3.4 Reactivation of inactivated enzyme

Reactivation rates of inactivated enzymes were studied as follows. After incubating the enzyme with inactivator, the inactivated enzyme was freed of excess inactivator by concentration using 30 kDa nominal molecular weight cut-off centrifugal concentrators

(Amicon Centricon-30) followed by dilution of the concentrated enzyme stock (100-200 μL) with buffer to a final volume of 2000 μL . This was repeated three times and the retentate was diluted to a final volume of buffer containing 1 mg/mL BSA, and appropriate transglycosylation ligands, if any. The enzyme samples were then incubated at 37°C and reactivation was monitored by removing aliquots at different time intervals and assaying for activity as described above. The spontaneous reactivation rate constant was determined by fitting the data to a first order rate equation.

4.3.5 Determination of apparent K_i' values

Apparent K_i' values for inhibitors were determined by assaying the appropriate enzyme in the presence of substrate and various concentrations of inhibitors. Initially, a V_m and K_m determination for this particular dilution of enzyme was performed. Then the same amount of enzyme was added to cells each containing the same substrate concentration ($\sim K_m$) and varying inhibitor concentrations. The steady-state enzymic rates were determined by monitoring nitrophenolate release. A plot of $1/V$ versus inhibitor concentration intersects a line given by $1/V_m$ at $-K_i$.

4.4 Determination of the Stereochemical Course of Hydrolysis of HBG

The buffer used in this experiment was 100 mM acetate solution, pH 4.8, in D_2O , prepared by adjusting the pH of a 100 mM solution of sodium acetate in D_2O with a 100 mM solution of acetic acid in D_2O . The ^1H -NMR spectrum of a sample of 1.1 mg (3.3

μmol) of *p*-nitrophenyl β -D-glucuronide in 400 μL buffer was recorded on a Brüker AC-200 spectrometer, then HBG (200 μL , 0.95 mg/mL), previously exchanged with buffer using a 30 kDa nominal molecular weight cut-off centrifugal concentrators (Amicon Centricon-30), was added. ^1H -NMR spectra were recorded at different time intervals.

4.5 Labelling and proteolysis of glycosidases for electrospray MS analysis

HBG (30 μL , 3.7 mg/mL) was incubated with 2FGlcAF (4 μL of 50 mM stock) at 37°C for 10 minutes in 100 mM sodium acetate buffer, pH 4.8; complete inactivation (>99%) was confirmed by enzyme assay as above. This mixture was immediately subjected to peptic digestion: β -glucuronidase (10 μL native or 34 μL 2F-glucopyranosyluronic acid-enzyme, 3.7 mg/mL) was mixed with pepsin (10 or 34 μL , respectively, 0.4 mg/mL in 300 mM, pH 2.0 sodium phosphate) and 300 mM sodium phosphate buffer pH 2.0 (10 or 34 μL , respectively). The mixture was incubated at 37°C for one hour, frozen, and analyzed immediately by liquid chromatography/mass spectrometry (LC/MS) upon thawing.

EBG (36 μL , 4.2 mg/mL) was incubated with 5FGlcAF (4 μL of 10 mM stock) or 2FGlcAF (4 μL 50 mM of stock) at 37°C for 15 minutes in 100 mM potassium phosphate buffer, pH 6.8; complete inactivation (>99%) was confirmed by enzyme assay as above. These mixtures were immediately subjected to peptic digestion: the samples were mixed with pepsin (40 μL , 0.4 mg/mL in 2.1 M sodium phosphate buffer, pH 1.6) followed by

2.1 M sodium phosphate, pH 1.6 buffer (40 μ L). The mixture was incubated at 37°C for 30 minutes, frozen, and analyzed immediately by liquid chromatography/mass spectrometry (LC/MS) upon thawing.

IDUA (40 μ L, 2.7 mg/mL) was incubated with 2FIduAF (3 μ L of 200 mM stock) at 37°C for 15 minutes in 100 mM 3,3-dimethylglutarate, pH 4.5; complete inactivation (>99%) was confirmed by enzyme assay as above. This mixture was immediately subjected to peptic digestion: α -iduronidase (10 μ L native or 43 μ L 2F-iduronyl-enzyme, 2.7 mg/mL) was mixed with pepsin (7 or 30 μ L, respectively, 0.3 mg/mL in 2.1 M sodium phosphate buffer, pH 1.6) and 2.1 M sodium phosphate buffer, pH 1.6 (7 or 30 μ L, respectively). The mixture was incubated at 37°C for 60 minutes, frozen, and analyzed immediately by liquid chromatography/mass spectrometry (LC/MS) upon thawing.

4.6 Electrospray MS conditions for peptide analysis

Mass spectra were recorded on a PE-Sciex API 300 triple quadrupole mass spectrometer (Sciex, Thornhill, Ontario, Canada) equipped with an Ionspray ion source. Peptides were separated by reverse phase HPLC on an Ultrafast Microprotein Analyzer (Michrom BioResources Inc., Pleasanton, CA) directly interfaced with the mass spectrometer. In each of the MS experiments, the proteolytic digest was loaded onto a C18 column (Reliasil, 1 x 150 mm) equilibrated with solvent A (solvent A; 0.05% trifluoroacetic acid (TFA), 2% acetonitrile in water). Elution of the peptides was accomplished using a gradient (0-60%) of solvent B over 60 minutes followed by 100% solvent B over 2

minutes (solvent B: 0.045% TFA, 80% acetonitrile in water). Solvents were pumped at a constant flow rate of 50 $\mu\text{L}/\text{min}$. Spectra were obtained in the single quadrupole scan mode (LC/MS) or the tandem MS product ion scan mode (MS/MS).

4.6.1 MS scan mode parameters - HBG

In the single quadrupole mode (LC/MS), the quadrupole mass analyzer was scanned over a mass to charge ratio (m/z) range of 300-2400 Da with a step size of 0.5 Da and a dwell time of 1 ms per step. The ion source voltage (ISV) was set at 5.5 kV and the orifice energy (OR) was 50 V. In the tandem MS daughter ion scan mode, the spectrum was obtained by selectively introducing the parent ion ($m/z = 935$) from the first quadrupole (Q1) into the collision cell (Q2) and observing the product ions in the third quadrupole (Q3). Thus, Q1 was locked on $m/z = 935$; Q3 scan range was 50-950; the step size was 0.5; dwell time was 1 ms; ion source voltage (ISV) was 5 kV; orifice energy (OR) was 50 V; $Q0 = -10$ V; $Q2 = -47$ V.

4.6.2 MS scan mode parameters - EBG

In the single quadrupole mode (LC/MS), the quadrupole mass analyzer was scanned over a mass to charge ratio (m/z) range of 300-2200 Da with a step size of 0.5 Da and a dwell time of 1.0 ms per step. The ion source voltage (ISV) was set at 5.5 kV and the orifice energy (OR) was 45 V. In the tandem MS daughter ion scan mode, the spectrum was obtained by selectively introducing the parent ion ($m/z = 974$ or 990) from the first quadrupole (Q1) into the collision cell (Q2) and observing the product ions in the third

quadrupole (Q3). Thus, Q1 was locked on $m/z = 974$ or 990 ; Q3 scan range was 50-1100; the step size was 0.5; dwell time was 2.0 ms; ion source voltage (ISV) was 5 kV; orifice energy (OR) was 45 V; $Q0 = -10$ V; $IQ2 = -50$ V.

4.6.3 MS scan mode parameters - IDUA

In the single quadrupole mode (LC/MS), the quadrupole mass analyzer was scanned over a mass to charge ratio (m/z) range of 300-2200 Da with a step size of 0.5 Da and a dwell time of 1.0 ms per step. The ion source voltage (ISV) was set at 5.5 kV and the orifice energy (OR) was 45 V. In the tandem MS daughter ion scan mode, the spectrum was obtained by selectively introducing the parent ion ($m/z = 885$) from the first quadrupole (Q1) into the collision cell (Q2) and observing the product ions in the third quadrupole (Q3). Thus, Q1 was locked on $m/z = 885$; Q3 scan range was 50-1100; the step size was 0.5; dwell time was 1.0 ms; ion source voltage (ISV) was 5 kV; orifice energy (OR) was 45 V; $Q0 = -10$ V; $IQ2 = -50$ V.

4.7 Radiolabelling of glucocerebrosidase

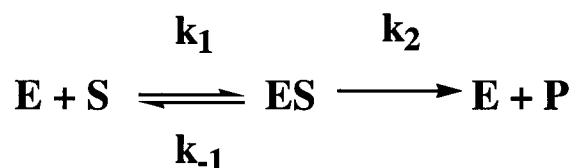
GCase (100 μ L, 60 U) was added to 4.15 mCi of 2,6-dideoxy-6- 18 F-2-fluoro- β -D-glucopyranosyl fluoride and incubated at 37°C for 7 hours. The solution was then passed through two Pharmacia Hi-Trap desalting columns connected in series (Sephadex G-25 Superfine) prewashed with 0.9% saline and using 0.9% saline as the eluant. One-millilitre fractions were collected and measured for radioactivity. After the fractions

were allowed to decay to background levels of radioactivity, they were concentrated using 10 kDa nominal molecular weight cut-off centrifugal concentrators (Amicon Centricon-10) and exchanged with buffer (20 mM sodium citrate, 60 mM sodium phosphate buffer, pH 5.5 containing 4 mM mercaptoethanol, 0.25% (v/v) Triton X-100, and 0.25% taurocholate). They were then assayed for GCase activity as above.

Appendix I: Enzyme Kinetics

Fundamental Equations of Enzyme Kinetics

In 1913, Michaelis and Menten proposed a simple model to account for the relationship between the rate of catalysis and the concentration of substrate.⁴⁴ Later, Briggs and Haldane (1925) expanded on this by introducing the concept of the steady state. The general scheme for an enzyme-catalyzed reaction is shown below. Free enzyme, E, combines with free substrate, S, to form an enzyme-substrate complex, ES, which is then turned over to yield product, P.



Under steady state conditions,

$$\frac{d[\text{ES}]}{dt} = k_1[\text{E}][\text{S}] - k_{-1}[\text{ES}] - k_2[\text{ES}] = 0 \quad (1)$$

The total concentration of enzyme $[\text{E}]_0$ is equal to the concentration of free enzyme $[\text{E}]$, plus the concentration of the enzyme bound in the ES complex, $[\text{ES}]$.

$$[\text{E}]_0 = [\text{E}] + [\text{ES}] \quad (2)$$

Solving for ES using equations 1 and 2, we get

$$[ES] = \frac{[E]_0[S]}{[S] + \frac{k_{-1} + k_2}{k_1}} \quad (3)$$

Assuming that the formation of products is the rate-limiting step (k_2), the initial velocity of the reaction, v , is equal to the rate of formation of product:

$$v = \frac{dP}{dt} = k_2[ES] \quad (4)$$

By substituting the expression for [ES] from equation 3 into equation 4, one obtains

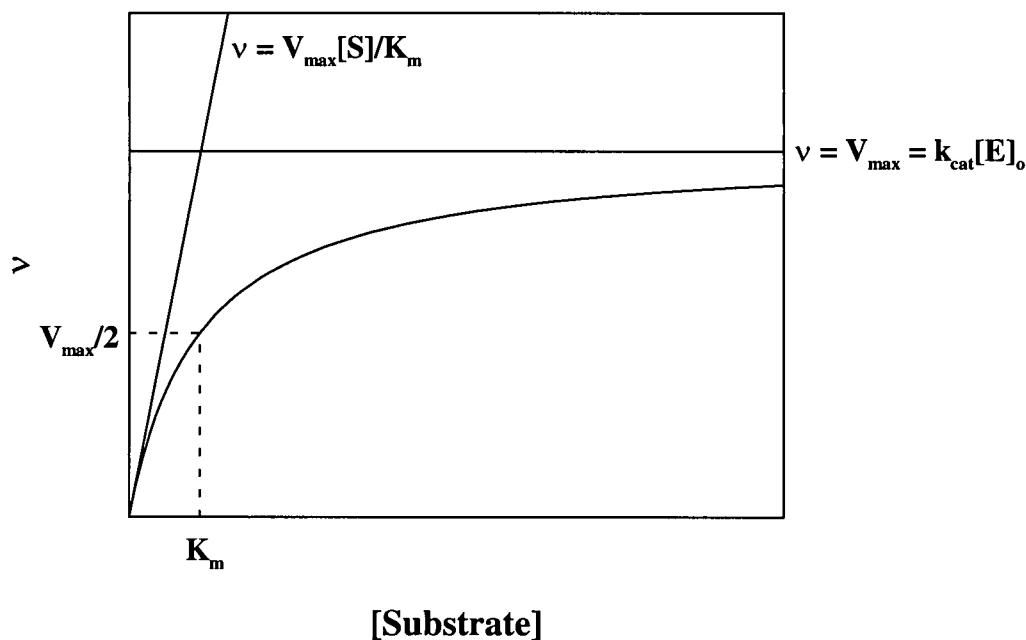
$$v = \frac{k_2[E]_0[S]}{\frac{k_{-1} + k_2}{k_1} + [S]} \quad (5)$$

The ratio of rate constants $(k_{-1} + k_2)/k_1$ is defined as K_m , the Michaelis constant while the rate constant k_2 is defined as the catalytic constant or k_{cat} (the turnover number). Therefore, equation 5 can be expressed in a more general format, also known as the Michaelis-Menten equation:

$$v = \frac{k_{cat}[E]_0[S]}{K_m + [S]} \quad (6)$$

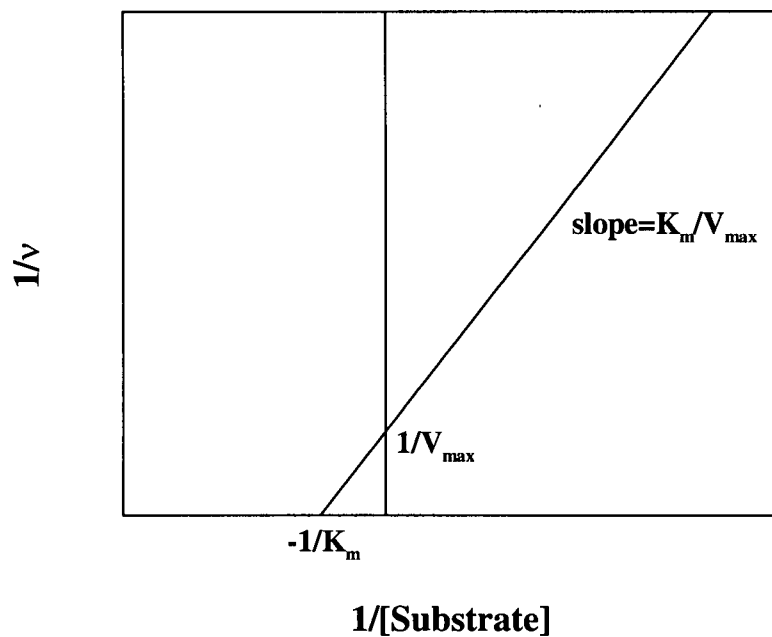
Therefore, when the initial rate of the reaction is equal to one-half the maximal velocity ($v=V_{\max}/2$), the substrate concentration is equal to K_m . In its simplest form, the Michaelis constant is a measure of the binding affinity of an enzyme for a particular substrate. An enzyme with a high binding affinity for a substrate has a low value of K_m .

A graphical representation of the Michaelis-Menten equation is shown below.



The Michaelis-Menten equation can also be plotted as a reciprocal plot ($1/v$ vs $1/[S]$).

This is known as a Lineweaver-Burke plot.



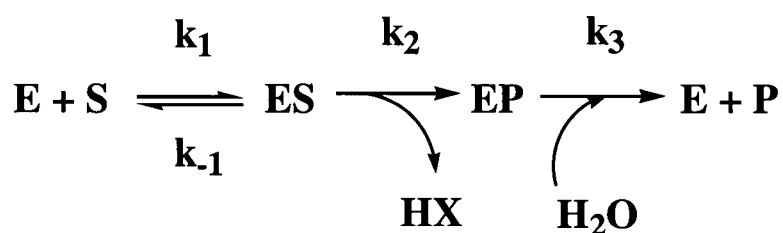
At high concentrations ($[S] \gg K_m$), v approaches its maximal value, V_{\max} , and the rate becomes independent of $[S]$. Thus, the Michaelis-Menten equation can be rewritten in the form:

$$V_{\max} = k_{cat}[E]_o \quad (7)$$

At low concentrations of $[S]$ ($[S] \ll K_m$), the initial rate of the reaction is proportional to $[S]$:

$$v = \frac{k_{cat}[E]_o[S]}{K_m} \quad (8)$$

The Michaelis-Menten approach can be expanded to more complex enzyme systems in which two or more distinct reaction steps occur. Such is the case for the double-displacement mechanism. The reaction scheme for this mechanism is as follows. Free enzyme, E, combines with free substrate, S, to form an enzyme-substrate complex, ES, with a rate constant, k_1 (association step). The conversion of ES to EP is termed the glycosylation step (k_2) and the turnover of EP to P is the deglycosylation step (k_3).



Assuming that a steady state concentration of both EP and ES is reached,

$$k_2[ES] = k_3[EP] \quad (9)$$

$$\frac{d[ES]}{dt} = k_1[E][S] - k_{-1}[ES] - k_2[ES] = 0 \quad (10)$$

The total concentration of enzyme $[E]_0$ is equal to free enzyme plus all of the enzyme bound species:

$$[E]_0 = [E] + [ES] + [EP] \quad (11)$$

By substituting for $[EP]$ using equation 9, one obtains

$$[E]_o = [E] + [ES] + \frac{k_2}{k_3}[ES] \quad (12)$$

By solving equation 12 for [E] and substituting for [E] into equation 10, followed by a rearrangement:

$$[ES] = \frac{k_1[E]_o[S]}{k_{-1} + k_2 + \frac{k_1(k_2 + k_3)}{k_3}[S]} \quad (13)$$

At steady state, the rate of product formation is equal to

$$\frac{dP}{dt} = k_3[EP] = k_2[ES] \quad (14)$$

Substituting equation 13 into equation 14, yields an expression in the form of the Michaelis-Menten equation:

$$v = \frac{\frac{k_2 k_3}{k_2 + k_3} [E]_o [S]}{\frac{k_3}{k_2 + k_3} \frac{k_{-1} + k_2}{k_1} + [S]} \quad (15)$$

From the form of the Michaelis-Menten equation:

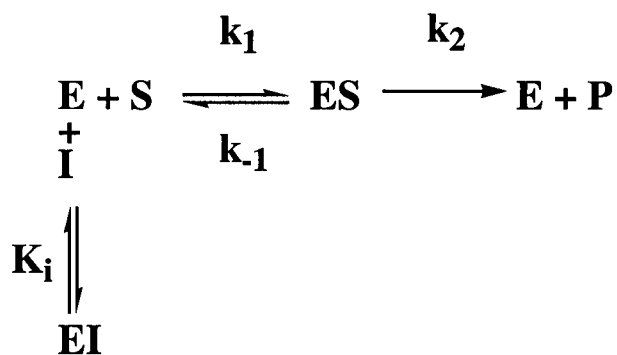
$$k_{cat} = \frac{k_2 k_3}{k_2 + k_3} \quad (16)$$

$$K_m = \frac{k_3}{k_2 + k_3} \frac{k_{-1} + k_2}{k_1} \quad (17)$$

Therefore, it becomes evident that the values obtained experimentally for k_{cat} and K_m are composed of the individual rate constants.

Enzyme Kinetics in the Presence of a Reversible Competitive Inhibitor

A competitive inhibitor competes directly with the substrate for binding at the enzyme's active site. This reaction is summarized by the following equilibrium:



Here, K_i is the dissociation constant for the enzyme-inhibitor complex:

$$K_i = \frac{[\text{E}][\text{I}]}{[\text{EI}]} \quad (18)$$

The total concentration of enzyme is now equal to

$$[E]_o = [E] + [ES] + [EI] \quad (19)$$

The free enzyme concentration can be calculated by rearranging equation 6 under the steady state condition

$$[E] = \frac{\frac{k_{-1} + k_2}{k_1} [ES]}{[S]} = \frac{K_m [ES]}{[S]} \quad (20)$$

Rearranging equation 18 and substituting equation 20 into it we get

$$[EI] = \frac{[E][I]}{K_i} = \frac{K_m [ES][I]}{[S]K_i} \quad (21)$$

substituting equation 21 into equation 19 we get

$$[E]_o = [ES] \left\{ \frac{K_m}{[S]} \left(1 + \frac{[I]}{K_i} \right) + 1 \right\} \quad (22)$$

which can be rearranged to give

$$[ES] = \frac{[E]_o [S]}{K_m \left(1 + \frac{[I]}{K_i} \right) + [S]} \quad (23)$$

Finally, from equation 4 we get the expression

$$v = k_2[ES] = \frac{k_2[E]_0[S]}{K_m \left(1 + \frac{[I]}{K_i} \right) + [S]} = \frac{V_{\max}[S]}{K_m \left(1 + \frac{[I]}{K_i} \right) + [S]} \quad (24)$$

Thus, a competitive inhibitor increases the apparent K_m by a factor of $1+[I]/K_i$. The value of V_{\max} remains unchanged since at high $[S]$ the inhibitor is displaced from the enzyme.

The double reciprocal plot of equation 24 is of the form

$$\frac{1}{v} = \frac{K_m \left(1 + \frac{[I]}{K_i} \right)}{V_{\max}} \frac{1}{[S]} + \frac{1}{V_{\max}} \quad (25)$$

where $K_m(1+[I]/K_i)/V_{\max}$ is the slope and $1/V_{\max}$ the y-intercept. Plots of this equation at various $[I]$ yield lines that intersect at $1/V_{\max}$. This is diagnostic of competitive inhibition. From these data, K_i can be determined.

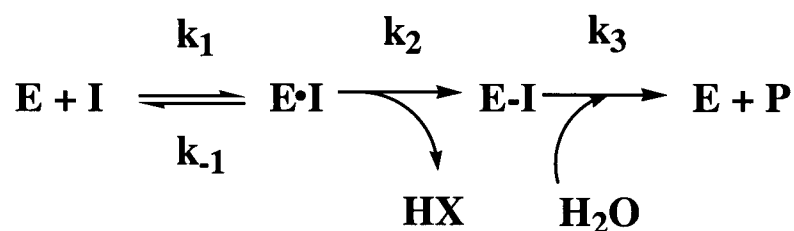
A simpler method of determining K_i if one knows the inhibitor behaves competitively is to use the following equation (rearranged from equation 25), also known as a Dixon plot:

$$\frac{1}{v} = \frac{K_m + [S]}{V_{\max}} \frac{1}{[S]} + \frac{K_m[I]}{K_i V_{\max}[S]} \quad (26)$$

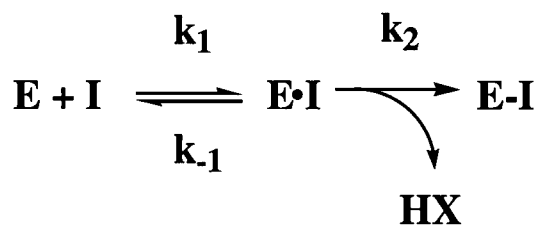
Setting $1/v = 1/V_{\max}$ gives $[I] = -K_i$.

Enzyme Kinetics in the Presence of a Mechanism-Based Inactivator

The inactivation of an enzyme, E, by a mechanism-based inactivator and its eventual reactivation by water is shown in the following scheme:



If $k_3 \ll k_2$, such that k_3 (or k_{cat}) approaches zero, then an extremely stable glycosyl-enzyme intermediate will accumulate and the enzyme will be inactivated. The model then simplifies to:

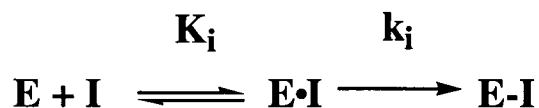


This model predicts a time-dependent inactivation of the enzyme. If $[I] \gg [E]$, then $[I]$ can be assumed to be essentially constant during the reaction and pseudo first-order

kinetics with respect to [E] will be observed. The equation for this process is analogous to the Michaelis-Menten equation:

$$v = \frac{k_i[E][I]}{K_i + [I]} \quad (27)$$

where k_i is the rate constant for inactivation ($k_i = k_2$) and K_i is an apparent dissociation constant for all forms of enzyme-bound inactivator ($K_i = k_{-1}/k_1$). The model then appears as:



Equation 27 can be rewritten as:

$$v = k_{obs}[E] \quad (28)$$

where

$$k_{obs} = \frac{k_i[I]}{K_i + [I]} \quad (29)$$

Equation 28 can be expressed as a differential equation:

$$\frac{d[E]}{dt} = k_{obs}[E] \quad (30)$$

which can then be solved with respect to time to give

$$\ln[E] = -k_{obs}t \quad (31)$$

If $K_i \gg [I]$, then equation 29 simplifies to

$$k_{obs} = \frac{k_i[I]}{K_i} \quad (32)$$

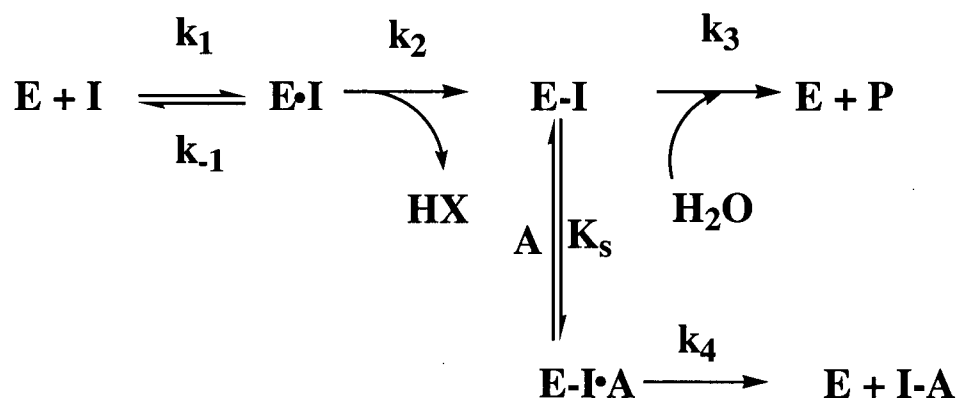
Thus far, we have discussed the case where $k_3 \ll k_2$ and $k_3 \sim 0$. However, if $k_2 > k_3$ and $k_3 > 0$, then the intermediate will slowly turn over and a steady-state rate will be established. An apparent K_i' under steady state conditions is given by the equation:^{23,110}

$$K_i' = \frac{K_i}{1 + k_i / k_{cat}} \quad (33)$$

where $K_i = k_{-1}/k_1$, $k_i = k_2$ and $k_{cat} = k_3$. In this case, K_i' represents a minimum value for the actual dissociation constant K_i .

Reactivation Kinetics

The model describing the inactivation of an enzyme and its eventual reactivation can be modified to include an alternate pathway by which the inactivated enzyme can turn over, i.e. through attack by a ligand (A) other than water:



The equation describing the reactivation process is written as follows:⁷⁷

$$-\frac{d[\text{E}-\text{I}]}{dt} = \left(k_3 + \frac{k_4[\text{A}]}{K_s + [\text{A}]}\right)[\text{E}-\text{I}] \quad (34)$$

Thus, when the reaction is carried out with a large excess of the reactivating ligand A over enzyme, the reaction will become pseudo-first order with respect to E-I, and at saturating concentrations the observed first-order rate constant (k_{obs}) will be equal to ($k_3 + k_4$). Under these circumstances, the increase in free enzyme with time can be related to the full activity of the sample by

$$[E] = [E]_o(1 - \exp[-k_{obs}t]) \quad (35)$$

Appendix II: Graphical Representation of Spontaneous Hydrolysis Data

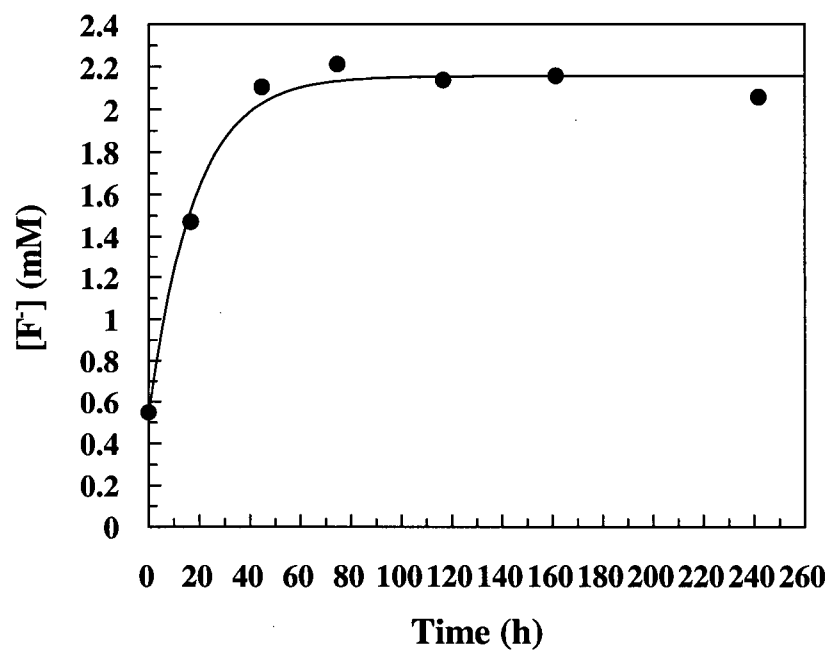


Figure AII-1: Spontaneous hydrolysis of 2FGF (2.5 mM) at 50°C, pH 6.8.

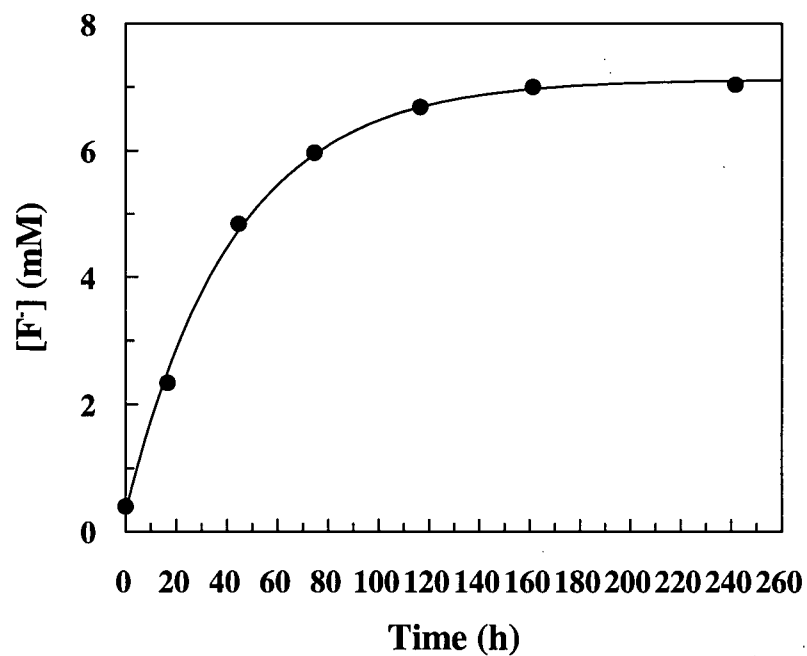


Figure AII-2: Spontaneous hydrolysis of 2FMF (7.5 mM) at 50°C, pH 6.8.

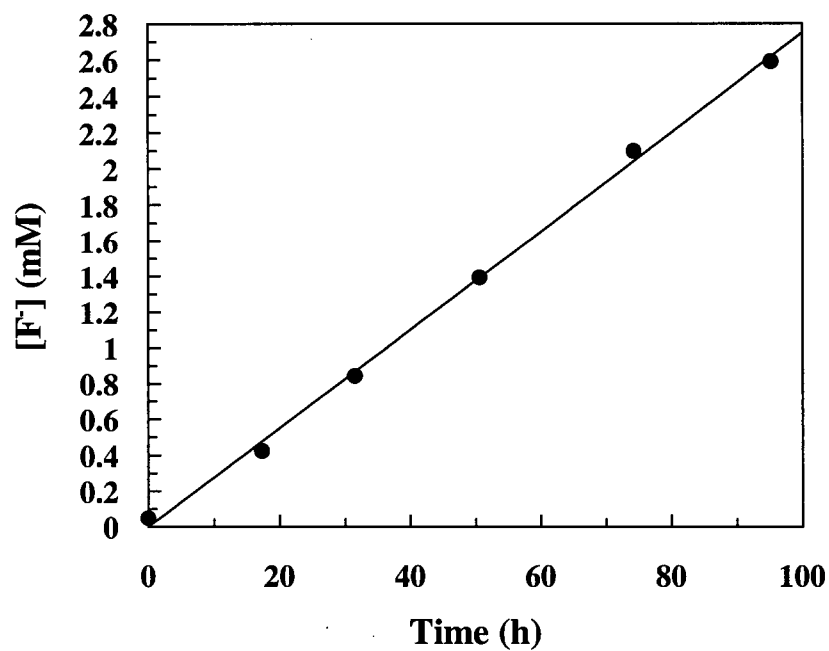


Figure AII-3: Spontaneous hydrolysis of 2,6diFGF (5 mM) at 50°C, pH 6.8.

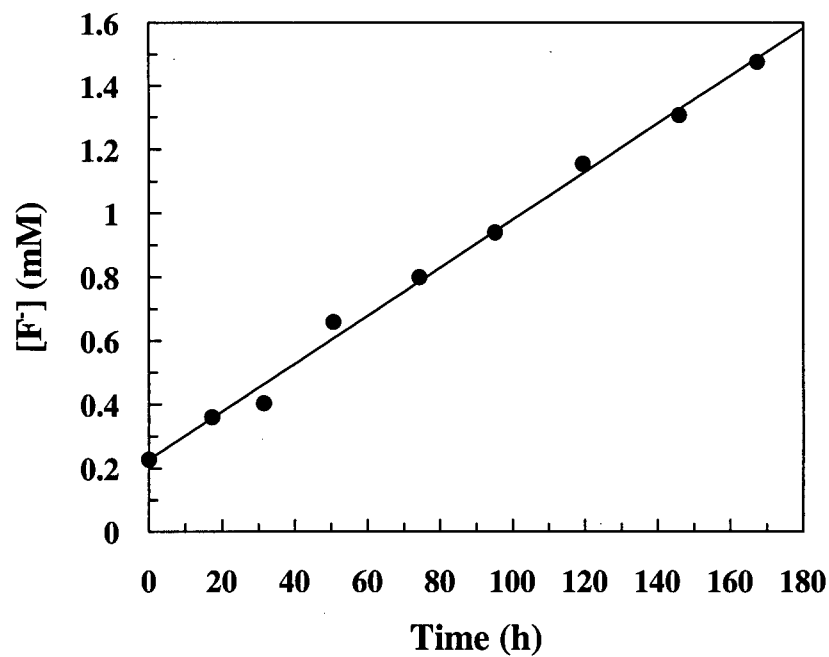


Figure AII-4: Spontaneous hydrolysis of 2FGlcAF (5 mM) at 50°C, pH 6.8.

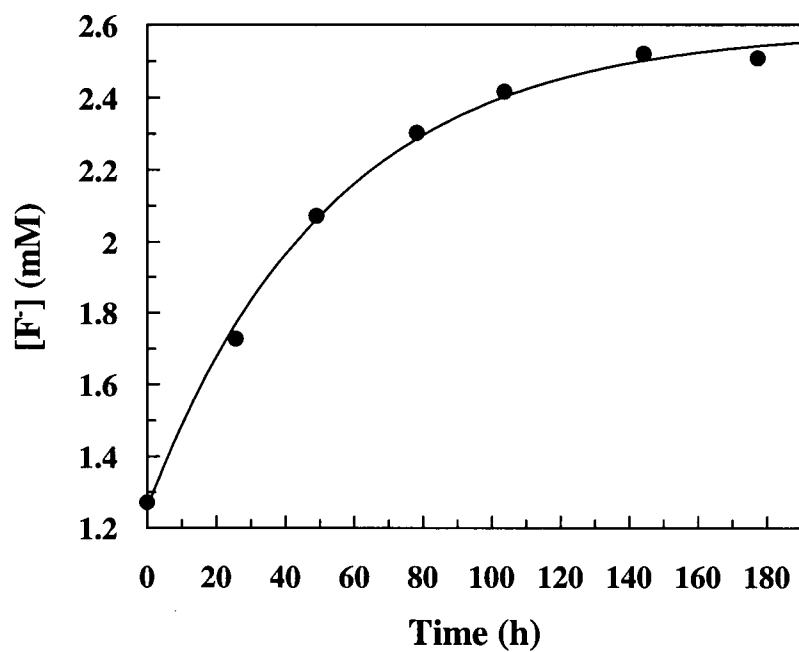


Figure AII-5: Spontaneous hydrolysis of 2FManAF (2.5 mM) at 50°C, pH 6.8.

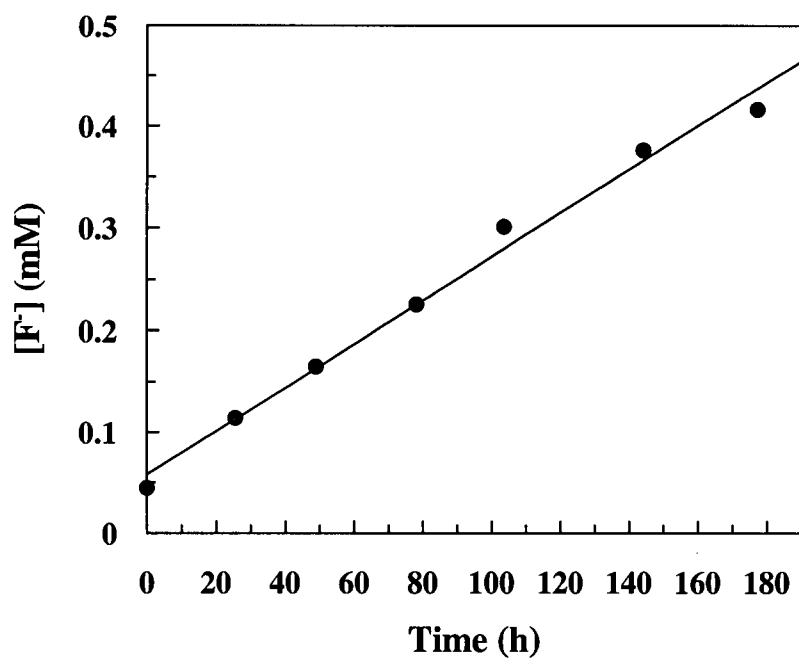


Figure AII-6: Spontaneous hydrolysis of 5FGlcAF (5 mM) at 50°C, pH 6.8.

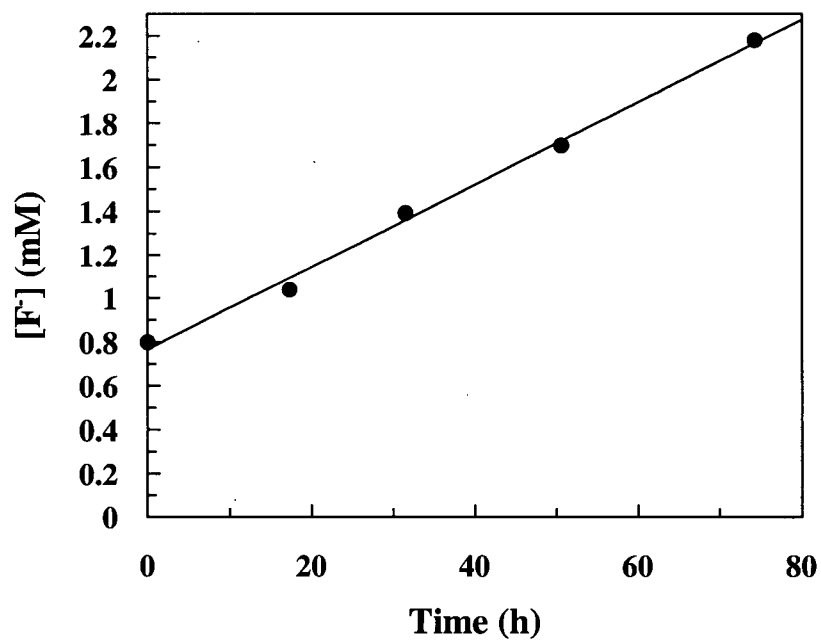


Figure AII-7: Spontaneous hydrolysis of 5FIdoAF (5 mM) at 50°C, pH 6.8.

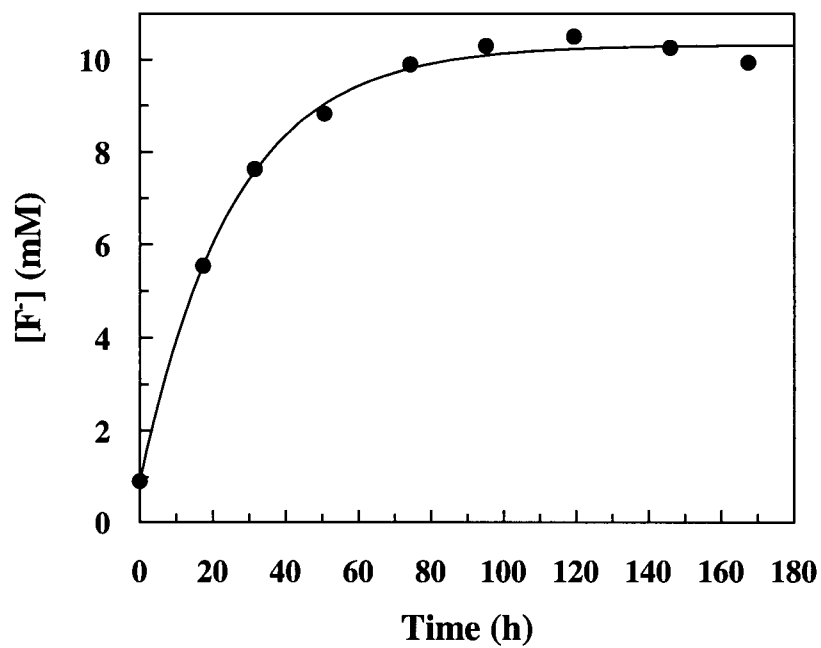


Figure AII-8: Spontaneous hydrolysis of 2FIdoAF (10 mM) at 50°C, pH 6.8.

References

1. Henrissat, B. *Biochem. J.* **1991**, 309-316.
2. Henrissat, B.; Bairoch, A. *Biochem. J.* **1993**, 781-788.
3. Henrissat, B.; Callebaut, I.; Fabrega, S.; Lehn, P.; Mornon, J.-P.; Davies, G.
Proceedings of the National Academy of Sciences USA **1995**, 92, 7090-7094.
4. Henrissat, B.; Bairoch, A. *Biochem. J.* **1996**, 695-696.
5. Henrissat, B.; Davies, G. *Current Opinion in Structural Biology* **1997**, 637-644.
6. D. E. Koshland, *J. Biol. Rev.* **1953**, 28, 416-436.
7. White, A.; Withers, S. G.; Gilkes, N.; Rose, D. *Biochemistry* **1994**, 33, 12546-12552.
8. Jacobson, R. H., Zhang, X-J., Dubose, R. F., and Mathews, B. W. *Nature* **1994**, 369, 761-766.
9. Jain, S.; Drendel, W. B.; Chen, Z.-w.; Mathews, F. S.; Sly, W. S.; Grubb, J. H.
Nat. Struct. Biol. **1996**, 3, 375-381.
10. White, A.; Tull, D.; Johns, K.; Withers, S. G.; Rose, D. R. *Nat. Struct. Biol.* **1996**, 3, 149-154.
11. Notenboom, V.; Birsan, C.; Warren, R. A. J.; Withers, S. G.; Rose, D. R.
Biochemistry **1998**, 37, 4751-4758.
12. Sidhu, G.; Withers, S. G.; Nguyen, N. T.; McIntosh, L. P.; Ziser, L.; Brayer, G. D.
Biochemistry **1999**, 38, 5346-5354.
13. Tao, B. Y.; Reilly, P. J.; Robyt, J. F. *Biochim. Biophys. Acta* **1989**, 995, 214-220.

14. Mooser, G.; Hefta, S. A.; Paxton, R. J.; Shively, J. E.; Lee, T. D. *J. Biol. Chem.* **1991**, *266*, 8916-8922.
15. Sinnott, M. L.; Withers, S. G.; Viratelle, O. M. *Biochem. J.* **1978**, *175*, 539-546.
16. Kempton, J. B.; Withers, S. G. *Biochemistry* **1992**, *31*, 9961-9969.
17. Banait, N. S.; Jencks, W. P. *J. Am. Chem. Soc.* **1991**, *113*, 7958-7963.
18. Bennet, A.; Sinnott, M. L. *J. Am. Chem. Soc.* **1986**, *108*, 7287-7294.
19. Weber, J. P.; Fink, A. L. *J. Biol. Chem.* **1980**, *255*, 9030-9032.
20. Sinnott, M. L.; Souchard, I. J. L. *Biochem. J.* **1973**, *133*, 89-98.
21. Sinnott, M. L.; Withers, S. G. *Biochem. J.* **1974**, *143*, 751-762.
22. Sinnott, M. L. Glycosyl group transfer. In *Enzyme Mechanisms*; Page, M. I.; Williams, A. Eds.; Royal Society of Chemistry: London, 1987; pp. 259.
23. Legler, G. *Adv. Carb. Chem. Biochem.* **1990**, *48*, 319-384.
24. Wolfenden, R. *Acc. Chem. Res.* **1972**, *5*, 10-18.
25. Fersht, A. *Enzyme Structure and Mechanism*, 2nd ed.; Freeman: New York, 1985.
26. Ermert, P.; Vasella, A.; Weber, M.; Rupitz, K.; Withers, S. G. *Carbohydr. Res.* **1993**, *250*, 113-128.
27. Black, T.; Kiss, L.; Tull, D.; Withers, S. G. *Carbohydr. Res.* **1993**, *250*, 195-202.
28. Keresztessy, Z.; Kiss, L.; Hughes, M. A. *Arch. Biochem. Biophys.* **1994**, *315*, 323-330.
29. Bombard, S.; Maillet, M.; Capmau, M. L. *Carbohydr. Res.* **1995**, *275*, 433-440.
30. Howard, S.; G. Withers, S. *Biochemistry* **1998**, *37*, 3858-3864.
31. Kanfer, J. N.; Raghaven, S. S.; Mumford, R. A. *Biochim. Biophys. Acta* **1975**, *391*, 129-140.

32. Herrchen, M.; Legler, G. *Eur. J. Biochem.* **1984**, *138*, 527-531.
33. Gebler, J. C., Aebersold, R., and Withers, S.G. *J. Biol. Chem.* **1992**, *267*, 11126-11130.
34. Yuan, J.; Martinez-Bilbao, M.; Huber, R. E. *Biochem. J.* **1994**, *299*, 527-531.
35. Zechel, D. L.; Withers, S. G. Glycosyl Transferase Mechanisms. In *Comprehensive Natural Products Chemistry*; Poulter, C. D. Ed.; Elsevier Science: Oxford, 1999; Vol. 5; pp. 279-314.
36. Withers, S. G.; Warren, R. A. J.; Street, I. P.; Rupitz, K.; Kempton, J. B.; Aebersold, R. *J. Am. Chem. Soc.* **1990**, *112*, 5887-5889.
37. Withers, S. G.; Street, I. P. *J. Am. Chem. Soc.* **1988**, *110*, 8551-8553.
38. McCarter, J. D.; Adam, M. J.; Braun, C.; Namchuk, M.; Tull, D.; Withers, S. G. *Carbohydr. Res.* **1993**, *249*, 77-90.
39. McCarter, J. D.; Withers, S. G. *J. Am. Chem. Soc.* **1996**, 241-242.
40. McCarter, J. D.; Withers, S. G. *J. Biol. Chem.* **1996**, *271*, 6889-6894.
41. Howard, S.; He, S.; Withers, S. G. *J. Biol. Chem.* **1998**, *273*, 2067-2072.
42. Gieselmann, V. *Biochim. Biophys. Acta* **1995**, 103-136.
43. Withers, S. G.; Rupitz, K.; Street, I. P. *J. Biol. Chem.* **1988**, *263*, 7929-7932.
44. Voet, D.; Voet, J. G. *Biochemistry*, 1st ed.; John Wiley & Sons: New York, 1990.
45. Paigen, K. *Progr. Nucleic Acid Res. Molec. Biol.* **1989**, *37*, 155-205.
46. Shipley, J. M., Klinkenberg, B. M., Wu, D. R., Bachinsky, J. H., and Sly, W. S. *Am. J. Hum. Genet.* **1993**, *52*, 517-526.

47. Tomatsu, S., Fukuda, S., Sukegawa, Y., Ikedo, S., Yamada, Y., Sasaki, H., Okamoto, T., Kuwahara, S., Yamaguchi, S., Kiman, T., Shintaku, H., Isshiki, G., and Orii, T. *Am. J. Hum. Genet.* **1991**, *48*, 89-96.
48. Vervoort, R., Lissens, W., and Liebaers, I. *Hum. Mutat.* **1993**, *2*, 443-445.
49. Wu, B. M., Tomatsu, S., Sukegawa, K., Orii, T., and Sly, W. S. *J. Biol. Chem.* **1994**, *269*, 23681-23688.
50. Sinnott, M. L. *Chem. Rev.* **1990**, 1171-1202.
51. Richard, J. P.; Huber, R. E.; Lin, S.; Heo, C.; Amyes, T. L. *Biochemistry* **1996**, *35*, 12377-12386.
52. Richard, J. P.; Huber, R. E.; Heo, C.; Amyes, T. L.; Lin, S. *Biochemistry* **1996**, *35*, 12387-12401.
53. Richard, J. P. *Biochemistry* **1998**, *37*, 4305-4309.
54. Sakon, J.; Adney, W. S.; Himmel, M. E.; Thomas, S. R.; Karplus, P. A. *Biochemistry* **1996**, *35*, 10648-10660.
55. Gallagher, S. R. GUS Protocols: Using the GUS gene as a reporter of gene expression; Academic Press, Inc.: San Diego, 1992; pp. 221.
56. Godsey, J. H.; Matteo, M. R.; Shen, D.; Tolman, G.; Gohlke, J. R. *J. Clin. Microbiol.* **1981**, *13*, 483-490.
57. Feng, P. C.; Hartman, P. A. *Appl. Environ. Microbiol.* **1982**, *43*, 1320-1329.
58. Scott, H. S.; Anson, D. S.; Orsborn, A. M.; Nelson, P. V.; Clements, P. R.; Morris, C. P.; Hopwood, J. J. *Proc. natl. Acad. Sci. USA* **1991**, *88*, 9695-9699.
59. Shull, R. M.; Kakkis, E. D.; McEntee, M. F.; Kania, S. A.; Jonas, A. J.; Neufeld, E. F. *Proc. Natl. Acad. Sci. USA* **1994**, *91*, 12937-12941.

60. Kakkis, E. D.; McEntee, M. F.; Schmidtchen, A.; Neufeld, E. F.; Ward, D. A.; Gompf, R. E.; Kania, S.; Bedolla, C.; Chien, S. L.; Shull, R. M. *Biochem. Mol. Med.* **1996**, 58.
61. Kakkis, E. D.; Muenzer, J.; Tiller, G. E.; Waber, L.; Belmont, J.; Passage, M.; Izykowski, B.; Phillips, J.; Doroshow, R.; Walot, I.; Hoft, R.; Neufeld, E. F. *N. Engl. J. Med.* **2001**, 344, 182-188.
62. Armand, S.; Vieille, C.; Gey, C.; Heyraud, A.; Zeikus, J. G.; Henrissat, B. *Eur. J. Biochem.* **1996**, 236, 706-713.
63. Durand, P.; Lehn, P.; Callebaut, I.; Fabrega, S.; Henrissat, B.; Mornon, J.-P. *Glycobiology* **1997**, 7, 277-284.
64. Durand, P.; Fabrega, S.; Henrissat, B.; Mornon, J.-P.; Lehn, P. *Hum. Mol. Gen.* **2000**, 9, 967-977.
65. Nieman, C. E. *Human α -L-iduronidase: Substrate synthesis and mechanistic analysis*; University of British Columbia: Vancouver, 2000.
66. Lal, G. S. *J. Org. Chem.* **1993**, 58, 2791-2796.
67. Burkhardt, M. D.; Zhang, Z.; Hung, S.-C.; Wong, C.-H. *J. Am. Chem. Soc.* **1997**, 11743-11746.
68. Albert, M.; Dax, K.; Ortner, J. *Tetrahedron* **1998**, 54, 4839-4848.
69. Györgydeák, Z., and Thiem, J. *Carbohydr. Res.* **1995**, 268, 85-92.
70. de Nooy, A. E. J., and Besemer, A. C. *Tetrahedron* **1995**, 51, 8023-8032.
71. Heeres, A.; Doren, H. A. v.; Gotlieb, K. F.; Bleeker, I. P. *Carbohydr. Res.* **1997**, 221-227.
72. Stelakatos, G. C.; Paganou, A.; Zervas, L. *J. Chem. Soc. C* **1966**, 1191-1199.

73. Somsák, L.; Ferrier, R. J. *Adv. Carbohydr. Chem. Biochem.* **1991**, *49*, 37-92.
74. Chiba, T.; Sinay, P. *Carbohydr. Res.* **1986**, *151*, 379-389.
75. Igarashi, K.; Honma, T.; Irisawa, J. *Carbohydr. Res.* **1969**, 577-578.
76. McCarter, J. D. *Mechanism-based inhibitors as in vitro and in vivo probes of glycosidase structure and mechanism*; University of British Columbia: Vancouver, 1995.
77. Street, I. P.; Kempton, J. B.; Withers, S. G. *Biochemistry* **1992**, *31*, 9970-9978.
78. Zechel, D. L.; Withers, S. G. *Acc. Chem. Res.* **2000**, 11-18.
79. Gebler, J., Gilkes, N. R., Claeysens, M., Wilson, D. B., Béguin, P., Wakarchuk, W. W., Kilburn, D. G., Miller, Jr., R. C., Warren, R. A., and Withers, S. G. *J. Biol. Chem.* **1992**, *267*, 12559-12561.
80. Howard, S., Braun, C., McCarter, J., Moremen, K. W., Liao, Y.-F., and Withers, S. G. *Biochem. Biophys. Res. Commun.* **1997**, *238*, 896-898.
81. McCarter, J. D.; Adam, M. J.; Withers, S. G. *J. Lab. Compd. Radiopharm.* **1992**, *31*, 1005-1009.
82. Zhang, Y.; Bommuwamy, J.; Sinnott, M. L. *J. Am. Chem. Soc.* **1994**, *116*, 7557-7563.
83. Sabini, E.; Sulzenbacher, G.; Dauter, M.; Dauter, Z.; Jorgensen, P. L.; Schulein, M.; Dupont, C.; Davies, G. J.; Wilson, K. S. *Chem. Biol.* **1999**, *6*, 483-492.
84. Ruth, L.; Eisenberg, D.; Neufeld, E. F. *Acta Crystallogr. D* **2000**, *56*, 524-528.
85. Takasaki, S.; Murray, G. J.; Furbish, F. S.; Brady, R. O.; Barranger, J. A.; Kobata, A. *J. Biol. Chem.* **1984**, *259*, 10112-10117.
86. Grace, M. E.; Desnick, R. J.; Pastores, G. M. *J. Clin. Invest.* **1997**, *99*, 2530-2537.

87. Tybulewicz, V. L. J.; Tremblay, M. L.; LaMarca, M. E.; Willemsen, R.; Stubblefield, B. K.; Winfield, S.; Zablocka, B.; Sidransky, E.; Martin, B. M.; Huang, S. P.; Mintzer, K. A.; Westphal, H.; Mulligan, R. C.; Ginns, E. I. *Nature* **1992**, *357*, 407-410.
88. Beutler, E.; Gelbart, T. *Blood Cells Mol Dis* **1997**, *23*, 2-7.
89. *JAMA* **1996**, *275*, 548-553.
90. Meikle, P. J.; Hopwood, J. J.; Clague, A. E.; Carey, W. F. *JAMA* **1999**, *281*, 249-254.
91. Poorthuis, B. J.; Wevers, R. A.; Kleijer, W. J.; Groener, J. E.; Jong, J. G. d.; Weely, S. v.; Niezen-Koning, K. E.; Diggelen, O. P. v. *Hum. Genet.* **1999**, *105*, 151-156.
92. Winchester, B.; Vellodi, A.; Young, E. *Biochem. Soc. Trans.* **2000**, *28*, 150-154.
93. Russell, C. S.; Clarke, L. A. *Clin. Genet.* **1999**, 389-394.
94. Murray, G. J.; Jin, F.-S. *J.Histochem. Cytochem.* **1995**, *43*, 149-158.
95. Zirzow, G. C.; Sanchez, O. A.; Murray, G. J.; Brady, R. O.; Oldfield, E. H. *Neurochem. Res.* **1999**, *24*, 301-305.
96. McCarthy, T. J.; Schwarz, S. W.; Welch, M. J. *J. Chem. Ed.* **1994**, *71*, 830-836.
97. Fowler, J. S.; Wolf, A. P. *Acc. Chem. Res.* **1997**, *30*, 181-188.
98. MacGregor, R. R.; Halldin, C.; Fowler, J. S.; Wolf, A. P.; Arnett, C. D.; Langstrom, B.; Alexoff, D. *Biochem. Pharmacol.* **1985**, *34*, 3207-3210.
99. Chirakal, R.; Firnau, G.; Garnett, E. *J. Label. Cmpds. Radiopharm.* **1989**, *26*, 228.
100. Street, I. P.; Rupitz, K.; Withers, S. G. *J. Am. Chem. Soc.* **1988**, *110*, 8551-8553.
101. Namchuk, M. N.; Withers, S. G. *Biochemistry* **1995**, *34*, 16194-16202.

102. Barker, G. R. Triphenylmethyl Ethers. In *Methods in Carbohydrate Chemistry*; Whistler, R. L.; Wolfrom, M. L. Eds.; Academic Press Inc.: New York and London, 1963; Vol. 2.
103. Dax, K.; Wolflehner, W.; Weidmann, H. *Carbohydr. Res.* **1978**, *65*, 132-138.
104. Eckelman, W. C.; Gibson, R. E. The design of site-directed radiopharmaceuticals for use in drug discovery. In *Nuclear imaging in drug discovery, development, and approval*; Burns, H. D.; Gibson, R. E.; Dannals, R. F.; Siegl, P. K. S. Eds.; Birkhauser: Boston, 1993; pp. 113-134.
105. Glew, R. H.; Gopalan, V.; Hubbell, C. A.; Devraj, R. V.; Lawson, R. A.; Diven, W. F.; Mannock, D. A. *Biochem. J.* **1991**, *274*, 557-563.
106. Csuk, R., and Glanzer, B. I. *Adv. Carbohydr. Chem. Biochem.* **1988**, *46*, 73-177.
107. Ho, K. J. *Protein Express.* **1991**, *2*, 63-65.
108. Grubb, J. H.; Kyle, J. W.; Cody, L. B.; Sly, W. S. *FASEB J.* **1993**, *7*, 1255a.
109. Unger, E. G.; Durrant, J.; Anson, D. S.; Hopwood, J. J. *Biochem. J.* **1994**, *304*, 43-49.
110. Wentworth, D. F.; Wolfenden, R. *Biochemistry* **1974**, *13*, 4715-4720.